UNIVERSITA' DEGLI STUDI DI SIENA
DIPARTIMENTO DI BIOTECNOLOGIE, CHIMICA E FARMACIA

DOTTORATO DI RICERCA IN
SCIENZE E CHIMICHE FARMACEUTICHE

CICLO XXXII

COORDINATORE: PROF. STEFANO MANGANI

Synthesis of intermediates for the preparation of Active Pharmaceutical Ingredients (APIs)

CHIM/06 - CHIMICA ORGANICA

TUTOR
Professor Maurizio Taddei

DOTTORANDO: Salvatore Princiotto

ANNO ACCADEMICO: 2018/2019

Alla mia famiglia

Sommario

1. Maytansine and maytansinoids

1.1 Maytansinoids and their activity

Maytansinoids are ansa macrolide derivatives extracted from shrubs of *Maytenus ovatus*. [1] Their pharmacological activity has been widely studied in the last decades, due to their cytotoxic and anticancer properties. [2–5] In particular, in late 70s Issell and Crooke described maytansine **1** as the first macrolide isolated from plants rather than microorganisms, though showing different mechanism of action. [4] Antibacterial effect from the known macrolides was explicated by inhibition of bacterial DNA-dependent RNA-polymerase, while maytansine antitumor activity was proved to be given by metaphase arrest of the mitotic cycle, similarly to *Vinca* alkaloids. [6]

Along with maytansine, also maytanprine **2** and maytanbutine **3** were extracted, with similar but less extent antitumor effect than maytansine itself. [5] All of the three homologues contain a chlorinated aromatic nucleus, with a substituted epoxide, an ester, a cyclic carbamate and a conjugated diene within the ansa system. Maytanprine and maytanbutine differ from maytansine because of the methyl groups present on the ester portion. (Scheme 1)

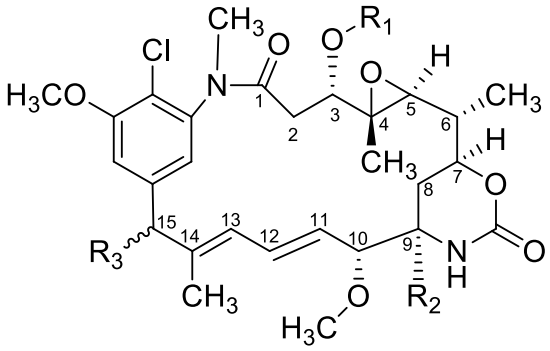

	R_1	R_2	R_3	
1	$COCH(CH_2)N(CH_3)COCH_3$	OH	H	**Maytansine**
2	$COCH(CH_2)N(CH_3)COCH_2CH_3$	OH	H	**Maytanprine**
3	$COCH(CH_2)N(CH_3)COCH(CH_3)_2$	OH	H	**Maytanbutine**

Scheme 1. Maytansine and its analogues

Clinical studies about antitumor activity were initially performed on patients that were refractory to other treatments. The trials were conducted on several types of solid tumors (colorectal, pancreatic, adenocarcinoma, renal, prostate, ovary, breast, melanoma, head and neck cancers), [4] but closed soon after because of the low therapeutic window, due to the high toxicity and side effects, in particular gastrointestinal (vomiting and diarrhea, often followed by constipation), neurotoxicity (weakness, lethargy, dysphoria, insomnia), myelosuppression (thrombocytopenia). [4]

1.2 Mechanism of action of maytansinoids

Maytansinoids can be classified as microtubule-targeting agents, a class of compounds able to interact with different binding sites within tubulin, so that microtubule formation could be stabilized or destabilized. (Figure 1A) [7–10] In order to better understand this process, it is important to highlight the phenomenon that characterize the so-called microtubules dynamic stability. In fact, microtubules undergo natural randomized shortening and growth to guarantee positioning and movement of the organelles, as well as segregation of chromosomes during cell division. [11–13] Among the most representative examples of the stabilizing agents there are taxanes (Paclitaxel, Docetaxel), able to enhance microtubule polymerization, by binding to microtubule sites and effecting in microtubule aggregation, with consequent impossibility for the mitosis to proceed correctly. (Figure 1B) [14] On the other hand, destabilizing agents, such as colchicine, *Vinca* alkaloids and maytansinoids, influence the replicative cell cycle arresting metaphase in consequence of inhibition of microtubule dynamics. [7,14] In other words, interaction with tubulin binding sites results in the block of the stochastic shortening, lengthening and polymerization of microtubules, impeding the cell cycle to be completed.

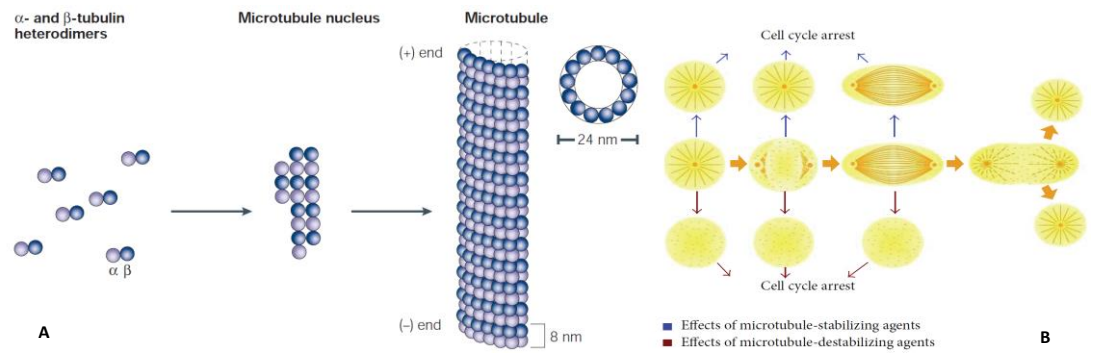

Figure 1A. microtubule formation from tubulin heterodimers; **1B** effects of microtubule stabilizing or destabilizing agents on microtubule dynamics and mitotic cell cycle

In particular, maytansinoids bind well determined sites placed at microtubules ends, so that their dynamics are strongly influenced and disrupted. Interestingly, two maytansine derivatives, known as S-methyl DM1 and S-methyl DM4, (Scheme 2) showed a better inhibition profile because of the ability to form aggregates besides the perturbation of microtubule dynamics. [15] Maytansine was not potent in the same way in this framework, because of the lack of stabilization and polymerization capability, though showing inhibitory activity against the Lewis lung carcinoma and B-16 melanocarcinoma solid murine tumor systems, together with antileukemic activity. Maytansine analogues, such as normaytansine, maytanprine and maytanbutine, but not maytansinol, showed a similar activity spectrum and potency. [15] Even bacteria-derived maytansinoids, known as ansamitocins, exhibit an activity spectrum and wide effective dose range similar to maytansine, showing antitumor activity against leukemia. [2] Ansamitocin P3 and P4 are also effective against melanoma, sarcoma, Ehrlich carcinoma [16] but were also proved to be less active against leukemia. [2,6]

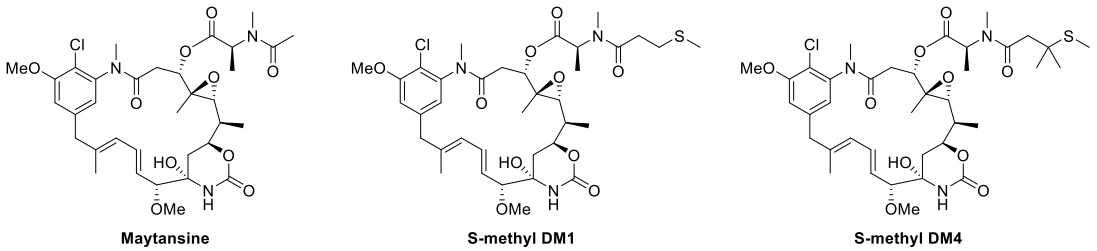

Scheme 2. Reported structures of DM1-SMe and DM4-SMe, compared to maytansine

Maytansine was evaluated as a cytotoxic agent in over 35 tumor types in more than 800 patients. [17] Only one patient with carcinoma recovered completely, whereas about 20 patients showed partial responses. Other maytansinoids activities than the

antiproliferative were tested. Efficacy against fungi, yeasts and plants was proved, while no activity was registered against growth of bacteria. Based on these results, applications for maytansine as a new drug were closed. [17]

1.3 Structure-Activity Relationship of maytansinoids

X-ray crystallographic studies were performed in order to better understand how biological activity by maytansinoids was achieved. The ansa macrolide is a 19-membered ring, with a hole of 5.4 Å in the center. - (Figure 2) - The upper side of the ring is more hydrophilic, while the lower face is mostly hydrophobic. The ester portion on the upper side acts as a shield against reactants approaching to the hydrophilic face; at the same time, the antileukemic activity could be due to the alkylation of carbinolamide and epoxydic regions, acting as false substrates. Ester moiety at C(3) is important for antileukemic activity and needs to maintain α-configuration (β-form is inactive), while hydrolysis brings to the formation of maytansinol **5** with no antileukemic potential and dramatic decrease in cytotoxic activity; anyway, almost all of the acyloxy derivatives that were synthesized maintained antitumor activity. [3,5]

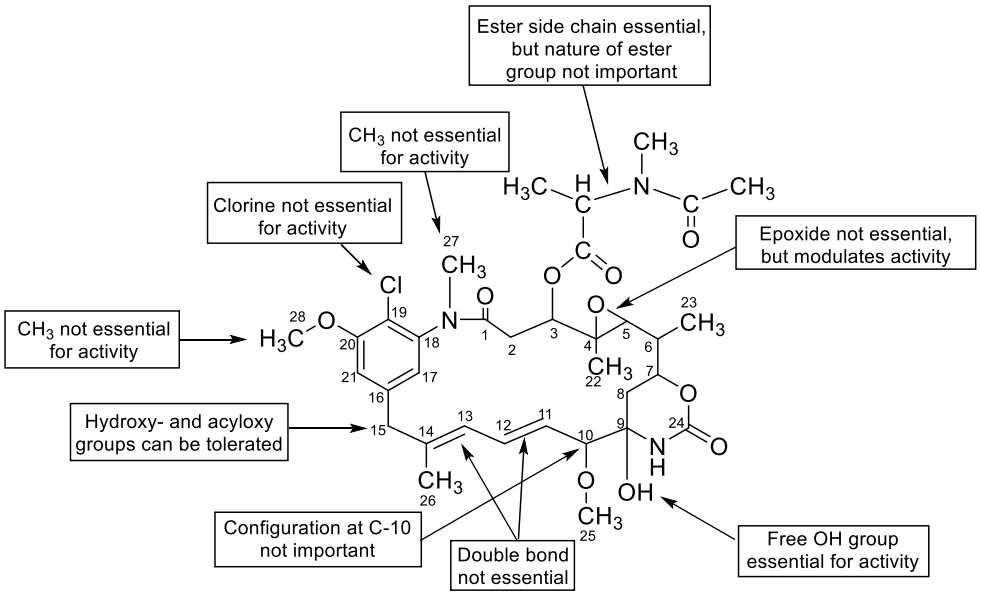

Figure 2. SAR of maytansine

Carbinolamide at C(9) is considered as an alkylating region: etherification of OH at C(9) results in loss of cytotoxicity. On the other hand, change of configuration of the

methoxy group at C(10) has no consequences on biological activity, whereas hydroxyl group at C(15) seems to promote cytotoxic efficacy. Aromatic substituents could tolerate modifications, maintaining the biological effects, so that methyl at phenolic C(20) and on the amide moiety are not essential, as well as aromatic chlorine and the epoxide, the latter seems rather to modulate cytotoxicity. [3]

1.4 Antibody Maytansinoid Conjugates (AMCs): structure and mechanism of action

In order to get through the too high and non-selective cytotoxicity of maytansine derivatives, in 1990s Takeda and coworkers prepared the first conjugate made up using maytansinoids and monoclonal antibodies (*m*Abs), so to explicate their antitumoral activity specifically on cancer cells. [18] In particular, it was exploited the ability of the antibodies to interact selectively with their substrate, an antigen that tuned out to be overexpressed on the surface of tumor cells, without any anomalous expression in healthy cells and tissues. [18] By such an approach, maytansine and its derivatives could have been used in a safer way, due to the selective attack on target cells, for both lymphomas and solid tumors. Typically, the antibody portion is responsible for the identification and interaction with its specific antigen overexpressed on tumor cells. In particular, due to the observed overexpression of certain antigens (for example, CanAg on colorectal cancer and HER2 on the breast metastatic cancer cells) and to the ability of maytansinoids to be effective against these tumors, it was thought to conjugate maytansine derivatives with *m*Abs able to specifically bind their antigens (CanAg for the antibody cantuzumab and HER2 for trastuzumab). [19] As a direct consequence, only cells overexpressing these antigens became a suitable target to induce the antibody-antigen interaction and the subsequent response. (Figure 3A)

Humanized antibodies trastuzumab were chosen for their ability to selectively bind HER2 antigen. Humanization provided for the engineering so to make them similar to endogenous proteins, avoiding in this way the response from immunological system against the conjugate. [20] In order to provide the most efficient carrying for the maytansinoid antitumoral molecules (called drug maytansionoid, DM), a suitable linker was employed with the role of guaranteeing the stability and integrity of the conjugate within the systemic circulation until the target cells have been reached. [21,22]

Only at this stage, the complex could be proteolytically digested and fragmented, to allow the maytansine derivative payload to exert its therapeutic anticancer activity. [23]

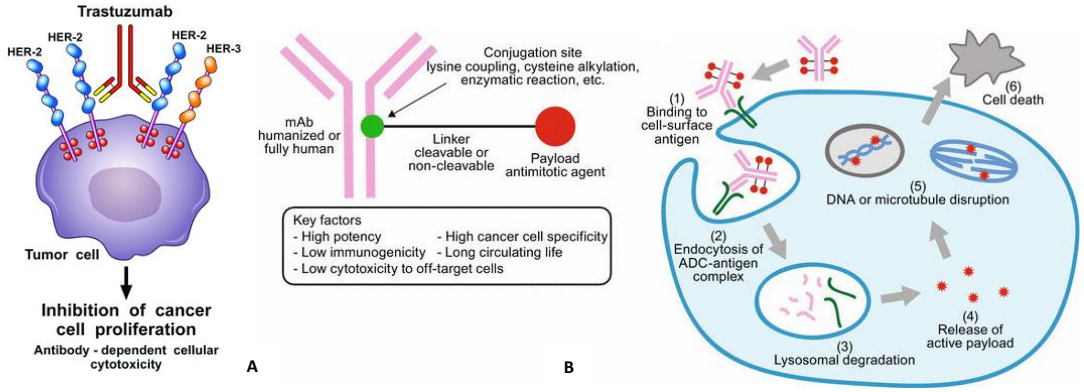

Figure 3A. Specific interaction of trastuzumab with HER2 antigens; **3B**. mechanism of action of ADCs.

As it is represented above, (Figure 3B) the selective interaction between antigen and antibody (1) allows the internalization of the complex within the tumor cell by endocytosis (2). Here, the conjugate moves towards the lysosomal compartment where it is degraded by proteolytic enzymes (3). Maytansinoid payload, at this point (4), is free and ready to permeate the nucleus and inhibit the mitotic cycle of its target (5), bringing to cell death (6).

By now, only ado-trastuzumab emtansine (or trastuzumab-DM1) is commercially available as Kadcyla® (**4**), for the treatment of HER2-positive metastatic breast cancer. [24] Kadcyla® shows trastuzumab as the monoclonal antibody, a maleimide cyclohexane-1-carboxylate (SMCC) moiety as the linker and the sulfide derivative of maytansine DM1 as the payload. (Scheme 3) Unfortunately, other maytansinoid-containing ADCs (such as cantuzumab mertansine) did not succeed in clinical trials. [25]

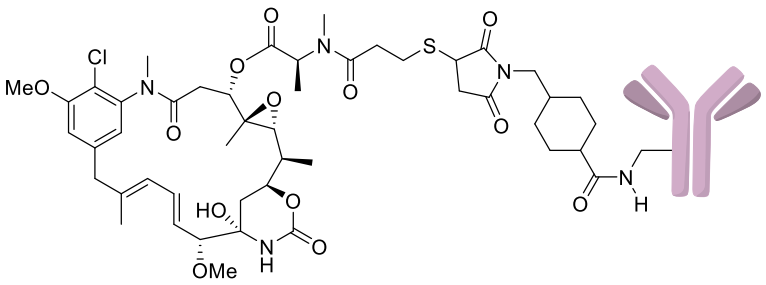

Scheme 3. Schematic representation of trastuzumab-SMCC-DM1

Once AMC was digested by proteolytic cleavage within the lysosomal compartment, [26] further modifications took place, in order to make the payload free to act as the cytotoxic agent. Among the most common linkers used to test the stability and efficacy of conjugated-DM1, N-Succinimidyl-3-(2-pyridyldithio)propionate (SPDP) and N-succinimidyl-4-(2-pyridyldithio)pentanoate (SPP) represented the best substrates for the glutathione reductive cleavage: subsequent liberation of sulfhydryl DM1, the actual therapeutic agent, free to inhibit microtubule formation and to induce apoptotic death in target cancer cells. [26] From the metabolic point of view, linker SPDP showed the fastest clearance, because of the absence of steric hindrance adjacently to the disulfide portion. Anyway, it was demonstrated that the most stable conjugates resulted trastuzumab-SMCC-DM1, non-reducible by glutathione, and trastuzumab-SSNPP-DM4, with three adjacent methyl groups, one on the antibody side and the other two on the payload side. [22] (Scheme 4) In particular, it was observed that in the former case DM1 was released in a non-relevant measure during 7 days, highlighting the high extracellular stability of the AMC and the subsequent increase in selective antitumor activity and reduction of cytotoxicity on healthy cells. [22] To validate this observation, several HER2 positive cell lines resistant to trastuzumab were treated with trastuzumab-SMCC-DM1, showing dose-dependent growth inhibition, with concurrent no response to non-conjugated trastuzumab. In contrast, normal cell lines exposed to trastuzumab-SMCC-DM1 showed minimum cell growth inhibition, evidencing the selectivity of action. [27]

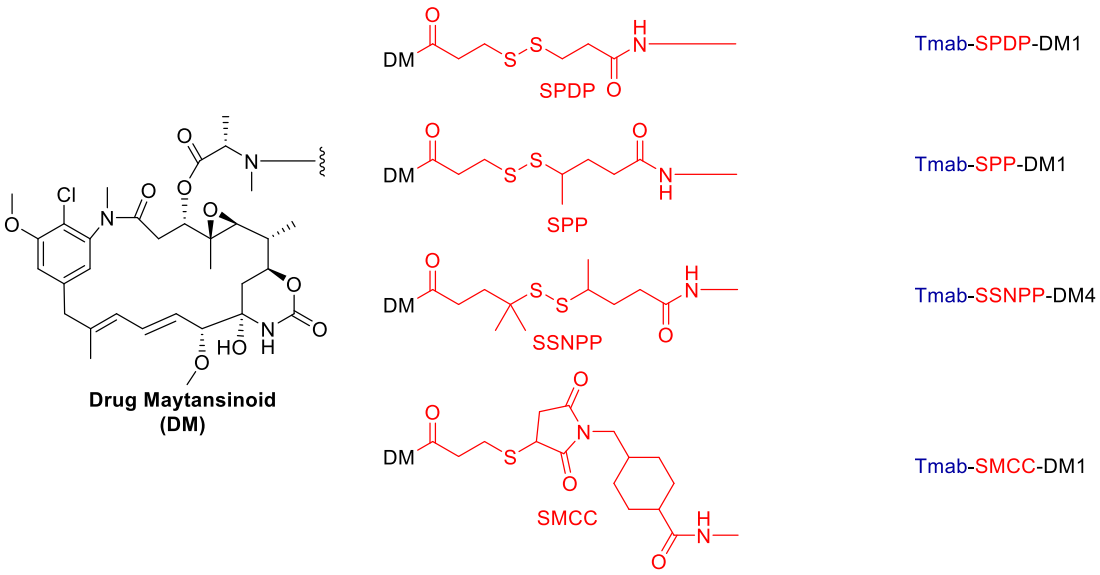

Scheme 4. Different linkers exploited to build AMCs. Hindrance next to the disulfide portion is responsible for the metabolic stability. SMCC shows a sulfide and, consequently, is not reducible

It was besides demonstrated that incubation with Ab-SMCC-DM1 resulted in a 5-fold more potency than administered free DM1, while monoclonal antibodies alone acted as cytostatic agents, so that they were capable to inhibit cell growth and proliferation, but without bringing to cell death. [28] These observations demonstrated that target cell death occurred due to the cytotoxic agent DM1 released within the cytoplasmic environment. [22]

In order to confirm that apoptosis depended on the activity of the conjugate, proteolytic cleavage of PARP was examined. Indeed, PARP cleavage to a 23 kDa fragment would have acted as an indicator of apoptotic cell death, observed to be released exclusively in tumoral cell lines treated with the conjugate. Mice treated with trastuzumab-SMCC-DM1 showed complete remission after 126 days; in contrast, initial tumor regression was observed after treatment with trastuzumab, followed by a re-growth after treatment cessation. Important to note, administration of the conjugate on already treated tumors resulted in further tumor decrease, indicating that no resistance occurred. [22] It was observed that an excess of unconjugated antibody prevented further complex-antigen interaction and that no internalization took place. [29] In fact, antigens represented the key to enter within the intracellular environment but, at the same time, the limitation for the interaction to occur when the concentration of the conjugate was too high.

1.5 AMC stability and metabolism

Several studies based on investigation about metabolic fate of SPP-linker-based conjugate administration clearly indicated DM1-lysine derivative **1** as highly present intracellularly. Its concentration, in fact, increased within 10 hours until, after 24 hours, when only DM1 was observed in the cytoplasmic compartment. [30,31] This observation showed that the metabolism of the SPP derivative brought at first to the lysine-derivative **1** and, then, to the disulfide reduction, with obtainment of DM1. (Scheme 5)

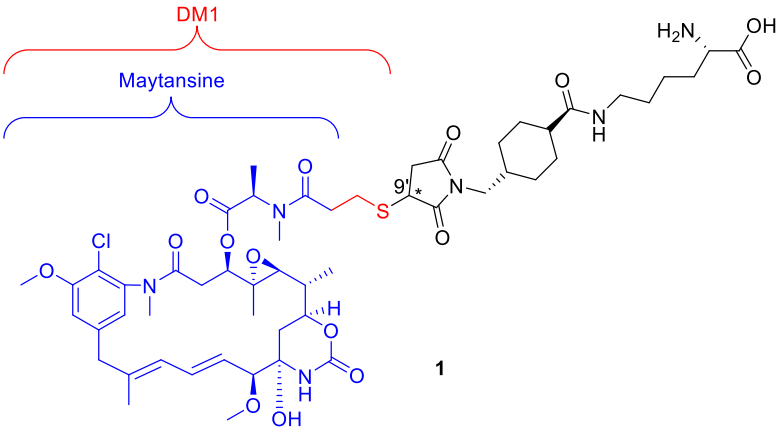

Scheme 5. Metabolic modification of Ab-SPP-DM1 to lysine derivative **1** and free DM1.

On the other hand, administration of SMCC-DM1 conjugate provided for the lysine derived metabolite **2**, stable even after 24 hours, because of the lack of the reducible disulfide group. [22] More in-depth studies about the cytotoxic activity of DM1, as conjugated, free or in form of lysine-derivative **2** demonstrated that their potency in inducing cell death by mitotic arrest were similar and that all of them exploited similar mechanisms of action. Same considerations were made for conjugated SPDB-DM4. The most abundant metabolite after 9 hours was identified as the cysteinyl-derivative **3**, due to a disulfide exchange, followed by the lysine-derivative **4** and S-methyl DM4, the latter due to the action of some S-methyl transferase. [22] (Scheme 6)

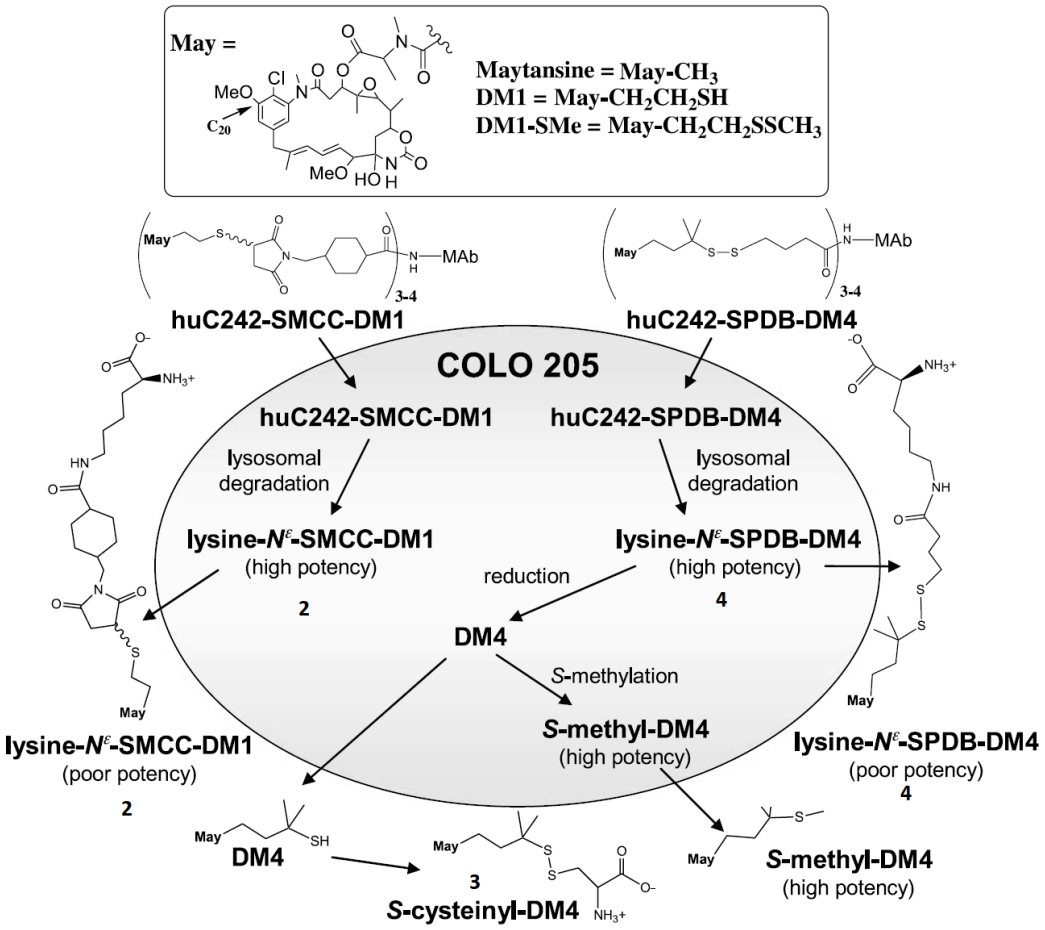

Scheme 6. Metabolic pathway for non-reducible SMCC-DM1 and disulfide SPDB-DM4. Both of them undergo lysine derivatization, but DM1 remains in form of **2** until further proteolytic degradation, while DM4 derivative **4** is reduced and methylated, to give S-methyl DM4.

All of these derivatives were considered to be within the cell at a steady-state concentration because of the saturation of the intracellular target. [26] Appreciable amount of DM4 was revealed after 26 hours, when most of the metabolites were cleaved by the reduction of the disulfide portion. [26] Characterization of the two most represented metabolites was performed, so that S-methyl DM4 and lysine-SMCC-DM1 **2** were synthesized and tested for their cytotoxicity against COLO 205 cells and Namalwa cells. [26] In particular, S-methyl DM4 was highly cytotoxic (in the picomolar range), about 50-fold more potent than lysine-SMCC-DM1 **2**, present in a positively charged form, so that its penetration towards the inner of the cell was highly inefficient, if compared to the lipophilic S-methyl DM4. The simultaneous presence of the lysine-derivative **2** (from uncleavable SMCC-DM1) and S-methyl DM4 (from cleavable

SPDB-DM4) showed that, once the target was reached, both of them had roughly the same potency. To confirm this consideration, the presence of protease inhibitors to impede the formation of both the metabolites resulted in no cytotoxic activity. Administration of DM4 isomer, with D-N-methyl-alanine moiety instead of the original L-form, was performed. Intracellular presence and potency were evaluated and it was evident that the lysine-, cysteine- and S-methyl derivatives of the D-isomer were not appreciably accumulated within the cells, due to the lower affinity of these metabolites towards the intracellular target and consequently effluxed to the extracellular compartment. [26]

1.6 Facing multidrug resistance (MDR)

Like several others cytotoxic agents, it was observed that maytansinoids could undergo multidrug resistance mediated by MDR1, a transporter able to delivery out of the cells the free payload, subsequently reducing its potency and its cytotoxic activity. [32] Given that MDR1 has more affinity towards hydrophobic substrates, Kovtun et al. focused their attention on the enhancement of the maytansinoids potency, by diminishing their affinity for MDR1. [32] To do that, it was hypothesized that a hydrophilic linker interposed between the antibody and the maytansinoid could be exploited, so that a tetraethyleneglycol (PEG_4) moiety was identified as a suitable candidate to be introduced. Administration of the new, more hydrophilic conjugate Ab-PEG_4-DM1 (Scheme 7) resulted in a better retention of the lysine metabolite of PEG_4-DM1, if compared to the lysine derivative from SMCC-DM1 **2**, to clearly indicate a less ability of the MDR1 transporter to efflux the metabolite. [32] The consequence of a better potency towards the target could be explained by several factors: the inhibition of MDR1 transporter by lysine-PEG_4-derivative; intrinsic higher potency than DM1 and its metabolites, so that less amount of lysine-PEG_4-DM1 was necessary to interact efficiently with the intracellular target; besides, this latter hypothesis was partially unreliable because of the same potency demonstrated by PEG_4 and non-PEG_4 metabolites of DM1 conjugates on MDR1-negative cells. Moreover, lysine-PEG_4-DM1 could have very low affinity towards the MDR1 transporter or could interact poorly with it. It was reported that only diffusion through the cellular double layer

favored the binding between the molecule and the transporter. [33,34] The higher hydrophilicity of lysine-PEG$_4$-DM1 could result in a worse diffusion and less like interaction with the protein, as it was proved by the reduced cytotoxicity of lysine-PEG$_4$-DM1 compared to lysine-SMCC-DM1 **2**, probably due to the impossibility to efficiently penetrate the cellular membrane.

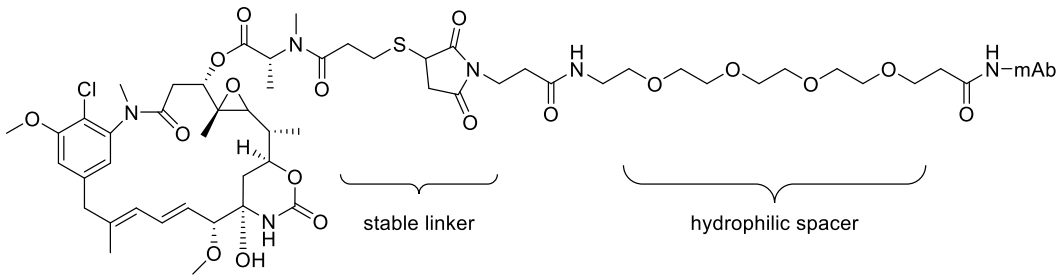

Scheme 7. Structure of hydrophilic DM1 conjugate in presence of PEG$_4$-linker.

1.7 AMCs and bystander effect

Another important factor that could influence the potency of maytansinoid conjugates and their antitumor efficacy consisted of the ability to kill cells within the nearest tumor surroundings, the so-called bystander effect. [35–37] More specifically, the conjugates were able to interact selectively with tumor cells expressing the antigen, so that internalization and degradation could take place. At this point, the possibility for the free payload to be effluxed out of the cell did not provide for a drawback, but rather for an advantage in this framework. In order to confirm this hypothesis, Kovtun et al. incubated COLO205 cells (antigen positive) or Namalwa cells (antigen negative) with conjugates huC242-DM1 (cleavable) or huC242-SMCC-DM1 (non-cleavable). [38] After 48 h, medium from the antigen positive cells showed a 3-fold decrease of the cleavable huC242-DM1 conjugate concentration, as well as a 4-fold increase in free maytansinoid presence; (Scheme 8A) same analysis performed on antigen negative Namalwa cells revealed exclusively the presence of the unmodified conjugate, to highlight that interaction with the specific antigen was necessary to allow the internalization and that disulfide reduction was needed for the liberation of the active payload. (Scheme 8B) Then, antigen negative Namalwa cells were incubated in the medium containing the free maytansinoid, demonstrating that non-selective cytotoxic

activity took place when exposed to the free antitumor agent, while no effect was evident after incubation with the medium containing the huC242-DM1 conjugate.

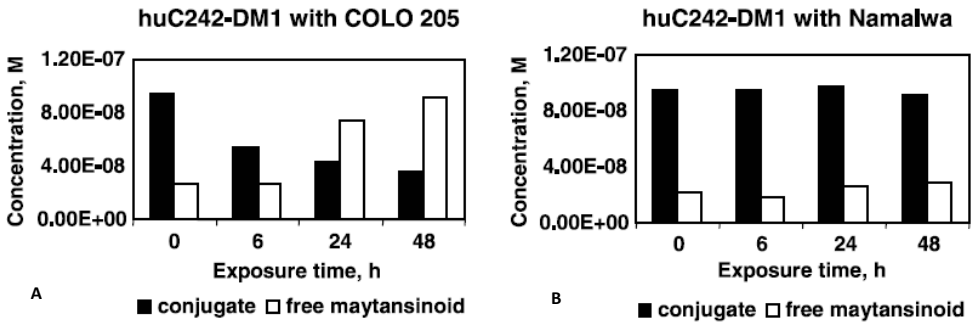

Scheme 8A. concentration of free DM1 depending on Ab-Ag mediated internalization and proteolysis. **8B**. Constant level of the conjugate highlight its stability on Ag negative substrates.

On the other hand, incubation of COLO205 and Namalwa cells with huC242-SMCC-DM1 afforded only a modest increase in unselective cytotoxicity, mostly depending on the lower potency (until 10000-fold less potent) of the metabolites deriving from huC242-SMCC-DM1 with respect to those from the disulfide reduction of huC242-DM1. When both of the cell types were present together within the same tumor formation, huC242-DM1 was able to reduce the tumor growth acting on both target and non-target cells through bystander effect, whereas huC242-SMCC-DM1 did not have efficacy, because of the lack of non-selective activity on antigen negative cells. It is clear that such an approach could negatively influence even healthy cells in the surroundings of the tumor localization. Nonetheless, this could be considered a minor drawback, thinking that only a few healthy cells in the intimate proximity would be involved. Moreover, damage to the tumor supporting tissues could be only considered as a positive factor in order to allow the complete eradication of the tumor.

1.8 Synthetic aspects of AMCs

Once it was clear that maytansine alone could have not been used in therapy due to its reduced therapeutic window, the attention was focused on some appropriate starting material for the synthesis of conjugated analogues. The most accessible precursor in this sense appeared to be ansamitocin P3 (**AP3**), a mixture of isopropyl and isobutyl ester at C(3). (Scheme 9)

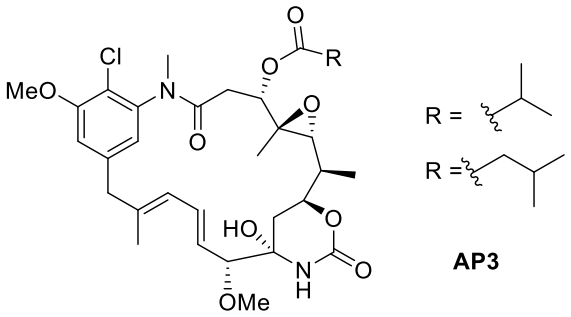

Scheme 9. Structure of ansamitocin P3 (AP3)

It was found to be easily collected as product of fermentation by *Actinosynnema pretiosum* and showed both antileukemic and antitumoral properties. [2,6] This biosynthetic pathway importantly enhanced the capability of production of such a key intermediate to the AMCs obtainment. In fact, hydrolysis of AP3, no matter of which kind of ester portion was present, afforded maytansinol **5**. [39] (Scheme 10)

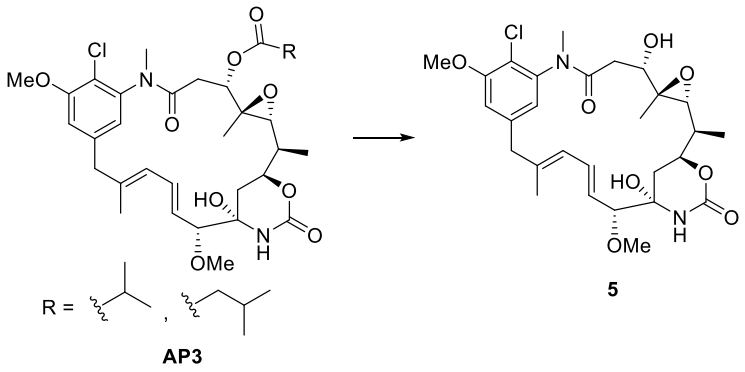

Scheme 10. Conversion from AP3 to maytansinol **5**

Maytansinol is a less potent cytotoxic agent than its precursor, but with a high potential as synthetic material, since the hydroxyl group at C(3) could be easily and variously functionalized. Due to the extensive presence of different orthogonal functional groups, maytansinol is achieved through reaction in very strictly controlled conditions. Traditional hydrolysis has to be avoided because of occurring of β-elimination at pH conditions above 9, with subsequent formation of α,β-unsaturated maysine **6**. [39] (Scheme 11)

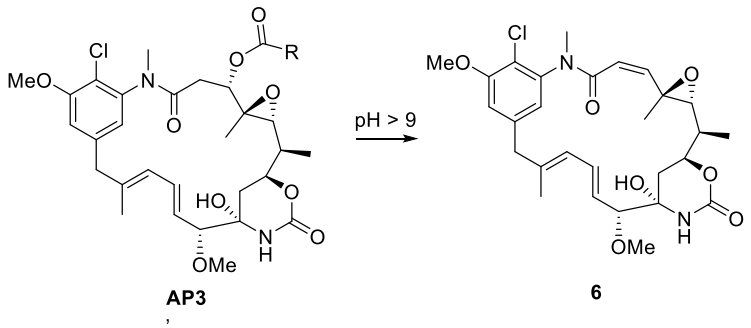

Scheme 11. Degradation of AP3 in alkaline conditions to maysine **6**

Initially, such a conversion was attempted by $LiAlH_4$ as the reducing agent, but with no satisfying results, given the very low yields and the presence of several byproducts. [39] Different reducing agents were furtherly tested (Red-Al®, DIBAL, $NaBH_4$), along with different types of esterases and lipases, but with the same disappointing results. Indeed, typical reaction conditions provided for a partially quenched reductant, lithium aluminum trimethoxy hydride, $LiAlH(OMe)_3$, prepared *in situ* at very low temperature (-45 to -35 °C), slowly added and let reacting with AP3 for no more than 5 hours at the same temperature.

Colder reaction environment resulted in a lot of residual starting material, whereas longer reaction time or temperatures higher than indicated had as a consequence the epoxide ring opening and the loss of integrity (and activity) of the desired derivative. When AP3 was treated with $LiAlH_4$, carbinolic OH was converted in the corresponding aluminum salt **7a**, so the addition of the hydride on the carbonyl ester afforded intermediate acetal **7b**. Treatment of the crude had to be performed at very low temperature (-40 °C) by adding water dropwise: in this way the pH would have raised until 12, so that the acetal bridge of **7b** (otherwise remarkably stable) could have been broken. Neutralization by formic acid and purification of the crude gave maytansinol **5**.

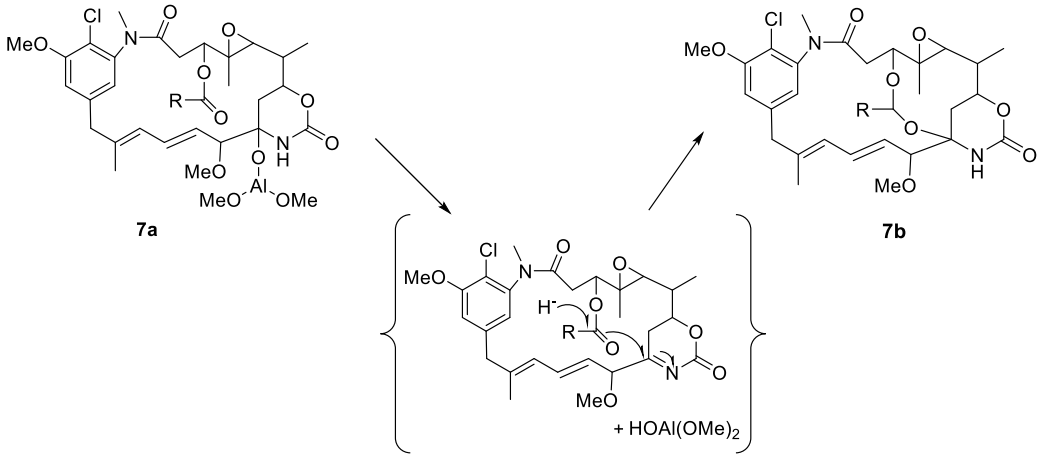

Scheme 12. Representation of mechanism from ester **7a** to the formation of acetal **7b**

Once in hand the free hydroxyl group of maytansinol, it was necessary to prepare the linker portion, able to connect the maytansinoid to the suitable residues on the antibody. [40] Different mercaptocarboxylic acids were considered, even if (for convenience) here only mercaptopropanoic acid **8** was reported. Reaction with S-methyl methanethiosulfonate **9** afforded the corresponding disulfide carboxylic acid **10**, ready to be activated as N-hydroxy succyinimidyl ester **11**. Coupling reaction with N-methyl-L-alanine, in presence of EDC, allowed the formation of enantiomerically pure L-alanyl derivative **12**. (Scheme 13)

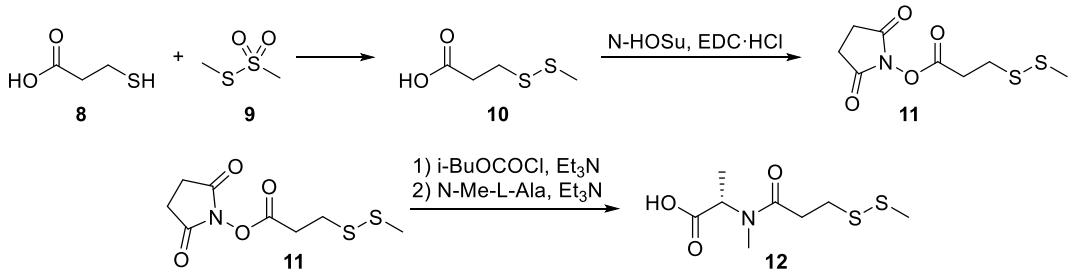

Scheme 13. Preparation of disulfide linker **12**, starting from 3-mercaptopropanoic **8**

The last step before bioconjugation with the antibody provided for the acylation of hydroxyl group on maytansinol **5** by carboxylic portion of L-alanine moiety **12**. This esterification reaction was performed in presence of DCC as coupling agent and zinc chloride as Lewis acid. At the end of the reaction, 10-20% of maytansinol was still present as unreacted, even after attempts using an excess of acid, DCC or Lewis acid. Use of $ZnCl_2$ was anyway justified by the fact that alkaline acyl transfer catalysts (such

as DMAP or Et_3N) would have not been compatible with the stability of the desired reaction product; besides, as Lewis acid, $ZnCl_2$ should have further activated the DCC-adduct towards nucleophilic attack by maytansinol hydroxyl group.

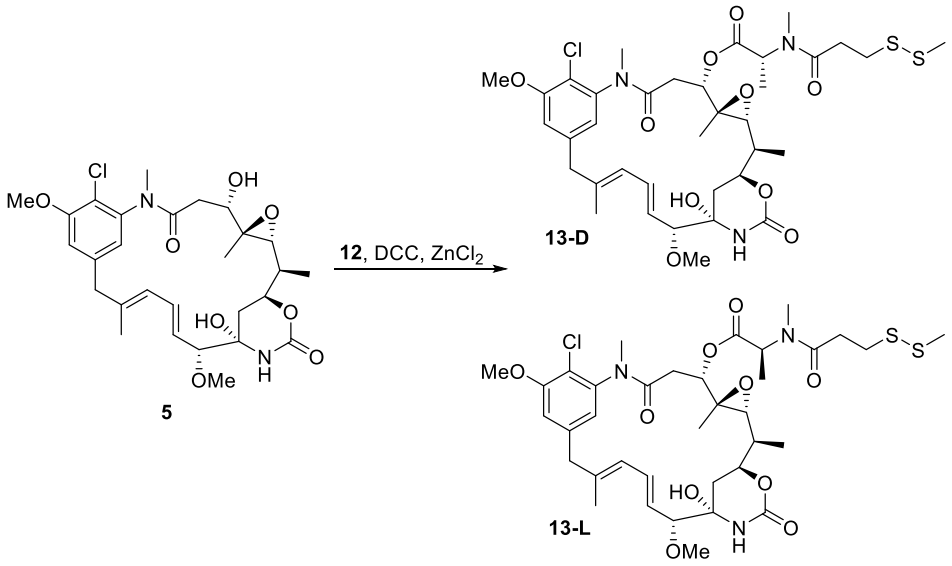

Scheme 14. Esterification reaction of maytansinol **5** in presence of acid **12** and DCC/$ZnCl_2$

The above described esterification resulted at the end in a diastereoisomeric mixture of D- and L-alanyl derivatives **13-D** and **13-L** (desired **DM1-SMe**), in almost 1:1 ratio, (Scheme 14) indicating that, in these conditions, epimerization on alanine moiety occurs. Esterification reaction of the hydroxyl group of **5** gave, as a consequence, a mixture of both the diastereoisomeric forms **13-D** and **13-L**. Preparation of adequate AMCs was then continued by reductive cleavage of the disulfide bridge. Due to the high sensitivity of maytansinoid derivatives towards alkaline environment conditions, corresponding thiols were achieved by treatment in neutral aqueous buffer with dithiothreitol (DTT). [40] DTT is indeed widely used in biochemistry to reduce disulfide bonds of oxidized cysteine residues.

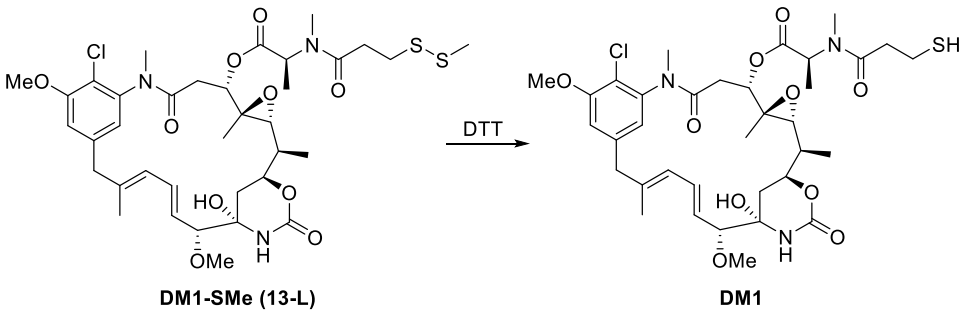

Scheme 15. Biochemical reduction of DM1-SMe in presence of DTT

However, purification of desired thiols was not very easy using HPLC chromatography in reverse phase columns, in presence of aqueous eluent mixture. In fact, oxidation to give dimeric maytansinoid **14** dramatically diminished the water solubility, so that a huge amount of **DM1** was not recovered. Only use of normal phase columns in presence of non-aqueous eluant allowed the obtainment of desired maytansinoid thiols.

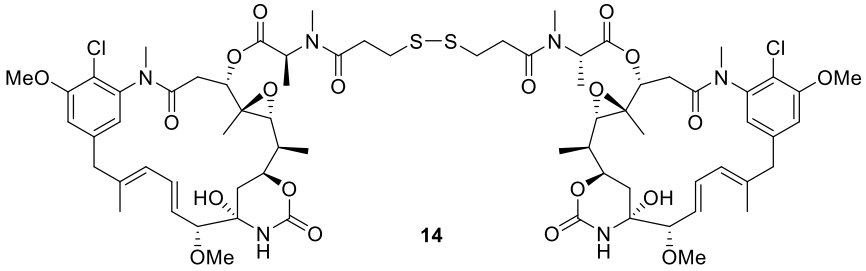

Scheme 16. Structure of disulfide dimer **14** from oxidation of **DM1**

Conjugation with antibodies was performed by two steps. In first place, the antibody was treated with N-hydroxy succyinimidyl disulfide derivatives **NHS-SPP** or **NHS-SPDB**, acting as the linkers, to give **Ab-SPP** and **Ab-SPDB**, respectively. (Scheme 17)

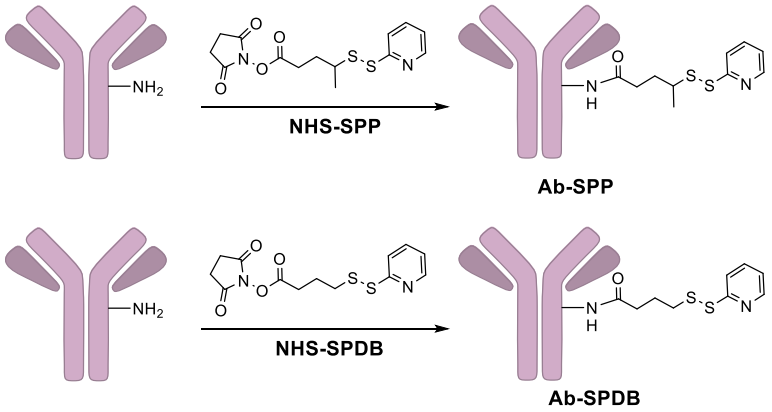

Scheme 17. Functionalization by SPP and SPDB linkers on the lysine residue of the antibodies

As the final result, 4-5 stable amidic bond were present per antibody together with the same amount of disulfide portion, bearing a pyridyldithio group. Disulfide exchange upon treatment with the appropriate thiol maytansinoid (**DM1** and **DM4** are here reported) resulted in the formation of a covalent disulfide bond between maytansinoid and linker attached to the antibody. In particular, conjugation of **DM1** with the antibody exploiting SPP spacer, allowed the obtainment of **Ab-SPP-DM1**, hindered by a methyl group on the antibody side of the disulfide portion. On the other hand, **DM4** was coupled to a non-hindered spacer (SPDB), with the resulting conjugate **Ab-SPDB-DM4** containing two hindered methyl groups on the payload side. (Scheme 18)

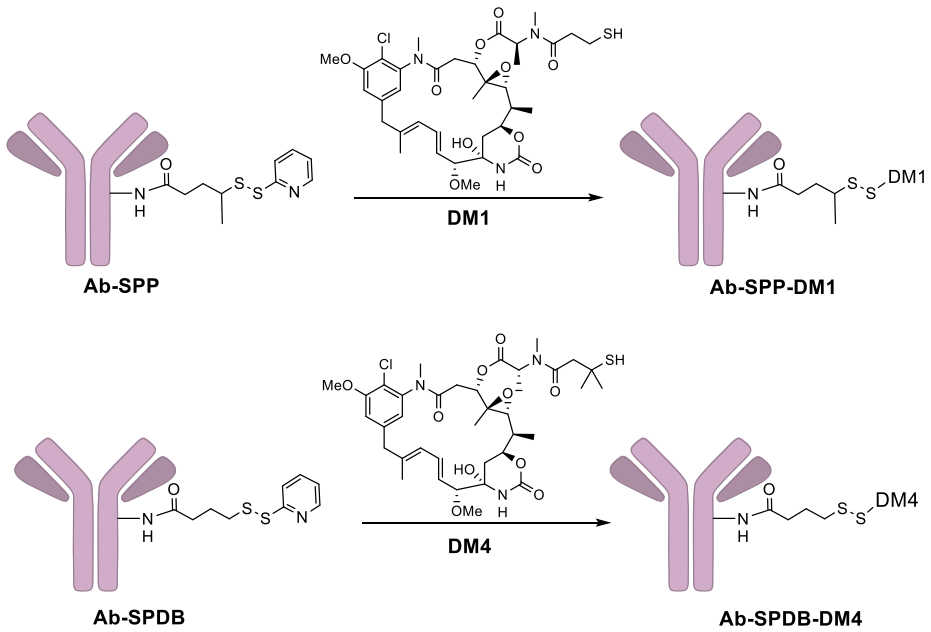

Scheme 18. Antibody conjugation of Ab-SPP with **DM1** and of Ab-SPDB with **DM4**

Though, differences from the steric point of view between the two **DM1** and **DM4** derivatives did not influence the degradation of the complex within the target cell, neither their cytotoxic activity. Anyway, after *in vitro* evaluation, it was confirmed the high selectivity of action of the conjugates towards cancerous cells, rather than healthy cells. [40]

2. Results and discussion

As it was previously reported, the best approach for the obtainment of biological active maytansinoid derivatives (such as **DM1** and **DM4**) provided for a well-regulated and in-depth described synthetic process. As a result, following the above synthetic protocol, ansamitocin P3 was selected as starting material, being commercially available as product of fermentation from *Actinosynnema pretiosum*. Thus, reductive hydrolysis was performed in order to obtain maytansinol, followed by functionalization with the adequate mercaptocarboxylic acid. Reductive modifications and bioconjugation on lysine or cysteine residues on the specific antibody provided, at the end, for the desired AMC.

Analyzing each of the steps needed for the preparation of the bioconjugate **Ab-SPP-DM1**, it was possible to hypothesize some variations and try to improve the previously described methodology.

2.1 Alternative reductive hydrolysis of AP3

As it was reported by Widdison et al., reductive hydrolysis was the best choice in order to maintain the integrity of any other functional group present on the ansamitocin scaffold than the ester moiety. [40] Several attempts have been done during the reactivity studies about the starting molecule, in order to understand if it was possible to achieve the same product maytansinol, overcoming the use of unstable and very moisture-sensitive reactants.

The first option that was considered in this sense was to use some aluminum hydride surrogate, more stable and less sensitive than $LiAlH(OMe)_3$. The tri *t*-butoxy analogue $LiAlH(Ot\text{-}Bu)_3$, in particular, was described as a white solid, commercially available, stable enough if handled and stored in dryers under inert gas. The presence of the *t*-butoxy substituents gave to the reactant an important steric hindrance, so that more energy would have been required to allow the reductive hydrolysis to happen. In fact, to better understand the possibility to use it on the target ester, $LiAlH(Ot\text{-}Bu)_3$ was added at -30 °C to a solution of **AP3** in THF and, then, left stirring from -30 °C to

room temperature within 8 hours. Monitoring by TLC analysis revealed only the presence of the starting material, with no formation of other spots, such the desired product or any other byproducts. The crude mixture was then left stirring overnight at room temperature, thinking thermodynamic conditions could have favored the reductive hydrolysis. Unfortunately, even after warming at 40 °C for other 8 hours, **AP3** resulted only partially affected by the hydride, indicating that probably the *t*-butoxy substituents were too bulky to allow efficiently the attack to the ansamitocin ester. Purification of the crude gave only modest yield of maytansinol **5** (16%), together with the residual unconverted starting material (66%). (Scheme 19)

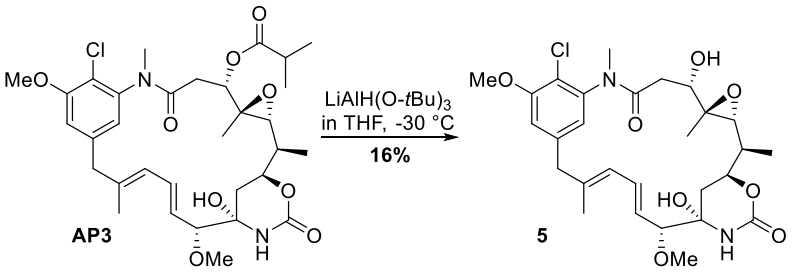

Scheme 19. Reductive hydrolysis of AP3 to 5 in presence of LiAlH(O-*t*Bu)$_3$

The reaction was repeated adding LiAlH(Ot-Bu)$_3$ at different temperatures and was conducted in presence of large excess of the hydride species. Unfortunately, none of these attempts gave better results than the conversion to maytansinol previously reported. This indicated that the relative stability of LiAlH(Ot-Bu)$_3$ was in contrast with the conditions required by the ester to be converted in alcohol: more harsh reaction conditions, useful for the hydride exertion, were not compatible with the integrity of the macrocyclic ansamitocin P3.

2.2 Transesterification approaches on AP3

Because of the degradation of the macrocyclic structure in alkaline environment (pH > 9), it was challenging to consider the application of some hydrolytic approach not affecting, in particular, the epoxide and the carbinolamide portions. However, it was hypothesized that obtainment of the desired secondary alcohol **5** could have been achieved by transesterification attempts, trying to switch the equilibrium towards the formation of a more stable ester than the isopropyl/isobutyl one present on **AP3** (for

convenience, only isobutyl ester will be represented in the following schemes in which **AP3** is reported).

Seebach et al. described in 1991 the transesterification in presence of catalytic amount of DBU and an excess of LiBr. [41] Due to the alkaline nature (though hindered) of DBU, the reaction was performed at very low temperature (-20 °C) and monitored every two hours for 8 hours. TLC and ESI-MS analysis revealed still the presence of starting material, along with degradation products, way less polar and with lower molecular weights than **AP3**. Attempting to force the transesterification conditions with longer reaction time and higher temperatures, it was only possible to observe by-products deriving from the complete degradation of **AP3**. (Scheme 20)

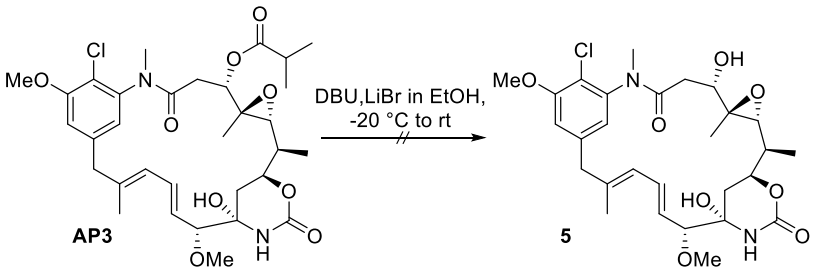

Scheme 20. Attempted transesterification following Seebach protocol

Crouch et al. worked on transesterification reactions using solid NaOH in heterogeneous environment, in presence of transfer phase catalysts. [42] In particular, tetrabutylammonium hydrogen sulfate (TBAH) was used in catalytic amount, with a large excess of NaOH (2-10 eq). In order to avoid immediate degradation of **AP3**, it was necessary to keep the reaction at very low temperature for a brief interval of time. Three attempts were made, with 10, 5 and 2 equivalents of NaOH, monitoring the reaction within 20 minutes at -40 °C, but none of them showed the formation of the desired product **5**. By TLC and ESI-MS analysis, it was possible to appreciate the complete disappearing of the starting material, along with degradation products such as those deriving from the epoxide and the cyclic carbamate opening. Even in heterogeneous conditions, it was once again demonstrated the instability of the ansamitocin system in alkaline environment. (Scheme 21)

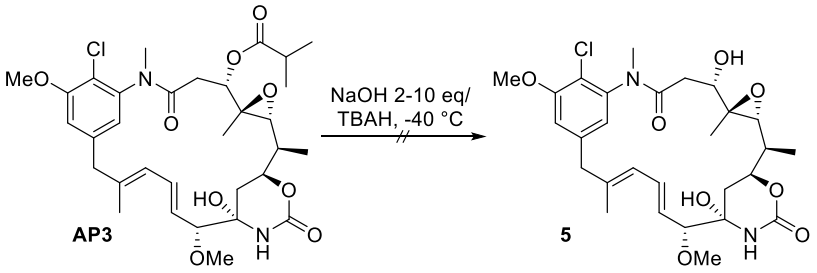

Scheme 21. Transesterification attempt on **AP3** in heterogeneous environment

Shinada et al. reported the application of transesterification protocol to macrocyclic compounds, in which several different functional groups were present. [43] Between the inorganic salts that were tried, K_2HPO_4 was demonstrated to be the most appropriate, due to the almost absence of side reactions, if compared to K_2CO_3, Na_2CO_3, $KHCO_3$ and $NaHCO_3$. In particular, use of catalytic amount (10 mol %) of K_2HPO_4 at reflux for several hours worked well for the complex amino acidic moiety they worked with. The reaction conditions were then commensurate to our substrate, so that the temperature was maintained between -20 °C and 25 °C. In such conditions, the starting material was recovered, without any sign of formation of other products. When the reaction was performed heating at 45 °C, **AP3** was entirely consumed within 1 hour, but only degradation products were found in the crude, with no trace of the desired secondary alcohol **5**. (Scheme 22)

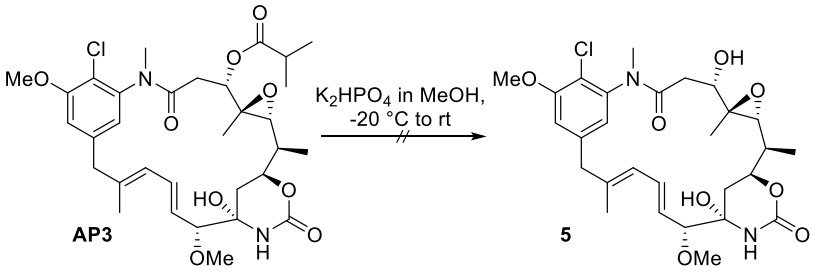

Scheme 22. Transesterification attempt on **AP3** in presence of bibasic potassium salt

Last attempt exploiting hydrolyzing agents potentially active on the proposed ester was based on the use of sodium methanethiolate (CH_3SNa). This organic base has been widely employed as potent nucleophile, able to easily displace various leaving groups in the context of substitution or addition reactions. Transesterification reaction, in this

sense, would have afforded the corresponding thioester **15**, together with the sodium salt of the alcoholate, as the deprotonated maytansinol **5**. Reaction was then performed in dry THF as the solvent, adding CH_3SNa to the stirring solution placed in a cooled bath at 0 °C. TLC monitoring after 40 minutes revealed the complete consuming of the starting ester, whereas many other spots were present at different R_f. It was hypothesized that the methanethiolate moiety was able to attack the most sensitive functional groups present upon **AP3**, so that opening of both the epoxide and cyclic carbamate happened. Probably, also the ester hydrolysis took place, but simultaneously to these above described undesired modifications. (Scheme 23)

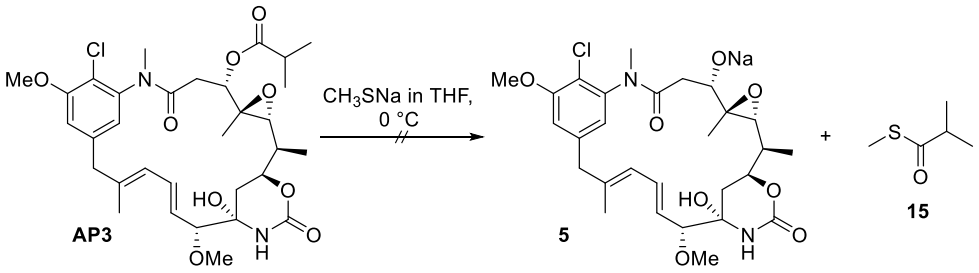

Scheme 23. Attempted transesterification of **AP3** with CH_3SNa

Having confirmed that transesterification attempts in presence of alkaline environment resulted always in degradation of the starting ester, due to the lability of the other functional groups present on the molecule, it was considered to perform some other approach exploiting other methods than Bronsted bases.

Nicolaou and Salomon described the mild transesterification of methyl esters in presence of trialkyltin hydroxide or bis(trialkyltin) oxide. [44,45] Tin derivatives, in this context, could act in fact as weak Lewis acids, allowing the activation of the ester carbonyl, that could be then converted to the corresponding acid; or as the nucleophile, able to attack the electrophilic center of the ester through the oxygen, allowing the formation of a tin carboxylate species, easily hydrolyzed to the desired acid. (Scheme 24)

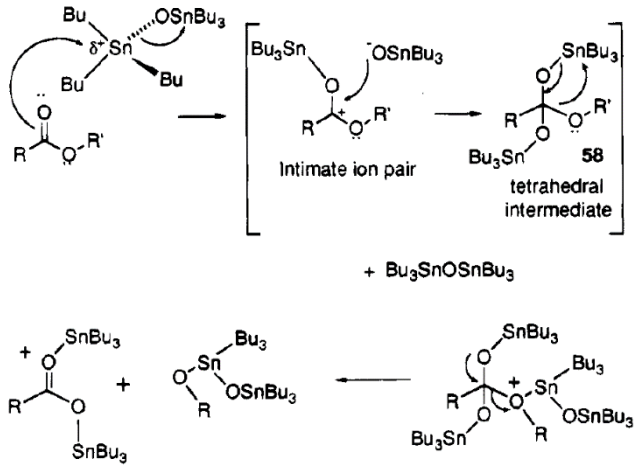

Scheme 24. $(Bu_3Sn)_2O$-catalyzed transesterification: proposed reaction mechanism [44]

Trying to transfer this protocol to **AP3**, the ester was treated with an excess (3 equivalents) of trimethyltin hydroxide (Me_3SnOH at room temperature and the reaction was monitored every 2 hours and carried out for 48 hours. Unfortunately, no product was detected, apart from starting material, indicating that the mix of isopropyl and isobutyl esters was probably very stable when exposed to these reaction conditions, if compared to the simple methyl ester. Same result occurred when 2 equivalents of bis tributyltin oxide $(Bu_3Sn)_2O$ were used on **AP3**, even when toluene was used instead of THF as the solvent and in presence of different reaction times and temperatures. (Scheme 25)

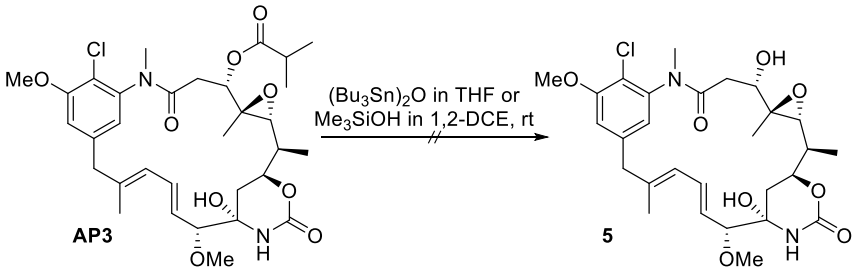

Scheme 25. Tin-based transesterification of **AP3** to obtain maytansinol **5**

Further efforts were made using titanium as a transition metal-based catalyst. Krasik reported that titanium catalyzed transesterification, mostly in presence of hindered alcohols and methyl and ethyl ester. [46] In order to apply the same protocol to the **AP3**, titanium ethoxide (10 mol%) was exploited. The reaction was performed twice, the first time in presence of methanol and the second time in presence of ethanol (maybe

more indicated since titanium ethoxide was used), both with toluene as the solvent. Unfortunately, also with following this protocol, after 48 hours, only starting material **AP3** was recovered, without any evidence of formation of products with different R_f by TLC analysis. Heating in microwave at 30, 40 and 60 °C for 10 minutes did not afford maytansinol **5**, but only degradation products. (Scheme 26)

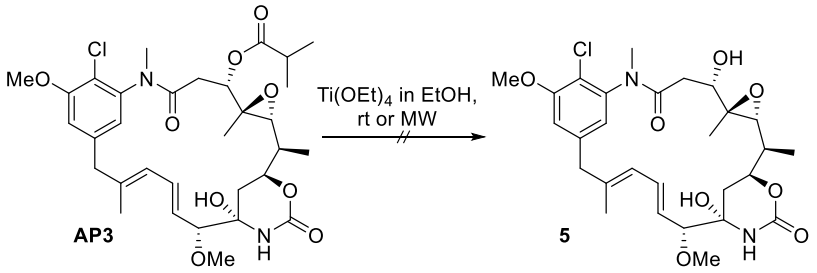

Scheme 26. Titanium-based transesterification of **AP3**, at rt or in microwave

Within the transesterification context, Grasa et al. reported the use of catalytic amount of N-Heterocyclic Carbenes (NHCs), mildly nucleophilic species able to allow the ester displacement. [47] In presence of another alcohol, it was favored the formation of the corresponding transesterified product, with the subsequent release of the alcoholic portion of the starting ester. NHCs mainly exploited in their work were iMes (imidazole-2-mesylitene) and Icy (imidazole-2-cyclohexylidene). (Scheme 27)

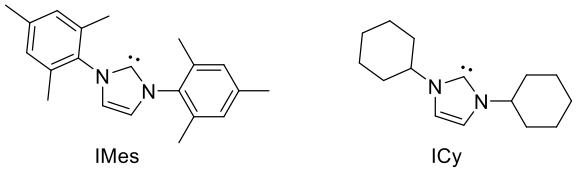

Scheme 27. IMes and Icy as N-heterocycle carbenes (NHCs)

Lai et al. performed some mechanistic studies, in order to propose plausible reaction mechanisms. [48] In particular, they hypothesized the deprotonation of the alcohol by the carbene, so that a tetrahedral intermediate **TI1** in equilibrium with **TI2** was formed, followed by dissociation and ester formation. (Scheme 28)

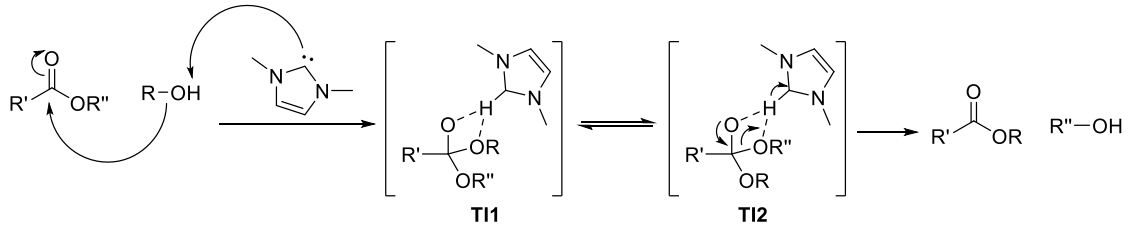

Scheme 28. Hypothesized mechanism of transesterification mediated by NHCs

Thinking that such kind of approach could be useful within the desired transesterification of AP3, IMes was used in catalytic amount (0.5 mol%), in dry THF as the solvent and in presence of a stoichiometric amount of dry methanol. Clearly, the reactive nature of the carbene needed for accurate control of the reaction conditions, since also a minimum quantity of moisture would have inactivated the NHC towards the transesterification purpose. Moreover, the crude was degassed before the addition of the catalyst, so to minimize the possibility of inactivation of IMes or undesired secondary reactions. Even with all of these precautions, after 96 hours and regular monitoring, only the starting material AP3 was present within the crude, indicating that IMes was not indicated for the transesterification of the hindered ester of AP3. It is also possible that handling of this NHC required even more attention in order to maintain its catalytic activity. (Scheme 28)

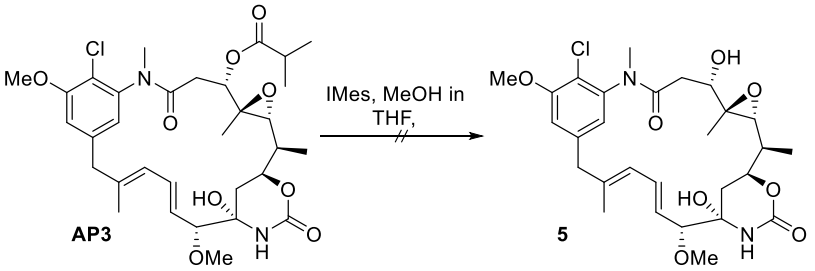

Scheme 28. Attempted NHC-based transesterification of **AP3** to maytansinol **5**

2.3 Optimizing the reductive hydrolysis conditions

Replication of the protocol providing for the use of $LiAlH(OMe)_3$ described from Widdison et al. was, then, the most obvious choice, although it did not represent the most reproducible and affordable way to generate the desired alcohol **5**. Because of the high sensitivity of the resultant species, produced *in situ* from $LiAlH_4$ and MeOH, even a minimum quantity of moisture and operative temperatures slightly higher than 15-20 °C resulted in the gelification of the solution. Besides, variations from the indicated interval of temperature between -40 and -45 °C during the dropwise addition were not tolerated: colder conditions would have not allowed the formation of the trimethoxy species, in favor of the more reactive dimethoxy one **$LiAlH_2(OMe)_2$**,

whereas warmer temperature would have accelerated the reaction rate, bringing to the formation of unreactive lithium tetramethoxide **LiAl(OMe)$_4$**. (Scheme 29)

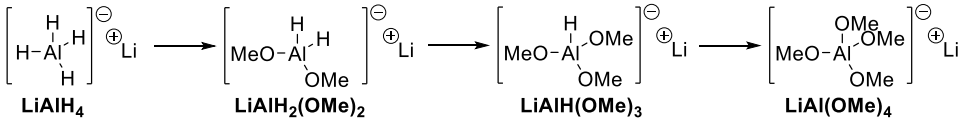

Scheme 29. Formation of methoxy derived species of $LiAlH_4$

Aside from these conditions, it would have been impossible to use the *in situ* prepared solution as the hydride source for the reductive hydrolysis of ansamitocin P3 ester, because of the physical impossibility to drop it by syringe addition. To minimize the probability for this to happen, it was very important to work with oven-dried Schlenk glassware, connected to an argon line, so that every trace of moisture was as much as possible far from the reaction environment. The addition was performed by not picking the solution up from the flask, but carefully cannulating it to the solution of ansamitocin at very low temperature, under argon pressure, while stirring both of the solutions. The low temperature was necessary because the reaction is highly endothermic, while a discharge needle was needed for the expulsion of the produced hydrogen gas. Important to note, the pressure of the gas introduced in the mother flask ($LiAlH(OMe)_3$ solution) was regulated so that one drop would have been added per second. Slower rate addition was not necessary, while faster addition would have resulted in the formation of a viscous solution, impossible to be adequately stirred. In such cases, after 6 hours at -35 °C, only unreacted ester was present within the crude. Furthermore, work-up of the resulting mixture represented another key step towards the obtainment of desired maytansinol. It was reported how addition of water at -25 °C was essential, followed, after 30 minutes at the same temperature, by formic acid and dilution with ethyl acetate. This procedure was recommended because of the formation of an acetal intermediate, that took place between the ester portion and the carbinolamide carbon (see scheme 12). Water addition, in fact, was necessarily performed at low temperatures because of the pH rising. In this way, the acetal moiety would be broken, but, at the same time, the stability of maytansinol would be preserved from the presence of basic conditions. Neutralization of the alkaline environment by formic acid dropping, dilution and filtration of the aluminum salts gave a crude mixture

containing the desired secondary alcohol **5** as the main product (not very reproducible yield, from 22% to 91%). (Scheme 30)

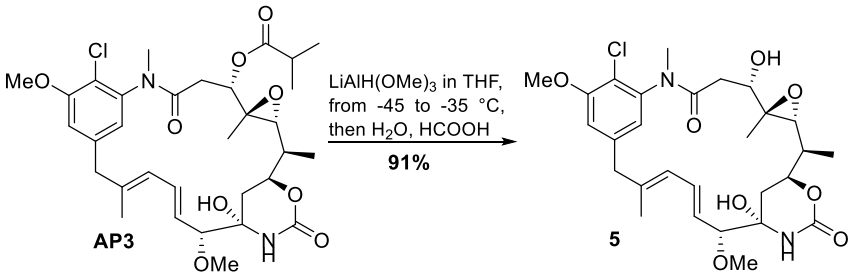

Scheme 30. Reductive hydrolysis of **AP3** to maytansinol **5** in optimized conditions

On the contrary, water dropping at higher temperatures than those here reported, resulted in a yellow bubbling solution, consisting of almost exclusively the acetal **7b**, described as highly stable in neutral conditions. [24] Still, when water was added at lower temperature or higher addition rate, the droplets tended to freeze and to increase the solution density, so that stirring became difficult and was hard for the acetal to be cleaved. Subsequent formic acid addition resulted in the fixation of the structure of previously reported acetal **7b**. (Scheme 12)

2.4 A feasible and safer alternative to cannulation

In this context, it seemed important to find some alternative approaches for the synthesis of maytansinol **5**, starting from **AP3**. The low reproducibility of the reaction derived from the very strict conditions that were required for the conversion to take place. Then, it was highly desirable to perform the reductive hydrolysis within a confined reaction environment, as much as possible avoiding the use of moisture-sensitive reactants or in presence very strictly dry and inert conditions.

Together with these aspects, one of the most important consideration to do when working with maytansinoids was their very high cytotoxic activity. As a consequence, there were safety protocols to be followed, in order to avoid any potential contact between the operators and the substance, as it was or in any kind of derivative forms. In laboratory scale, this was quite easy to be put in practice, paying attention to the basic rules of a chemistry lab (double gloves, specific lab coat for cytotoxic reactions,

specific laboratory equipment available only for cytotoxic agents handling). Besides, ansamitocin P3 and their derivatives showed an activity in the picomolar range (10^{-12} M), so that any adventitious interaction could result in some acute toxic effects for the operator. The possibility to isolate the reaction environment, in this sense, was considered as desirable from both safety and synthetic point of views. It was hypothesized that the best way to act in this direction was to confine the reactants in a close system, far from the technician and from sources of instability (atmospheric moisture, oxygen).

In fact, traditional setting of the reaction in batch was characterized by an elevated possibility of exposure to the cytotoxic agent, from the weighting to the dissolution to the work-up procedure. It was considered, then, to perform this kind of reaction greatly reducing the risk for the operator, confining the solution within tubes, that would have acted as the reaction vessel. Moreover, *in situ* preparation of the trimethoxy aluminum hydride species and its high moisture sensitivity, would have resulted in a more complicated system to be set up. Higher stability and commercial availability let allow to prefer, in this framework, the use of $LiAlH_4$ solution (1.0 M in THF). Exploiting the collaboration with the group of professor Vaccaro (University of Perugia), it was possible to develop a *continuous flow system* made up by two different syringe-pumps, connected to PTFE tube, ultimately flowing into a sealed flask, that acted as the quenching vessel. (Scheme 31)

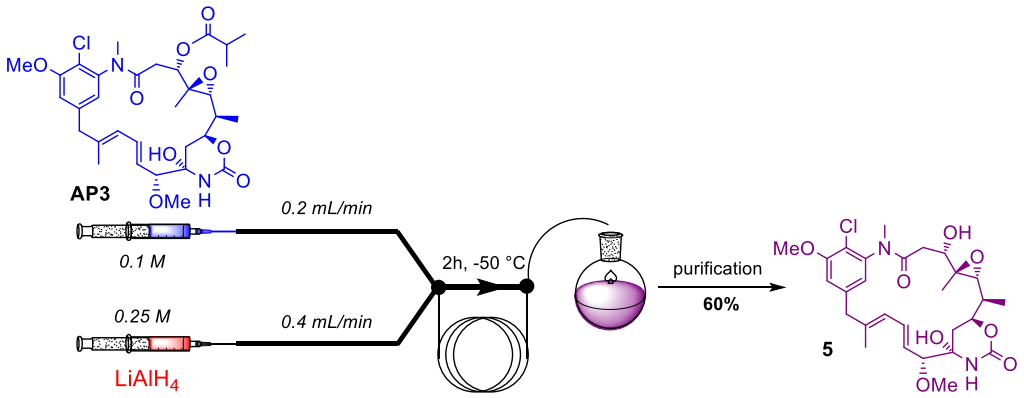

Scheme 31. Setting of the system for the application of continuous flow to reductive hydrolysis of AP3

More specifically, the reaction was conducted filling one syringe with **AP3** in THF (1 eq) and the other one with $LiAlH_4$ in THF (5 eq). The flow of the ansamitocin P3 solution was set to 0.2 mL/min, while that one of the $LiAlH_4$ solution was 0.4 mL/min. When the two solutions joined up, the temperature was set to -50 °C, low enough to control the reaction rate and the exothermicity and far more favorable in terms of cooling homogeneity, since PTFE tubes were less thick than any flask wall. After 2 hours, the reaction mixture was collected in a round bottom flask submerged itself in the cool bath, to which a vent was applied, in order to allow H_2 to escape and pumps not to be locked. Quenching of the collected solution by adding water, HCOOH and AcOEt, allowed to obtain a suspension which was filtered; the filtrate was then purified by flash chromatography, to give pure maytansinol **5** with a 60% yield. In order to better evaluate if this new reported approach for the reductive hydrolysis of **AP3** in continuous flow conditions was valid, the same $LiAlH_4$ solution in THF was exploited as the reducing agent, but conducting the reaction in traditional way. $LiAlH_4$ was then dropwise added to the solution of **AP3** in dry THF, always at -50 °C. Monitoring after 2 hours revealed no detectable products by TLC analysis, so that the quenching was performed after 6 hours. Purification of the deriving crude by chromatography afforded maytansinol **5** in 18% yield, together with at least other 3 byproducts, probably due to the reactivity of $LiAlH_4$ towards the several functional groups on **AP3**. Here is shown the TLC comparison between the chromatographed crude from continuous flow (Figure 4A) and the one from traditional batch reaction (Figure 4B).

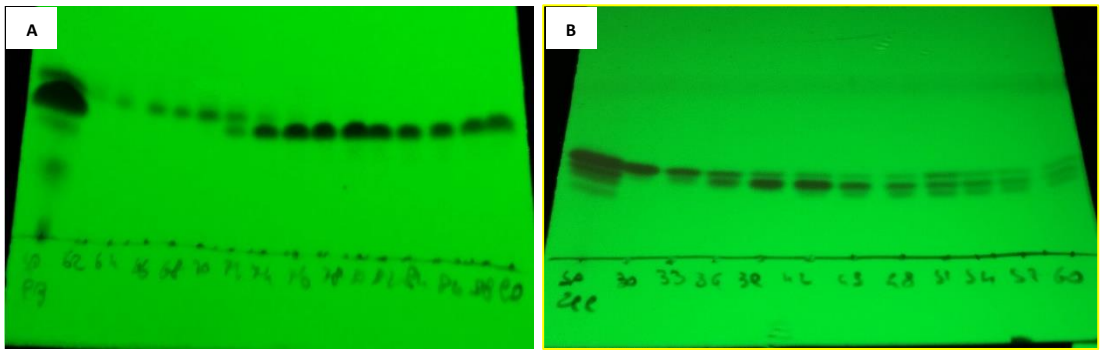

Figure 4A. TLC of the chromatographed crude from continuous flow reaction; **4B**. TLC of the crude from the traditional protocol reaction.

When the reaction where performed at -60 °C no better yields for the desired alcohol **5** were obtained (14%). Moreover, one attempt was performed at -70 °C, affording nothing more than the starting material, probably due to the slowed down reaction rate. Performing the same reaction for the last time, 12-crown-4 was added to the reaction environment, so that lithium cations within the reaction environment could have been sequestered. In fact, it was hypothesized that lithium ions could act oxyphilic coordinating agents, able to activate the epoxide and the carbinolamide portions towards the nucleophilic attack by the hydride source. Keeping lithium isolated from the ansamitocin P3 structure, it could have been possible to avoid certain secondary reactions by $LiAlH_4$. **AP3** was then treated with the reducing agent, in presence of the crown ether, at -50 °C and left stirring for 3 hours, until the temperature was raised to -15 °C. Usual work-up and flash chromatography afforded maytansinol **5** in superimposable yields (15%) and containing the same byproducts, if compared to those obtained without the crown ether, indicating that its use did not have significant role in decreasing side reactions on this molecule.

2.5 Replication of already reported synthesis of DM1-SMe

Once the maytansinol was isolated in sufficient amount, it was possible to proceed with the preparation of **DM1-SMe**, reproducing what was already described by Widdison et al., so to prepare some standard samples ready to be exploited for future analysis (HPLC, TLC, NMR). To do this, methyl disulfide linker **12** was prepared, by make reacting 3-mercaptopropanoic acid **8** and S-methyl-methanethiosulfonate to afford disulfide acid **10**. Activation in presence of isobutyl chloroformate was followed by the coupling reaction with N-methyl-L-alanine, providing for desired compound **12**. (Scheme 32)

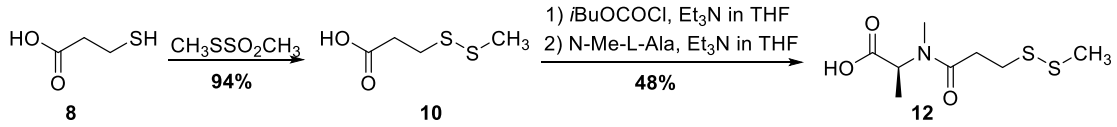

Scheme 32. Preparation of acid sulfide linker **12**

Final esterification reaction between maytansinol **5** and acid **12** afforded a diastereoisomeric mixture of L-aminoacyl and D-aminoacyl esters, separated by preparative TLC, to afford **13-L** (**DM1-SMe**) in very low yield (4%). (Scheme 33)

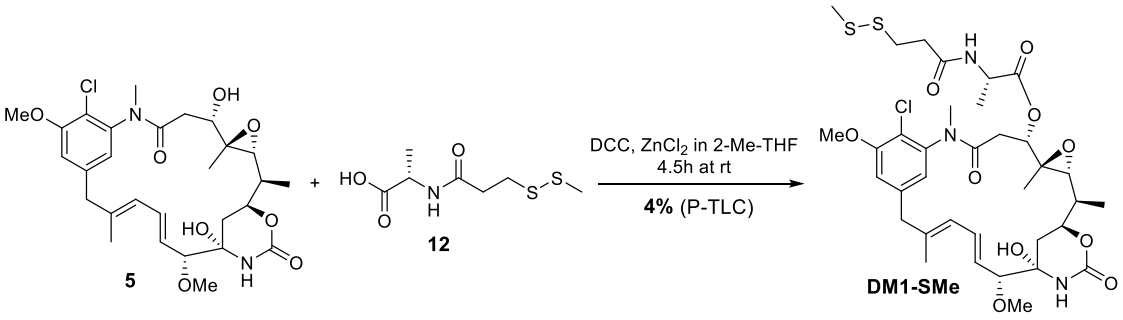

Scheme 33. Esterification of maytansinol **5** in presence of acid linker **12** to afford **DM1-SMe**

With the reference sample in hand, it was attempted to prepare **DM1-SMe** starting from maytansinol **5**, but passing through the formation of the deacetyl-maytansine moiety **16**. The final amide coupling with the disulfide acid **10** would have afforded **DM1-SMe**. At first, the amino acidic portion derived from N-methyl-L-alanine was prepared exploiting the approach developed by Leuch. (Scheme 34)

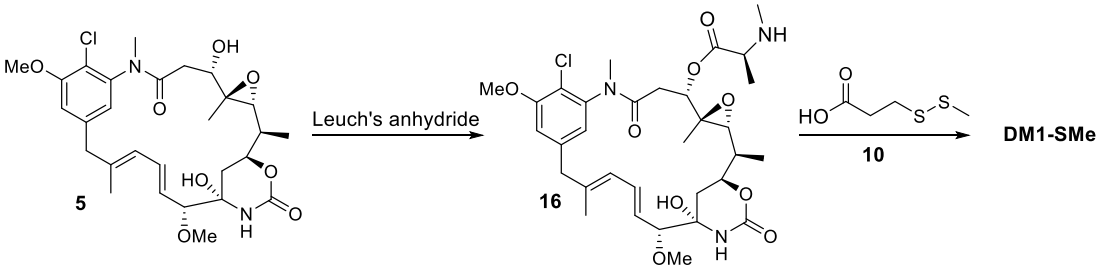

Scheme 34. Proposed approach for the synthesis of **DM1-SMe** by Leuch's anhydride

Originally, Leuch's anhydrides were used as a suitable approach for peptide couplings, avoiding any kind of protection on the aminic portion of the corresponding amino acid **L-AA**. [49] To do this, phosgene (or triphosgene) was employed, so to allow, under heating, the cyclization and the formation of a 5-membered ring, in form of cyclic anhydride **L-NCA** (N-carboxyanhydride, NCA), showing an amidic portion on one side of the reactant. (Scheme 35)

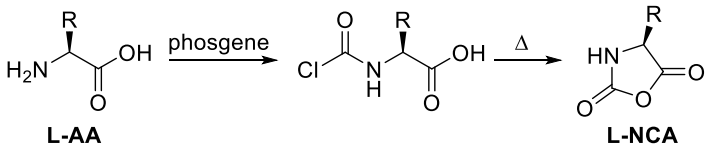

Scheme 35. Preparation of N-carboxyanhydride **L-NCA**, starting from amino acid **L-AA**

Although this approach was very advantageous in terms of coupling reaction yields, it was evident that the use of phosgene to induce the cyclization to NCAs implicates high toxicity issues. Akssira et al. [49] reported in their work an alternative way for the formation of NCAs, exploiting the presence of the *t*-butoxycarbonyl group on the aminic portion, though avoiding phosgene as the cyclization promoter, while using PCl_3 as chlorinating agent. Starting from these observations, L-alanine was protected in form of **Boc-L-ala** and methylated, to afford Boc-N-methyl-L-alanine **17**. Treatment with PCl_3 afforded, after 3 hours at 0 °C the desired Leuch's anhydride **18**, used without any further purification for the next coupling reaction. (Scheme 36)

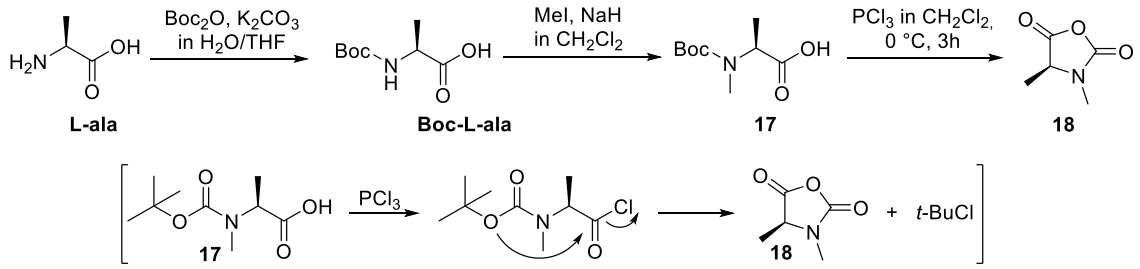

Scheme 36. Conversion of L-ala in NCA **18**

Maytansinol **5** was, then, dissolved in a 3:1 THF/DMF mixture and to the resulting solution $Zn(OTf)_2$ was added in one portion, followed by DIPEA and NCA **18**. After 48 hours at room temperature, the solvents were evaporated at reduced pressure and the crude was purified by chromatography. Desired product deacetyl-maytansine **16** was obtained in 26% yield as the desired diastereoisomer, with an 87% diastereoisomeric excess, highlighting the great advantage of this kind of approach, that was the reduced ratio of racemization during the coupling reaction in accordance with what was described Carrozzella et al. in their patent. [50] (Schema 37)

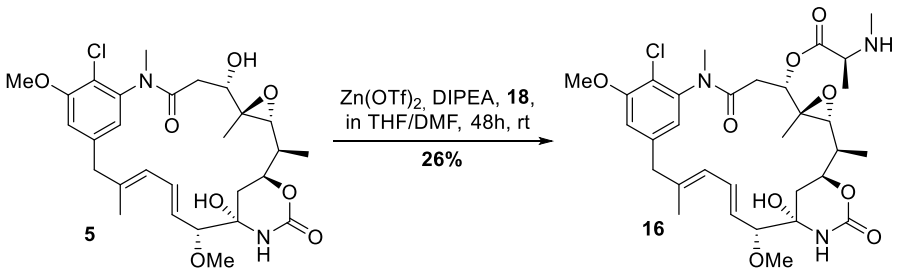

Schema 37. Esterification of maytansinol **5** performed in presence of NCA **18**

2.6 Diastereoselective synthesis attempts on model compound

All of the described methodologies reported here above were made in order to prepare the desired DM1-SMe following well established pathways. Since to date (and to our knowledge) nothing more than this was exploited for the preparation of DM1-SMe, in collaboration with Indena S.p.a., several non-infringing processes were designed. It was necessary to perform an in-depth review of all of the patented and published methodologies about maytansinoids and their chemical behavior, the allowed functionalizations and the convenience of using different approaches from what has been described until now. In this context, of course the stereoconvergent synthesis of DM1-SMe was appealing, considering that it could have been possible to provide for an important cytotoxic agent with the objective of lowering costs, enhancing yields and affording the desired product with complete stereoselectivity.

In principle, because of cost efficiency reasons, it was necessary to perform several attempts on model molecules, so to analyze the behavior of enantiomerically pure starting material towards the different reaction conditions. L-menthol was chosen as the model compound, given that it is an enantiomerically pure secondary alcohol, similarly to maytansinol **5**, but characterized by high stability, even if exposed to harsh conditions, and commercial availability.

In order to comprehend the stereochemistry around the already reported reaction, but on simpler substrates, enantiomerically pure acid disulfide **12** was esterified by optically pure L-(-)-menthol, in presence of DCC and $ZnCl_2$, as described by Widdison

et al. in their protocol. As expected, even using an enantiomerically pure alcohol, the esterification provided for the formation of a diastereoisomeric mixture of **19-D** and **19-L** in 1:1 ratio, same that happened when acid **12$_{rac}$** was employed (HPLC analysis), indicating that racemization takes place at this stage at alanine stereocenter. (Scheme 38)

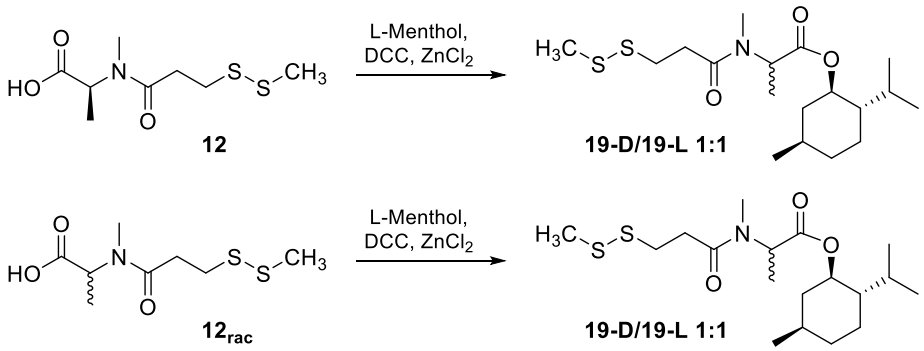

Scheme 38. Comparison between L-menthol esterification performed with acid **12**

Due to the activation by DCC as coupling agent, it was hypothesized that replacing it with some other activated ester, it was possible to increase the diastereoselectivity towards the desired L-aminoacyl product **19-L**. For this purpose, disulfide acid **12** was activated as pentafluorophenol ester **20**, more reactive and maybe more prone to give **19-L** in diastereoselective fashion. Surprisingly, esterification reaction with pentafluorophenol afforded the activated ester **20** in only 30% yield (obtained in the best case). Further coupling of **20** with L-menthol was performed both in presence and without DCC, in presence of $ZnCl_2$ as the Lewis acid or DIPEA as accelerating rate catalyst. Unfortunately, none of these attempts allowed to isolate the desired product **19-L**, neither its diastereoisomer, but only the unexpectedly stable PFP-ester **20**. (Scheme 39)

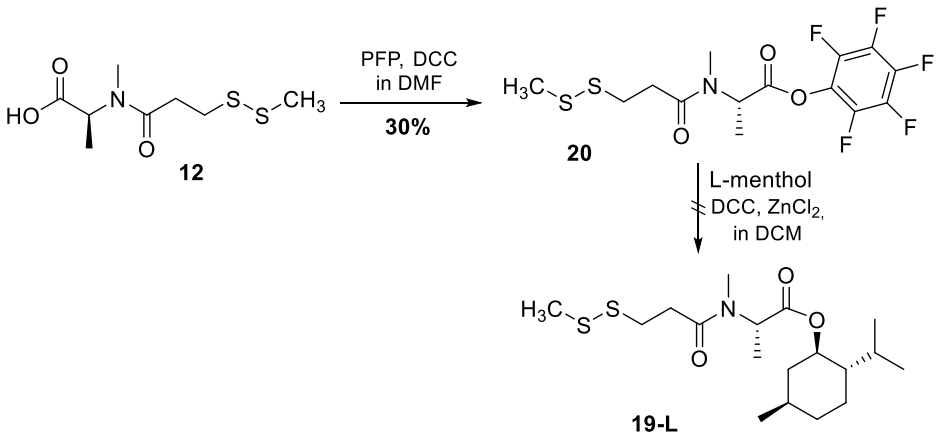

Scheme 39. Attempt of activation of **12** as PFP-ester **20** and subsequent coupling with L-menthol

Searching for some diastereoselective method for the activation of disulfide acid **12**, it was inspiring the publication from Dev and co-workers. [51] They reported the preparation and use as activating agent of ethyl-2-cyano-2-(2-nitrobenzenesulfonyloxyimino) acetate, o-NosylOXY, as valid and cheaper alternative to other toxic or expensive coupling reagents for the preparation of amides and ester, with complete retention of configuration and stereoselectivity. *o*-NosylOXY was prepared starting from *o*-nitrobenzenesulfonyl chloride and ethyl cyanohydroxyiminoacetate (commercially available as OXYMA), in presence of DIPEA. In the optimized conditions, it was reported that no racemization occurred performing peptide couplings, with even better results than with HBTU or HATU (comparable yields, but showing 5.9% and 1.6% of racemization, respectively). Disulfide acid **12** was treated in presence of *o*-NosylOXY and DIPEA with L-menthol and the reaction was left stirring for 16 hours at room temperature. Despite the great outcomes that were described within the article, it was not possible, even after several attempts at different temperatures and in different reaction times, to recover other than the starting acid **12**, with no trace of desired diastereoisomerically pure **19-L**. (Scheme 40)

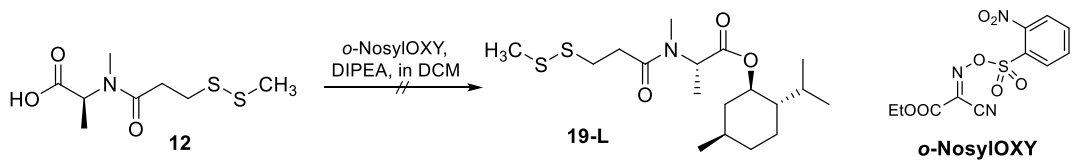

Scheme 40. One-pot attempt to obtain optically pure **19-L** from acid **12**, exploiting *o*-NosylOXY

Trying to explore some other non-infringing method exploiting the functionalization of the aminic group, it was found that *nitrophenyl sulfenyl* (Nps) group could have been a suitable protection. Even if its application was not very exploited due to the low stability to oxidative conditions (even from the atmospheric oxygen), Nps functionalization was described as a protecting group able to favor the peptidic coupling in stereoselective manner. In order to obtain optically pure esterification product **19-L**, N-methyl-L-alanine was treated under argon with *o*-nitrophenyl sulfenyl chloride, in presence of triethylamine for 16 hours. Chromatographic purification of the crude allowed to obtain protected amino acid **22** with a 98% yield, so that esterification with L-menthol could be performed, in presence of the standard reaction conditions (DCC, $ZnCl_2$). After 16 hours, the crude was purified by chromatography affording still a complex mixture of products in which it was possible to identify (ESI-MS, NMR) the presence of the aminoester **23**. Complete deprotection was not afforded following what was described by Zervas et al.; [52] instead, it was possible to obtain the free secondary amine **24** (21% yield in two steps) by pyridine addition (1 equivalent), followed by HCl 37% (1 equivalent) at 0 °C, then stirring for 24 hours at room temperature. (Scheme 41)

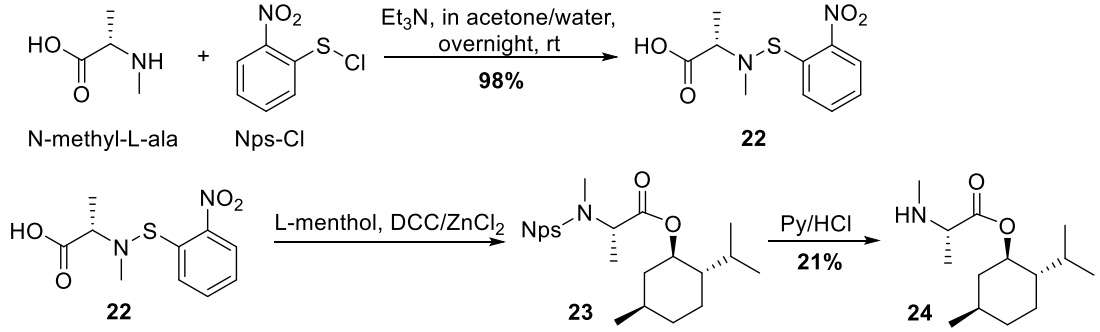

Scheme 41. Protection of N-methyl-L-alanine with Nps-Cl and subsequent esterification with L-menthol and deprotection

In order to verify the reproducibility of the reaction also on the macrocyclic substrate, Nps-protected N-methyl-L-alanine **22** was added to the solution of maytansinol in dry dichloromethane, in presence of DCC and $ZnCl_2$. Given that no conversion of the starting alcohol **5** was observed, the reaction was repeated using 2, 4 and 7 equivalents of the protected amino acid **22**, in presence of $Zn(OTf)_2$ instead of $ZnCl_2$ and

performed at room temperature or 45 °C, for 16 hours until 48 hours. Unfortunately, from all of these crude mixtures it was possible only to recover almost entirely pure maytansinol **5** (87-91%), indicating that, probably, these reaction conditions do not fit what is required by maytansinol to allow the esterification with acid **22**.

2.7 Key fragment design and application

Another interesting alternative was evaluated in order to diastereoselectively obtain **DM1-SMe**, but without involving any protecting group, though maintaining the most important features: to be a non-infringing method and to not be prone to racemization. From the retrosynthetic point of view, it is possible to disconnect DM1-SMe at the level of ester and amidic portions. The key fragment in this context was the amino acidic one, able to esterify maytansinol **5** and to give peptidic bond with the disulfide acid moiety **10**. (Scheme 42)

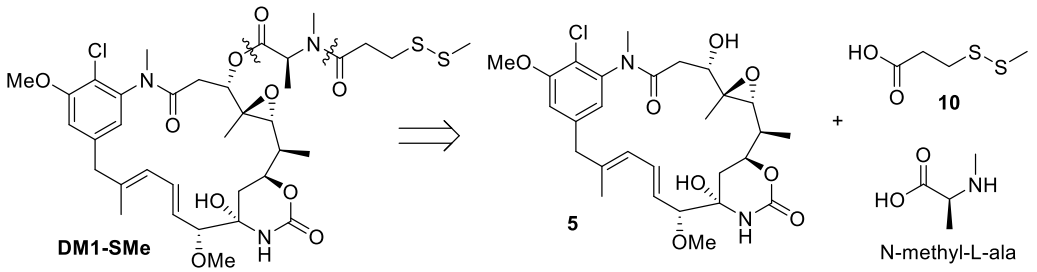

Scheme 42. Retrosynthetic analysis of **DM1-SMe**

It is evident that amino group could be obtained by reduction of the cyanide group, rearrangement of the amidic group or reduction of the azido group, among the most important methodologies. Considering that the portion of interest is an α-substituted C-2 fragment, cyanoformic acid **25** could not be useful, because of its low stability and difficult commercial affordability, together with the necessity of introduction in stereoselective manner in α-position prior to the cyano reduction; malonamic acid **26** could be easily, but not stereoselectively, substituted in α-position, though Hoffmann rearrangement would require harsh conditions, not tolerable by the maytansinoid scaffold; finally, azido alanine **27** could be easily afforded with stereochemistry retention and with no tendency to give racemization, thanks to the weak electron-donating nature of the azido group. (Scheme 43)

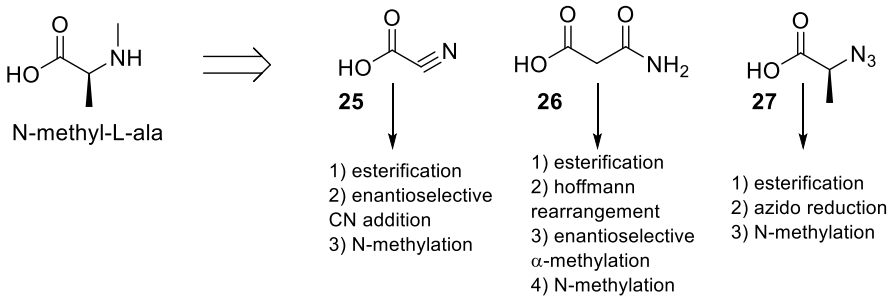

Scheme 43. Retrosynthetic analysis of N-methyl-L-alanine

Starting from the scaffold of L-alanine, Borger and Stick reported a simple and stereoselective methodology suitable for diazotransfer reactions. [53] To do that, it was necessary to prepare the diazotransfer reagent, imidazole-1-sulfonylazide **28**, obtained by reaction at 0 °C between sulfuryl chloride and sodium azide in acetonitrile, followed after 16 hours by the addition of imidazole. Treatment of the crude with ethanolic hydrochloric acid allowed the precipitation of **28 HCl** in form of hydrochloride salt. At this point, a suspension of L-alanine in MeOH was treated with K_2CO_3, $CuSO_4 \bullet 5H_2O$ and **28 HCl**. After 16 hours, the solvent was evaporated and the crude mixture diluted with water, treated with HCl conc until pH = 1 and extracted with ethyl acetate. Evaporation and treatment with petroleum ether gave in the ethereal phase pure L-azido-alanine **27** (99% yield). (Scheme 44)

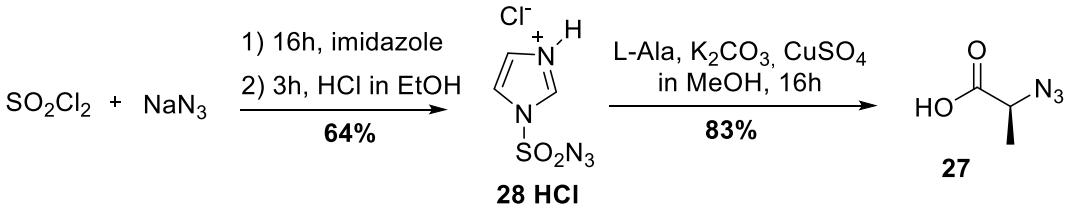

Scheme 44. Preparation of diazotransfer reagent salt **28 HCl** and its reaction to obtain L-azido-alanine **27**

Esterification of maytansinol **5** was performed in presence of DCC and $ZnCl_2$, as originally described by Widdison, in order to be sure that the reaction conditions were compatible with maytansinol stability. After several attempts, the best results were obtained when the reaction was quenched after 6 hours and when 1.1 equivalents of azido acid **27** were used. The relatively low yield of azido ester **29** (22%) was due to

unreacted maytansinol **5** that for some reason remained unconverted, even using 4 equivalents of the **27** or make the reaction lasting 48 hours. (Scheme 45)

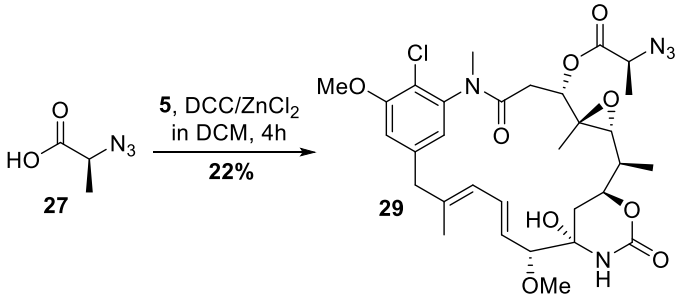

Scheme 45. Esterification of maytansinol **5** with **27** in presence of DCC/$ZnCl_2$

Most important, azidotransfer reaction was performed using racemic alanine as the substrate. In this way, resulting racemate azido alanine **27$_{rac}$** was used to perform the esterification of maytansinol **5**, under the standardized conditions. Comparison between the HPLC chromatograms of L-azido ester and racemate azido ester **29$_{rac}$** highlighted that, when L-azido acid **27** was used, L-azido ester **29** was afforded with a 95% of diastereoisomeric excess, confirming the hypothesis that azido group would have strongly reduced the racemization process. (Figure 5)

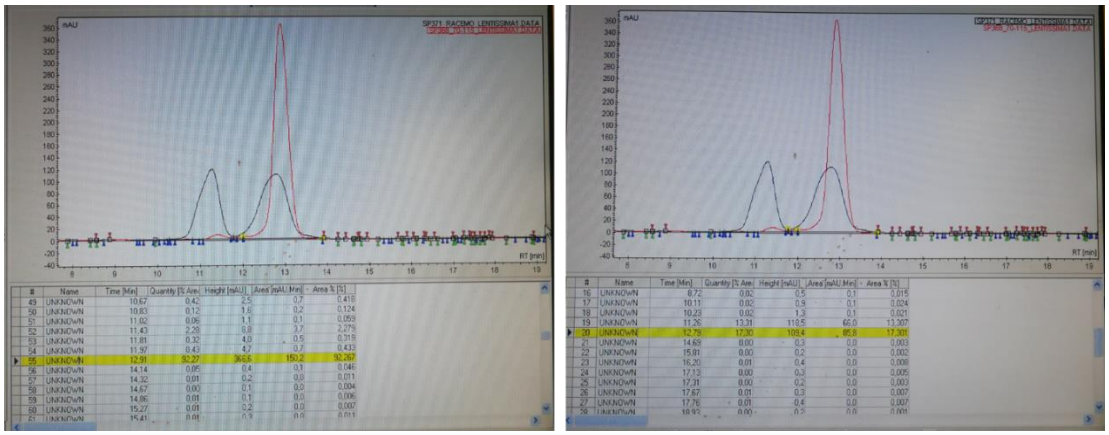

Figure 5. HPLC chromatograms of **29$_{rac}$** (black) and **29** (red) reporting retention times and integrated areas. HPLC conditions: C18 column, eluting with MeCN in water (55%-80% in 30 minutes)

With the azido ester **29** in hand it was possible to investigate some ways to convert the N_3 group in the methylamino moiety. In literature it was widely described the reduction in presence of PPh_3 for the obtainment of the primary amine but, in this case, it was

not easy because of the necessity to obtain the secondary amine. Alkylation of the eventually obtained primary amine would have resulted in the exhaustive alkylation, so that the quaternary amine would have been obtained.

Trying to overcome such a side reaction, Kato and co-workers developed a convenient methodology for the one-pot conversion of azides to N-monomethylamines. [53] This protocol was based on the formation of the aza-Wittig intermediate, iminophosphorane **30**, followed by treatment with paraformaldehyde, in order to obtain the imine **31**. Reduction by $NaBH_4$ afforded the N-monomethylamino derivative **32**. (Scheme 46)

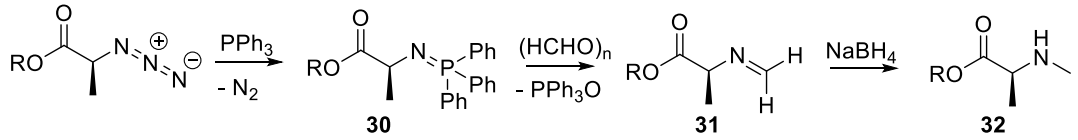

Scheme 46. Proposed one-pot N-monomethylamination of azides

Following what was here above described, L-azido ester **29** was treated with PPh_3 in dry THF and the reaction was left stirring for 16 hours. Then, paraformaldehyde was added in one portion followed, after 6 hours, by $NaBH_4$ addition at 0 °C. After 2 hours, the crude was diluted with dichloromethane and washed with $NaHCO_3$, then purified by careful chromatography, so that two main products were isolated: the less polar was the desired N-monomethylamino derivative **33** (27% yield), while the more polar one was the primary amine **34** (67% yield). (Scheme 47)

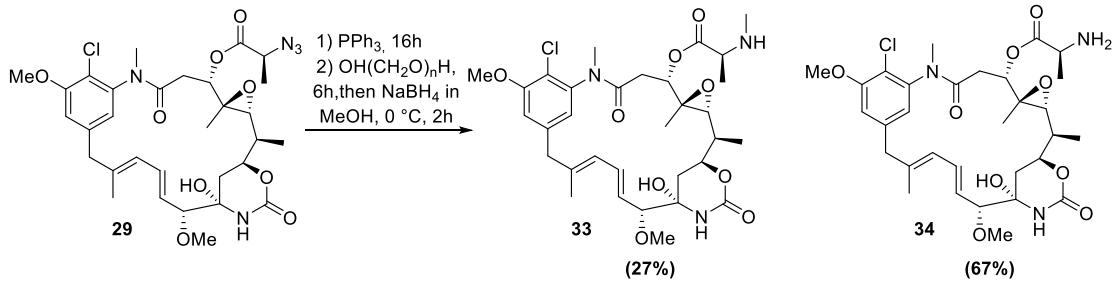

Scheme 47. Preparation of N-monomethylamine **33** starting from azido ester **29**

Even trying to optimize the reaction conditions as much as possible, this was the best result that was possible to obtain. However, given that the primary amine **34** represented the major product by using this approach, it was necessary to valorize such a product. Considering that, as said before, alkylation approach would have resulted

in per-alkylation, some other protocol was needed to be followed. Lebleu et al. provided for a new method to overcome the exhaustive alkylation of primary amines exploiting different methyl group sources, using some unusual solvent. [54] Fluorinated alcohols, in fact, were often employed because of their H-bond donation ability, counterbalanced by the H-bond acceptor nucleophiles, such as secondary and tertiary amines. For this reason, it was hypothesized that, in presence of hexafluoroisopropanol (HFIP) as H-bond donating substrate (acting as the solvent), secondary and tertiary amines would have been more stable, consequently reducing or avoiding the amine over-alkylation. Primary amine **34** was then dissolved in HFIP and treated with 1.5 equivalent of MeOTf, as the methyl donor. Quenching of the reaction by ethanolic ammonia was followed by solvent evaporation and chromatographic purification of the crude. Secondary amine **33** was obtained as pure in 51% yield, together with residual starting material **34** (13% yield) and dimethylamino derivative **35** (31% yield), indicating that complete conversion of primary amine would have worsen the ratio between secondary and tertiary amine. (Scheme 48)

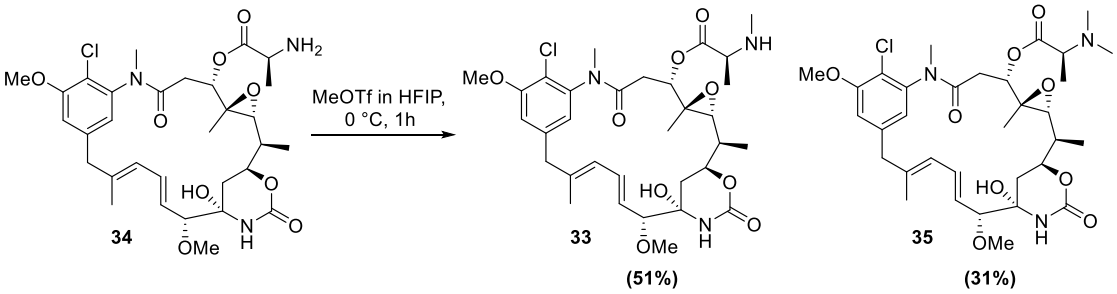

Scheme 48. Monoaminomethylation of primary amine **34** to afford desired **33**

At the end, secondary amine **33** was treated with methyl disulfide acid **10** in presence of EDC•HCl. The crude deriving from this last reaction was analyzed by HPLC and the resulting chromatogram compared with those obtained from the two different diastereoisomers **13-D** and **13-L**, confirming that only the desired diastereoisomerically pure L-form was present. (Scheme 49 and Figure 6)

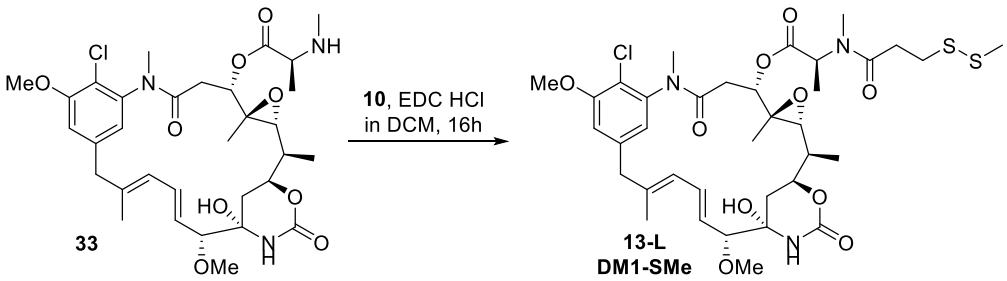

Scheme 49. Reaction of secondary amine **34** with methyl disulfide acid **10** to afford diastereoisomerically pure **13-L** (**DM1-SMe**)

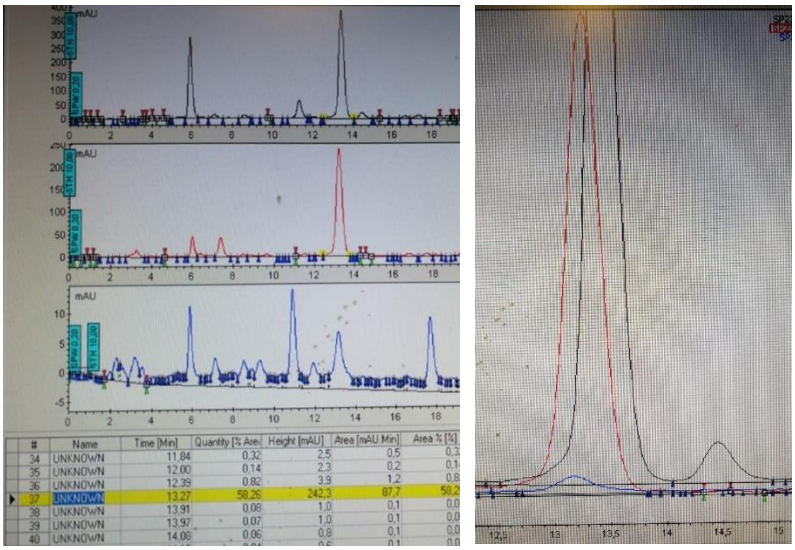

Figure 6A. Comparison between HPLC chromatograms of **13-D** (black), **DM1-SMe** (red) and the crude from reaction between **33** and **10** (blue); **6B** better reveals the minimum difference of retention time between **13-D** (13.49 min) and **DM1-SMe** (13.27 min) and the same retention time between **DM1-SMe** and the crude (13.18 min)

What was here above reported represents a new, unprecedently described methodology for the synthesis of enantiomerically pure **DM1-SMe**. The entire procedure was registered within the patent *"diastereoselective process for the preparation of thiol- or disulfide-containing maytansinoid esters and intermediates thereof"* in the date 18/4/2019, but still not published.

3. Inositols

3.1 Inositols: a brief introduction

Inositols, also called cyclitols (hexahydroxycyclohexanes), are a class of nine poly hydroxy cyclic compounds, widely diffused in nature in different forms. Their main characteristic is the diastereoisomeric relationship between seven of them (*allo*-, *epi*-, *muco*-, *cis*-, *neo*-, *myo*-, *scyllo*-inositol), present in *meso* form, in which the plain of symmetry divides the molecule in two specular and not superimposable parts, while the *chiro*-form is represented by two enantiomeric forms, D- and L-*chiro*-inositols. (Figure 7) Among them, the most abundant isomer is *myo*-inositol, widely present in mammalians and plants, essential for the growth and survey of the animal and vegetable organisms. [55] *Myo*-inositol takes part in the cellular membrane constitution, in form of phospholipid, essential for the structural integrity of the cell. [55] Moreover, it is one of the most important second messengers in intracellular cascade, allowing several essential physiological effects. [55]

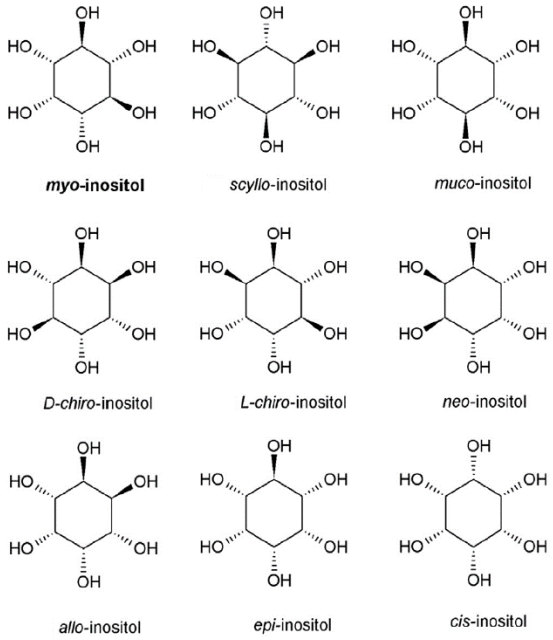

Figure 7. *myo*-inositol and its diastereoisomeric derivative inositols

On the contrary, *cis*-inositol is the only inositol not known in nature, obtained only by synthetic ways, in which all of the hydroxyl groups stand on the same side of the cyclohexane-hexol. [56]

Chiro-inositol shows a particular conformation of the alcoholic groups, so that two enantiomeric forms are possible. D-*chiro*-inositol seems to be effective against endothelial disfunctions within blood vessels, as well as it inhibits bone resorption by osteoclasts. [57] Low levels of D-*chiro*-inositol are linked to increased insulin resistance, while the presence of this particular form in several vegetable seeds (from pumpkins and *Cucurbita cicifolia* family) are responsible for the antihyperglycemic effect after assumption. [58] The most important D-*chiro*-inositol synthetic derivative is *pinitol*, 3-O-methylated-D-*chiro*-inositol, active as antihyperglycemic agent and able to decrease plasmatic glucose levels. [59] (Scheme 50) It is also suppressant of inflammatory and carcinogenic genes expression, reducing proliferation, apoptosis and angiogenesis. [60] Prostate cancer metastasis is inhibited by suppressing overexpression on the cellular surface of integrins, kinase phosphorylation and transcription factors activation. [61]

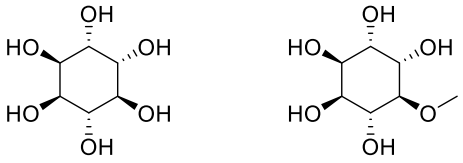

Scheme 50. D-*chiro*-inositol and its 3-O-methyl derivative, pinitol

On the other hand, L-*chiro*-inositol acts mostly on GLUT4-dependent glucose uptake, mimicking insulin administration effect. [62] *Quebrachitol*, the 2-O-methyl-L-*chiro*-inositol derivative, is a naturally occurring antioxidant agent. [63] It has also a great protective effect on acute gastric lesions by nitric oxide release and/or K^+-ATP dependent channel activation. [64]

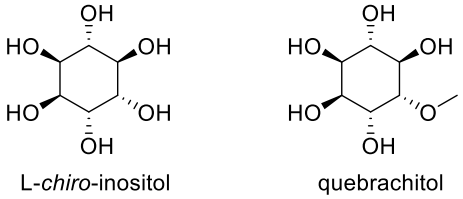

Scheme 51. L-*chiro*-inositol and its 2-O-methyl derivative, quebrachitol

3.2 *myo*-inositol: chemistry and biology

Myo-inositol is widely present in eukaryotic cells of plants and mammalians. [65] Endogenous biosynthesis is provided above all in testis, brain, kidney and liver starting by D-glucose. [66] It is phosphorylated by hexokinase to glucose-6-phosphate, arranged by *myo*-inositol-1-phosphate synthase (MIPS) and dephosphorylated by inositol monophosphatase (IMPase) to free *myo*-inositol, as a not chiral (*meso*) compound. [67]

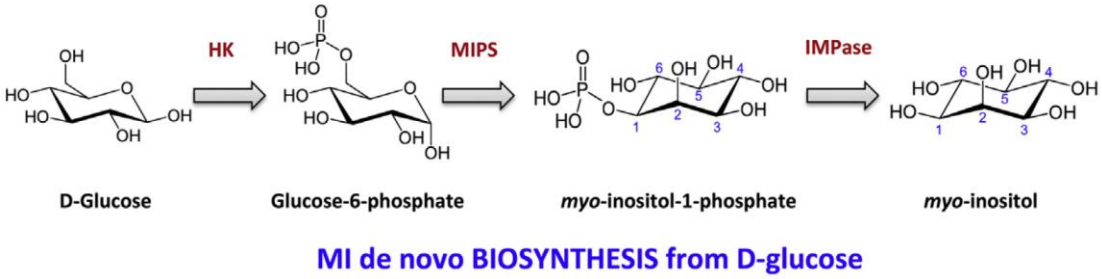

Scheme 52. Endogenous biosynthesis of *myo*-inositol, starting from D-glucose

Because of its important role in metabolic regulation, *myo*-inositol was initially categorized as a vitamin (vitamin B8). [56] Since it has been discovered its biosynthetic pathway, the assumption from external sources was not considered essential anymore. [55] While its endogenous synthesis is possible starting from D-glucose, it is also found within mammalian and vegetables in free form, variously phosphorylated or as phytic acid, the hexaphosphorylated inositol (IP_6). [55,68] Very high contents of *myo*-inositol are found in foods containing seeds, as well as fresh fruits and vegetables. In form of phytic acid is particularly abundant in almonds and nuts, oats and bran. [68] Uptake of IP_6 from dietary affords *myo*-inositol after hydrolysis from *phytases*, enzymes present on gastrointestinal mucosa able to hydrolyze all or part of the phosphate groups. [68] *Myo*-inositol in free form is instead absorbed from the gastrointestinal tract, thanks to Na^+/K^+-ATPase active transport. It is mainly accumulated in thyroid, seminal vesicles, liver and spleen. Organs with high levels of endogenous *myo*-inositol (brain, muscles, fat, testis) seem to be unable to concentrate it from the blood. [55] Next to endogenous biosynthesis, other ways to increase *myo*-inositol intracellular availability were observed, such as processing inositol phospholipids (phosphatidylinositol derivatives) and cellular uptake from active transport systems (after dietary supplementation). [55]

Among the latter, proton/*myo*-inositol transporter (HMIT) is able to co-transport *myo*-inositol together with one proton, while SMIT1 and SMIT2 are sodium dependent transporters, able to co-transport two sodium ions and one molecule of *myo*-inositol along the concentration gradient. [69,70] Glucose is a competitive substrate towards SMIT1, whereas SMIT2 is able to co-transport also D-*chiro*-inositol. (Figure 8)

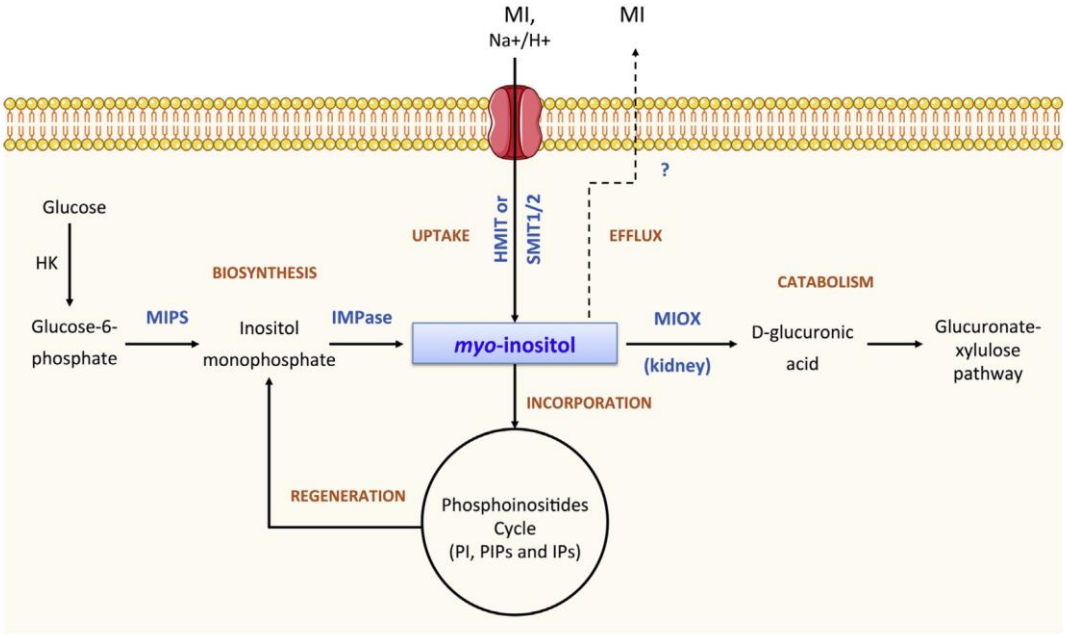

Figure 8. Representation of synthesis, uptake and catabolic fate of *myo*-inositol (**MI**) [56]

Polyphosphorylated inositols are widely present within human cells. Because of the lack of inositol kinases, it is likely that these derivatives are originated from dephosphorylation by phosphatases or hydrolysis of phosphoinositides. [56] Within the membrane, in fact, *myo*-inositol is present in form of phospholipid, in particular phosphatidylinositols, that can be further phosphorylated. Catabolic fate of *myo*-inositol depends on its conversion to D-glucuronic acid by *myo*-inositol oxygenase (MIOX) in the kidney before excretion. [71]

In cellular membrane inositol is present as phosphatidylinositol-4,5-biphosphate (PIP_2), responsible for endo- and exocytosis, as well as for the cytoskeleton integrity. [72] Hydrolysis of PIP_2 by phosphoinositidase C (PLC) affords inositol-1,4,5-triphosphate (IP_3) and 1,2-diacylglycerol (DAG), as essential intracellular second messengers. [72] While IP_3 is accumulated in cytosol and, then, is able to stimulate sarcoplasmic reticulum to release Ca^{2+}, DAG is known as regulator of PKC, a family

of phosphorylating enzymes involved in several intracellular signaling pathways. [73] (Figure 9)

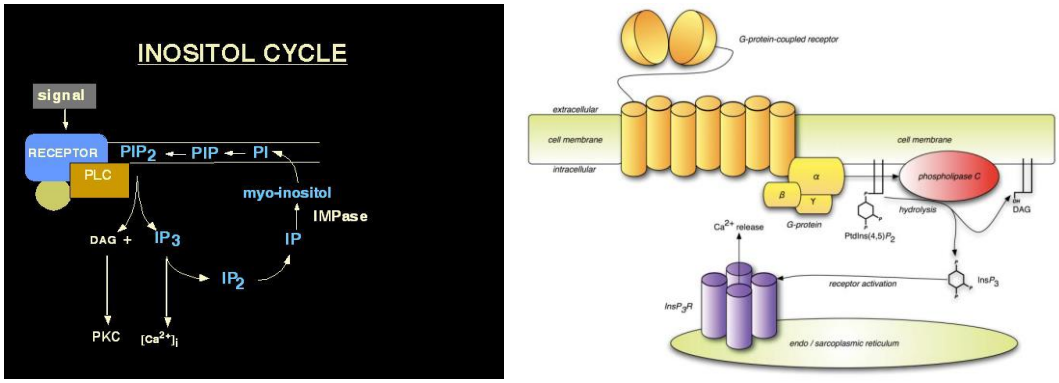

Figure 9. Representation of the "inositol cycle" within the cell

Besides, IP_3 serves also as substrate for the synthesis phytic acid (IP_6), the most occurring form of storage of free inositol and phosphorus. Further functionalizations on IP_3 afford differently phosphorylated inositol and inositol pyrophosphate derivatives. [72]

Functionalization of *myo*-inositol in animal cells brings to variously phosphorylated and substituted derivatives; however, methylation of one or more hydroxyl groups and their epimerization are not likely to happen within intracellular environment, but it is rather possible that they are assumed from other sources (pinitol, from some plant species) or obtained by synthetic routes (*allo*-, *epi*- and *cis*-inositols). Epimerization of *myo*-inositol to other naturally occurring inositols (*muco*-, *scyllo*-, D- and L-*chiro*- and *neo*-inositol) does not take place in vivo, except for the conversion of *myo*-inositol to D-*chiro*-inositol only in tissues expressing the specific epimerase. [56]

3.3 Role of *myo*-inositol derivatives in pathological conditions

Myo-inositol seems to be involved in several pathological conditions correlated to its deficiency. Here after, it will be explained how its role could be determinant in the pathogenesis of metabolic diseases, mostly involving hormonal disequilibrium.

3.3.1 Diabetes

Diabetes is described as a pathological condition in which no sensitivity to insulin is expressed, consisting of glucose homeostasis and that brings, as a consequence, to the

lack of glucose uptake from the cells and subsequent non-physiological high levels of glucose within the circulation (hyperglycemia). Diabetes mellitus of type 2, in particular, is characterized by increased insulin resistance and no response to the stimulation of circulating insulin on its receptors, as well as by insufficient insulin secretion from the pancreas. [74] Typical therapeutic approach consists of the administration of insulin sensitizing agents, able to improve cell response to the antiglycemic insulin action. [75] Abnormalities in *myo*-inositol metabolism could be related to insulin dependent processes, some of them bringing to increased *myo*-inositol excretion and its intracellular depletion. [76,77] In diabetes context, inositol derivatives have an important function deriving from the insulin-mimetic role of inositol phosphoglycans (IPGs), built on the *myo*-inositol and D-*chiro*-inositol cores. [78] In fact, inositols provide for the production and activation of phosphinositol-3-kinase (PI3K), with subsequent GLUT-4 transporter translocation: in this context, *myo*-inositol constitutes second messengers able to favor glucose uptake, while D-*chiro*-inositol is the scaffold for second messengers involved in glycogen synthesis and synthase activation. [62] (Figure 10)

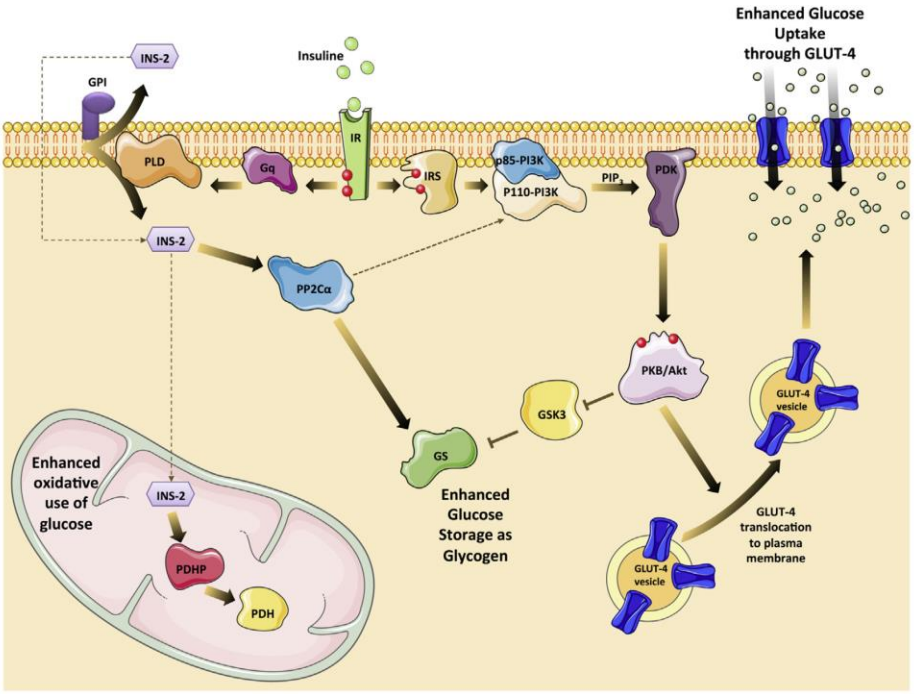

Figure 10. *myo*-inositol role in insulin-mediated response in type 2 diabetes mellitus

Myo-inositol is converted to D-*chiro*-inositol by specific epimerase activity within insulin sensitive tissues, such as muscles, fat and liver. [79] In type 2 diabetes mellitus increased glucose blood concentration is accompanied by high *myo*-inositol levels, given that its endogenous synthesis starts from glucose itself. Hyperinsulinemic conditions favor the conversion of *myo*-inositol to D-*chiro*-inositol, so that there is no physiological balance between the two diastereoisomeric forms. [80] Moreover, higher glucose uptake has, as a consequence, the extrusion of *myo*-inositol from the intracellular environment. This results in an increased metabolism and urinary excretion, due to the competitive relationship between glucose and *myo*-inositol towards the same transporter (SMIT1). [81] Supplementation with *myo*-inositol would therefore help in diabetic condition, because of its ability to favor insulin-mediated glucose uptake, exploiting its insulin mimetic activity. [81] Inosituria was found to be strictly correlated with glycosuria within insulin resistance conditions. Such *myo*-inositol depletion has as a direct consequence a sensitive decrease in phosphatidylinositol levels, heavily influencing the activity of Na^+/K^+ ATPase, that at this point is no more balanced and brings at first to important effects, mostly in neurons and axons, where myelin degeneration takes place, with subsequent affection of central nervous system and/or peripheral nervous system. [82] Moreover, inositol unbalance could be the cause for epimerization from *myo*- to D-*chiro*-inositol to not take place in insulin sensitive tissues. M*yo*-inositol extracellular low levels result in a decreased intracellular uptake and reduced cellular functions: as a consequence, the lower conversion from *myo*-inositol to D-*chiro*-inositol prevents the incorporation in phosphoglycans (acting as insulin second messengers), hence an increased specific tissue insulin-resistance would be observed. In particular, insulin stimulates glycosylphosphatidylinositols (GPIs) hydrolysis so to obtain IPGs: IPG-A (inositolphosphoglycans AMP-kinase inhibitor) deriving from the hydrolysis by phospholipases C (PLC) and D (PLD) on PGI and based on the *myo*-inositol scaffold, and IPG-P (inositolphosphoglycans phosphatase stimulator) deriving from membrane phospholipids hydrolysis and containing the D-*chiro*-inositol core. [78] While IPG-P stimulates glycogen synthesis and regulates the glucose-dependent release of insulin

from pancreatic β-cells, IPG-A favors intracellular glucose uptake, acting as an insulin-mimetic agent and enhancing GLUT-4 translocation. (figure 11)

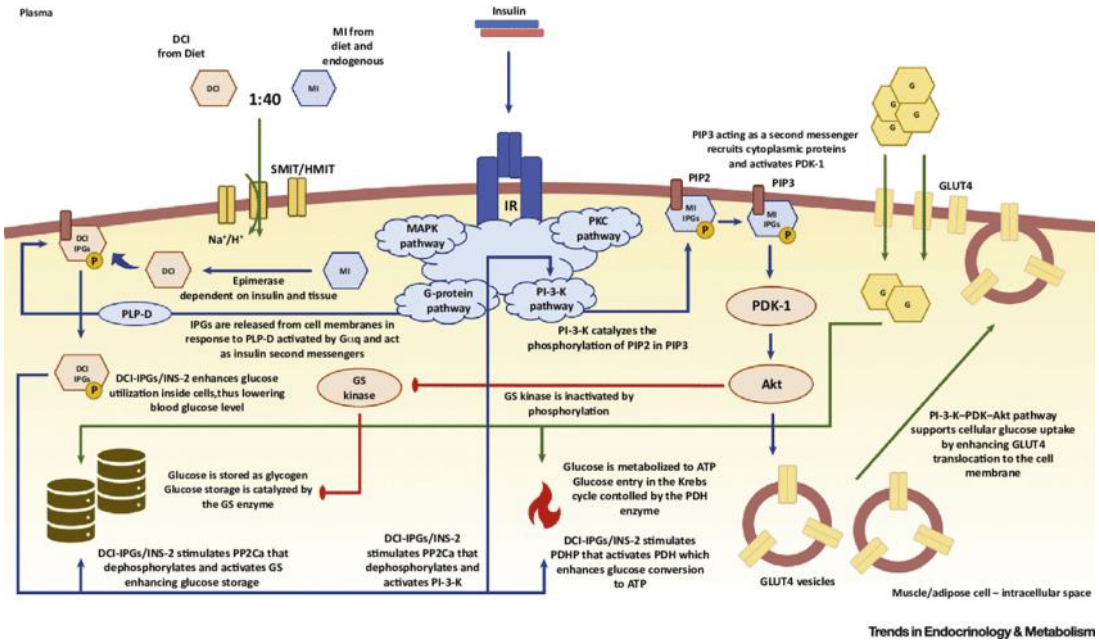

Figure 11. schematic representation of all of the pathways involved in hyperinsulinemic control, in presence *myo*-inositol or D-*chiro*-inositol derivatives [78b]

It is evident that type 1 diabetes (where no insulin is produced) could not have benefits from *myo*-inositol supplementation. However, high levels of *myo*-inositol supplementation were proved to be efficient in lowering blood glucose thanks to the increased translocation of GLUT-4 on cell surface and its activity as insulin mimic.

3.3.2. PCOS

Polycystic ovary syndrome (or PCOS) is a metabolic endocrine disorder, affecting women more often in reproductive age and characterized by hyperandrogenism and ovulatory dysregulation. [83] Causes of PCOS are still unknown, even if genetic background and lifestyle seem to strongly influence its development. PCOS is often associated to hyperinsulinemia and obesity. In particular, hyperinsulinemia could favor androgens production from ovaries, with consequent reduction of testosterone transporters, leaving high levels of testosterone itself in circulation and hyperandrogenism symptoms. [84] Moreover, it could impede folliculogenesis and ovulation, because of the intraovarian androgen high levels and of the possible alteration of the gonadotropin secretion. [56] It was demonstrated that enhancements in

hyperinsulinemic context, increasing insulin tissue sensitivity or decreasing the circulating insulin by pancreatic secretion inhibition could improve PCOS conditions. [56] In this context, *myo*-inositol supplementation was able to restore ovarian activity and to improve hormonal parameters and restore fertility, thanks to an improved insulin sensitivity together with lower insulinemia levels and concurrent lower circulating androgens. [85] The most plausible mechanism for *myo*-inositol efficacy within PCOS framework seems to be the main activity on insulin sensitivity improvement with consequent positive impact on hormonal and reproductive axis, [85] even reducing all of the correlated risk factors (dyslipidemia, obesity, cardiovascular risk). [56] The only direct effect of *myo*-inositol on the syndrome appeared to be connected to the augmented Ins(1,4,5)P_3 release, able to regulate oocytes development and maturation and the control of FSH blood levels, though being fundamental in infertility caused by PCOS. [86–88] Moreover, it was observed that D-*chiro*-inositol was able to regulate within the ovaries the insulin-induced androgens synthesis, favoring their release in response to insulin stimulation. In the ovaries, conversion from *myo*-inositol to D-*chiro*-inositol by epimerase allows, in physiological conditions, the presence in 100:1 ratio, respectively. [89] PCOS, as well as type 2 diabetes mellitus and insulin resistance, is capable to reduce epimerase activity, inducing low levels of D-*chiro*-inositol, with consequent low levels of IGPs used as second messengers in insulin resistance enhancement. Starting from this evidence, it was demonstrated that a small dose of D-*chiro*-inositol can improve insulin sensitivity, while simultaneous administration of *myo*-inositol and D-*chiro*-inositol helps in insulin resistance, in tissues where epimerase did not work well. [90,91] Given that ovaries are not insulin resistant tissues, hyperinsulinemia conditions do not worsen the epimerization from *myo*- to D-*chiro*-inositol, but *myo*-inositol depletion takes place, whereas D-*chiro*-inositol levels become very high. Unfortunately, this represents a drawback in PCOS considering that high dosages of D-*chiro*-inositol worsen ovarian response and oocytes quality, and that conversion from D-*chiro*-inositol to *myo*-inositol is not possible endogenously. In such a situation *myo*-inositol is not able to accomplish its insulin mimic activity, so that insulin resistance symptoms become more evident. Higher extracellular levels of *myo*-inositol have as a consequence hyperglycemic conditions,

due to the competition with glucose for the intracellular uptake. Supplementation with *myo*-inositol could help in controlling PCOS with concurrent hyperglycemic condition, given that increased insulin sensitization and lower insulinemia would allow to lower testosterone levels by increasing SHBG (Sex Hormone Binding Globulin) able to sequester circulating testosterone, though improving oocytes quality and ovarian response. [84]

3.3.3 Thyroid hormones disequilibrium

Myo-inositol is also widely involved in signaling within thyroid hormonal regulation. In particular, synthesis of thyroid hormones is regulated by phosphatidylinositol diphosphate (PIP_2) and cAMP cascades, strongly correlated to the production of H_2O_2 necessary for thyroid hormones to be fully functional. [92] Indeed, this step is fundamental in order that inorganic iodine could be correctly bind to tyrosine residues. Unbalance in H_2O_2 production, instead, could have as a consequence several illnesses ranging from hypothyroidism to thyroid tumor. [93] Autoimmune disease could be moreover originated from insufficient phosphatidyl inositol triphosphate (PIP3) signaling within intracellular cascade, due to the involvement of PIP_3 in B cells fate and of other inositol polyphosphates in T cells regulatory functions. [94]

Thyroid hormones synthesis starts with iodide uptake and binding of thyroid stimulating hormone (TSH) to its receptor TSH-R. [95] This interaction results in adenylate cyclase (AC) activation and cAMP cascade, finishing in the nucleus stimulation for THs synthesis and thyrocyte growth and differentiation. [96] In presence of an excess of TSH, another G-protein is activated, so that PLC and IP_3/DAG pathway are involved, affording H_2O_2 formation and subsequent iodination thanks to thyroid peroxidase (TPO), essential for the hormone biosynthesis. [97] Production of H_2O_2 normally would induce apoptosis in thyrocytes, but cAMP agonists and TSH prevent this condition thanks to PKA and PI3K actions. [98] In this context, inactivation of signaling members of phosphatidylinositol cascade results in natural killer (NK) cells defects and subsequent possible autoimmunity, cancer conditions and infections. [99] *Myo*-inositol showed to assist TSH and its intracellular cascade, helping in H_2O_2-mediated iodination. Treatment of hypothyroidism with *myo*-inositol, in fact, increased

second messenger signaling and improved sensitivity to TSH, as it is precursor of phosphoinositides and involved in phosphatidylinositol synthesis. [97] Lack of *myo*-inositol and its derivatives resulted in dysregulation of immune response and autoimmunity. It is at first incorporated into cells in form of phosphatidylinositol (involved in cell growth, metabolism regulation and lipid synthesis) that was then phosphorylated to give PIPs as important precursors for second messengers (IP_3 and DAG), regulating different kinases and, in the end, the levels of intracellular Ca^{2+}. Treatment of hypothyroid patients with *myo*-inositol in association to selenium helped in decreasing TSH high levels caused by autoimmune disease. [100] Balance of T3 and T4 hormones in autoimmune thyroiditis patients and reduced blood TPO and thyroglobulin, on the other hand, were treated with *myo*-inositol, since it helps thyrocytes in producing in a more efficient way T4 and modulating H_2O_2-mediated iodination through PLC-dependent pathway. [92] The subsequent increased intracellular Ca^{2+} favors an increased H_2O_2 generation, promoting iodine incorporation and availability in thyroid. [101]

3.3.4 Phytic acid in cancer

Phytic acid (IP_6) is the hexaphosphorylated form of *myo*-inositol. It is found in plants, cereals and legumes and behaves as phosphorous storage. Several studies reported a negative correlation between IP_6 and colon cancer, so that it was hypothesized that IP_6 could be internalized and then dephosphorylated, to give other inositol phosphate derivatives, with the capability of acting as tumor growth inhibitors. [102] Besides the high charged form in which IP_6 is found, is possible to orally administer phytate, favoring its absorption even far from gastrointestinal tract, thanks to specific transport mechanisms. Pinocytosis and receptor mediated endocytosis, in fact, allow the internalization within the cytoplasm, where IP_6 is then dephosphorylated to $IP_{1\text{-}5}$ analogues. [103] Different types of tumor cell lines are susceptible to IP_6, mostly leukemic ones, suggesting that different mechanism of action could be involved in anticancer activity showed on breast cancer cells, cervical cells and mesenchymal tumors. [104] Its potential as preventive agent was demonstrated at first *in vitro* in benzo[a]pyrene-induced cancers and confirmed by inducing tumor in different cell

lines, by treating them with azoxymethane and dimethylhydrazine carcinogens. Efficacy of IP_6 in cancer treatment was dose and time-dependent and its potential as therapeutic agent was shown after positive results upon treatment of different types of tumor in animals. Reduced number and dimension of neoplastic formations was highlighted, even on metastatic cancer cells. [105] *Myo*-inositol was tested itself as anticarcinogenic agent, although showing a less potent activity than IP_6. [106] Synergistic cancer inhibition with IP_6 was observed in studies on colon and mammary cancers. Mechanism of action is still not fully understood. It seems that less phosphorylated inositols, such as IP_3 and IP_4, are very important in signal transduction and cell growth and differentiation. [107] In this context PI3K phosphorylates phosphatidylinositol to give PIP_3, as well as other phosphorylated forms of phosphatidylinositols. Besides, IP_6 inhibits PI3K activity, influencing intracellular cascade, proliferation and differentiation of cancer cells. [108] Moreover, it seems that steric hindrance of IP_6 on heparin-binding domain of basic fibroblast growth factor could play an important role, because of the structure similarity with the pyranose of heparin (its natural substrate). [109] Another proposed mechanism is based on the antioxidant activity by Fe^{3+} chelation, so to efficiently suppress hydroxyl radical formation. Its particular conformation allows negative charged phosphate groups in position 1, 2 and 3 (axial, equatorial, axial) to interact specifically with iron, inhibiting in this way its catalytic activity towards hydroxyl radical formation. [110] (Scheme 53) This coordinating ability would allow also the binding of Zn^{2+} present in thymidine kinase, essential for DNA synthesis, even in cancer cells. [110] It is also known how IP_6 is capable to increase natural killer cells activity. [111]

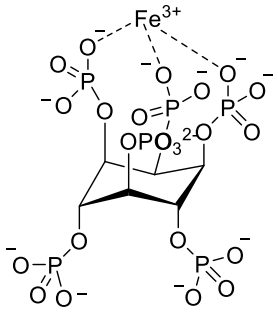

Scheme 53. Conformation of IP6 for the coordination and chelation of metals (iron is here reported)

The most appreciate characteristic of IP_6 as anticancer agent is its selective mechanism on cancer cells. It is well known that tumor cells are characterized by different metabolism, receptor expression and growth rate, even if it is still unclear how such specificity is possible. However, several studies indicated anticancer activity only on malignant cells. IP_6 is able to regulate and control cell cycle, blocking cell division or bringing cells to apoptosis, by arresting G1-phase and decreasing S-phase in human breast, colon and prostate cancer cell lines. [112]

Ability to suppress metastasis was highlighted and explained. In particular, tumor cells emit matrix metalloproteinases (MMPs) able to let metastatic cells to pass blood vessels, while IP_6 is able to inhibit this MMPs secretion. [113] Another peculiar characteristic of tumor condition is the development of new blood vessels, through the release of great amount of vascular endothelial growth factor (vEGF), whose levels resulted hugely decreased after treatment with IP_6. [114] In chemoprotective approach, IP_6 seemed to be responsible for some liver enzymes inhibition and for an increase in the levels of S-glutathione transferase, indicating cancer protection through the block of carcinogenic activity. [115]

Co-administration of IP_6 and *myo*-inositol demonstrated antitumor activity in patients with metastatic colorectal cancers. In fact, even when traditional chemotherapy was refused, significant reduction in tumor growth rate was shown. [116] Great advantage in IP_6 administration consisted in almost no side effects at the effective dose, together with a plethora of therapeutic applications, from kidney stones to hypercalciuria, to hypercholesterolemia, to diabetes. [117] However, such a strategy needs to be evaluated in its effectiveness and safety in further steps of clinical studies.

3.3.5 *myo*-inositol on bone resorption

Due to its ability to chelate Ca^{2+} salts and to inhibit crystallization exclusively by physicochemical action, even bone resorption could be treated with IP_6. [118] In fact, it finds therapeutic application in pathological conditions involving some cation sequestration, such as calcification (renal stones, cardiovascular calcification). [119,120] Supposed mechanism of action provides for inhibition of crystal development, avoiding at the same time the possibility of redissolution for the already formed

crystals. [121] To date, is possible to assert the positive influence of IP_6 assumption and its increased urinary secretion, correlated to reduced loss of bone mass and minimized risk of osteoporotic fractures.

3.4 Synthetic pathways to obtain *myo*-inositol and its derivatives

Synthesis of *myo*-inositol and its derivatives has been always intriguing, because of the potential therapeutic applications and the different activities of the synthetic analogues. One of the methods exploited to synthesize *myo*-inositol and its diastereoisomers provided for the functionalization of *p*-benzoquinone **36**, through the obtainment of *conduritols*. [122] Conduritols are products of natural origins often used as precursors for cyclitols and pseudo sugars, with remarkable biological activity as glycosidase inhibitors. [123] Their synthetic versatility is mainly related to the presence of four hydroxyl group on a cyclohexene moiety, where the double bond could be dehydroxylated to afford variously substituted inositols. (Figure 12)

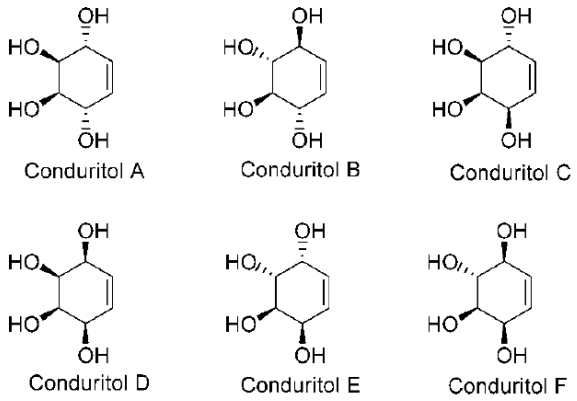

Figure 12. Six stereoisomeric forms of conduritols

In order to achieve the conduritol scaffold, *p*-benzoquinone **36** (scheme 54) was brominated on one of the two double bonds and reduced with $NaBH_4$ to afford the dibromide furtherly protected as acetate **(+)-38**. This allowed the inversion of the configuration of all of the carbon stereocenters, so that treatment with BnONa in BnOH/THF, afforded the conduritol B enantiomer (-)-**39**. Dihydroxylation of the double bond easily gave product **(-)-40**, as *myo*-inositol derivative. Reaction of **38** in presence of AcONa in AcOH afforded conduritol E enantiomer **(+)-41**, as precursor of *allo*-inositol derivative **(+)-42**, obtained after the double bond dihydroxylation.

Epoxidation of **(-)-39** and **(+)-41** gave **(-)-43** and **(+)-44**, that after ring opening afforded diols (-)-**45** and (+)-**46**, respectively *chiro*- and *neo*-inositol derivatives. (Scheme 54)

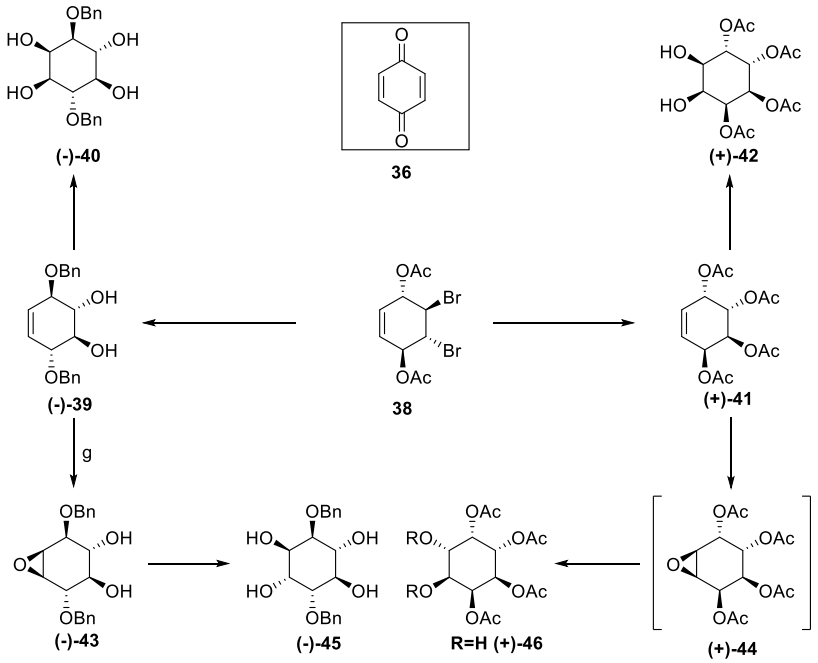

Scheme 54. Preparation of different inositol derivatives starting from *p*-benzoquinone **36**

For the synthesis of *epi*-inositol, dibromo diacetate **(+)-38** was directly dihydroxylated to give diol **(-)-47**. Then, protection as acetate, halogen elimination and double bond formation resulted in conduritol C analogue **(-)-48**, that was dihydroxylated and protected as acetate **49**. Alkaline hydrolysis gave *epi*-inositol. (Scheme 55)

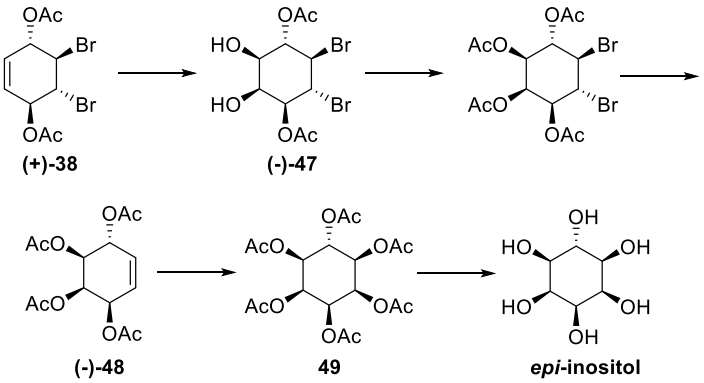

Scheme 55. Synthesis of *epi*-inositol from **(+)-38**

A concise way to obtain inositols was developed starting from optically pure (+) *proto*-quercitol, extracted from the stems of *Arfeuillea arborescens*. [124] It represented a very useful chiral building block for the synthesis and functionalization of cyclitol moieties, because of the presence of five contiguous hydroxyl groups, able to afford after protection with 2,2-dimethoxypropane a single bis-acetonide product **50**. Treatment with triflic anhydride and pyridine allowed the double bond formation (**51**), while deprotection in acidic conditions afforded conduritol F. Dihydroxylation of the double bond of bis-acetonide **51** brought to D-*chiro*-inositol and *epi*-inositol. (Scheme 56)

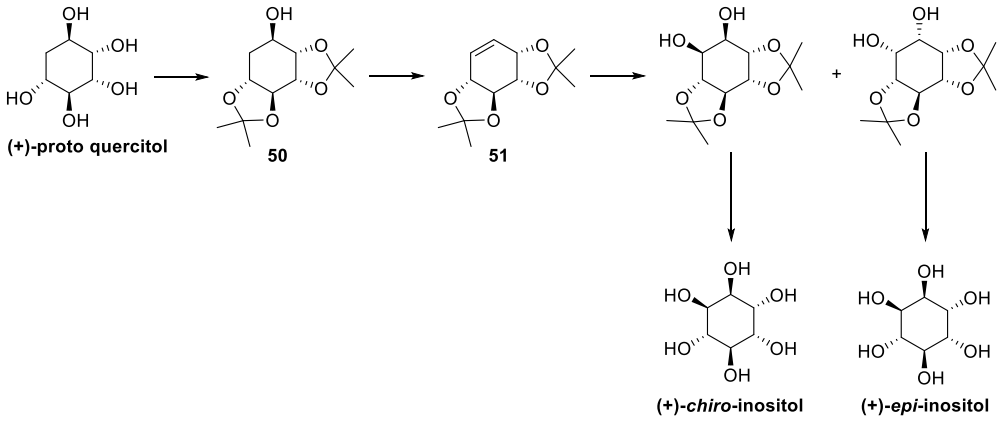

Scheme 56. Synthesis of D-*chiro* and *epi*-inositol starting from (+)-*proto* quercitol

Preparation of inositol derivatives starting from aromatics was described by Hudlicky et al. [125] In particular, *neo*-inositol was prepared in seven steps using bromobenzene **52** as starting material. Oxidation by dioxygenase enzymes, followed by diol protection as acetonide and double bond functionalization with dibromo dimethylhydantoine gave intermediate **53**. Epoxidation and ring opening afforded trans-diol **54**, prior to bromine elimination and residual double bond cis-dihydroxylation, to afford tetraol **55**. Deprotection of acetonide moiety afforded desired *neo*-inositol. (Scheme 57)

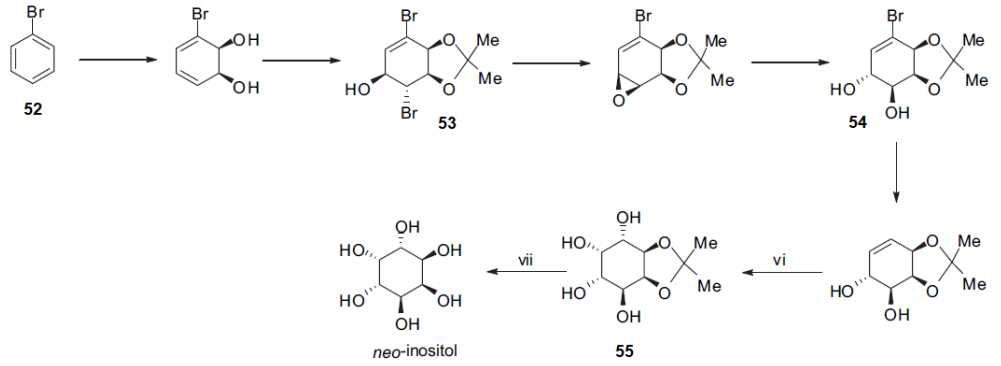

Scheme 57. Synthesis of *neo*-inositol starting from bromobenzene **52**

Bromobenzene oxidation followed by cis-dihydroxylation and acetonide protection gave access to cis-tetrahydroxy cyclohexane protected derivative **56**. Epoxidation and bromine elimination afforded epoxide **57**, opened in acidic environment in presence of water, to give deprotected *epi*-inositol. (Scheme 58)

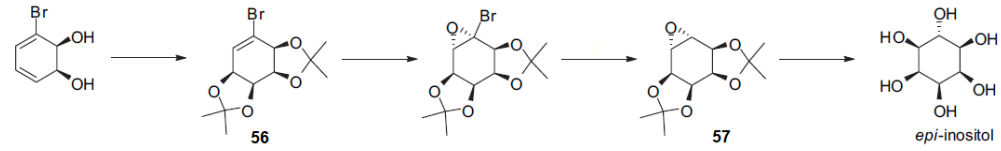

Scheme 58. Synthesis of *epi*-inositol starting from bromobenzene oxidation

In order to synthesize glycosylphosphatidylinositol derivatives in an enantiomerically pure way, Conrad et al. reported the preparation of the *myo*-inositol scaffold exploiting Ring Closing Metathesis (RCM). [126] Commercially available dimethyl 2,3-*O*-isopropylidene-*D*-tartrate **58** was converted in the bis-Weineb amide **59**, as direct precursor of diene **60**. RCM performed in presence of II generation Grubb's catalyst afforded the mono-acetonide conduritol B **61**. Protection as *p*-methoxybenzylated derivative gave **62**, that was then cis-dihydroxylated and selectively mono-allylated on the less hindered hydroxyl group to give **63**. Acylation of the residual -OH, followed by serendipitous monodeprotection of one of the two PMB-ethers, gave **64** as optimal precursor for the conjugation of glycosylphosphatidylinositol to give GPI-anchor **65**. (Scheme 59)

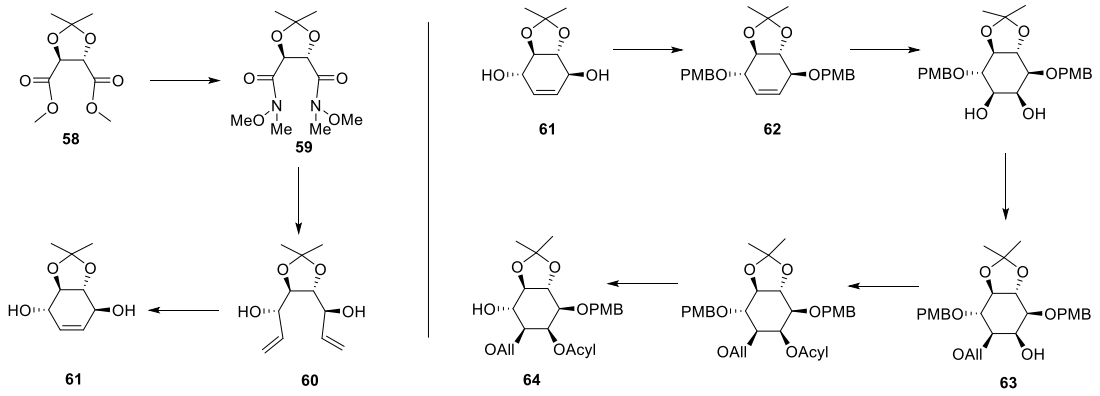

Scheme 59. Synthesis of *myo*-inositol derivative **64**, as precursor for GPI-anchor **65**

Another method to prepare inositol derivatives was developed by Kang et al. through N-heterocyclic carbene catalysts, allowing the ring closure by a benzoin-type cyclization on alditol substrates. [127] Dialdose analogs were prepared starting from the appropriate carbohydrate; D-mannose, for example, was used for the synthesis of the tetrabenzyl dialdose **66**, that was further let reacting with the NHC salt **67** in presence of triethylamine as the base. (Scheme 59)

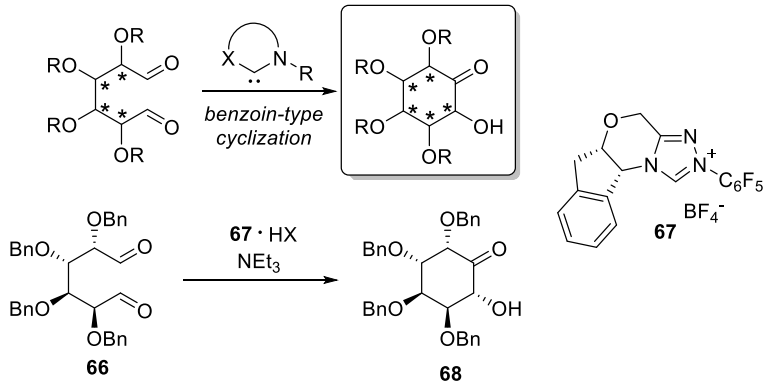

Scheme 59. Synthesis of ketone **68**, exploiting NHC **67** on dialdose **66**

Chiral triazolium salt **67** used in 5 mol% amount afforded ketone **68** as a single diastereoisomer in high yield. Interestingly, the same NHC used in the same reaction conditions on the enantiomeric form of **66** did not allow to isolate nothing other than the starting material, that was quantitively recovered. Having obtained the ketone in the desired configuration, the authors decided to submit it to stereoselective reduction in order to achieve the formation of inositol derivative in diastereoselective manner.

In particular, using $NaBH_4$ as hydride source on **68** it was possible to isolate in high yield and complete diastereoselectivity *allo*-inositol derivative **69**. This is because the hydride attack suffers more from steric factors when the present electronegative substituents favors an earlier transition state; in presence of an amino borane complex, the hydride is less ready to perform the reduction, so that the hydride attack on the late transition state is more sensitive to the torsional strain of the substituents, so that if R = TBDMS diastereoisomer **70** was obtained with high stereoselectivity. (Scheme 60)

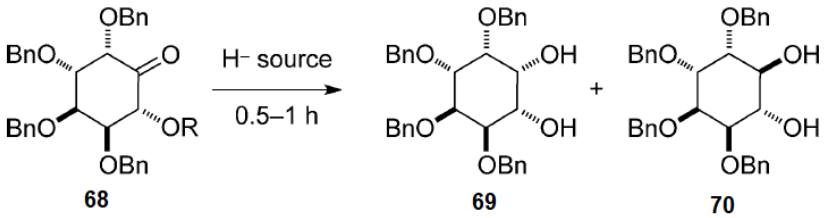

Scheme 60. Reduction of **68** furnished different diastereoisomers depending on the source (NaBH4 or amino borane complex) and substituent (R = H or R = TBDMS)

Takahashi et al. described the conversion of methyl-tri-O-benzyl glycosides starting from the oxidation following Moffatt's procedure, in order to obtain the unstable aldehyde **71** treated with acetic anhydride to give enol acetate **72**. [128] With this approach it was possible to obtain both Z (as the main product) and E isomers, easy to be purified by chromatography. Treatment of Z-isomer of glucose-like glycoside **73** with 5 mol % of $PdCl_2$ afforded with good yield a mixture of diastereoisomers, of which the most represented was the ketone with the α-acetoxy group in equatorial position (compound **74**). (Scheme 61)

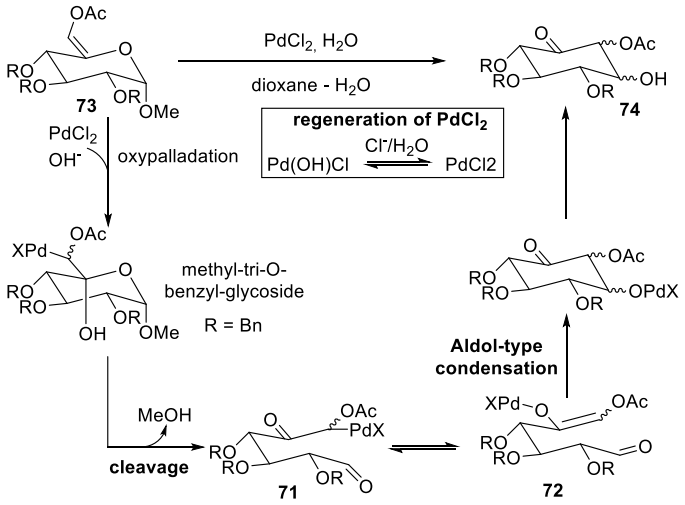

Scheme 61. Palladium-catalyzed Ferrier rearrangement towards cyclic ketone **74**

Within the same work, selective reduction was explored, in order to obtain all of the inositol diastereoisomeric forms. In particular, $Me_4NBH(OAc)_3$, usually employed to reduce β-hydroxy ketone to obtain anti-diols, and $NaBH_4$ in methanol were used. Reduction following Evans-Saksena protocol exploits the boron as the chelating agent, so that hydride transfer happens from the opposite side, compared to the chelation. In comparison, traditional reduction by $NaBH_4$ allowed the obtainment in diastereoselective and complementary way, with respect to boron hydride reducing agent. (Scheme 62)

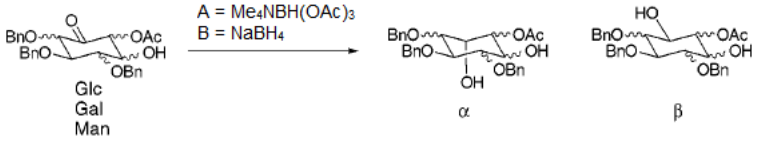

entry	substrate	method	conditions	yield	α : β	
1	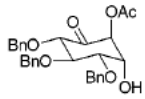	A	0 °C, 3 h	91 %	<1 : 99	→ D-*chiro*-inositol
2		B	0 °C, 0.5 h	84 %	87 : 13	→ *muco*-inositol
3	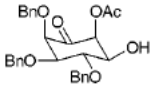	A	r.t., 24 h	46 %	70 : 30	
4		B	-78 °C, 0.5 h	90 %	<1 : 99	→ *epi*-Inositol
5	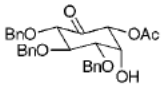	A	r.t., 3 h	94 %	<1 : 99	
6		B	0 °C, 0.5 h	97 %	>99 : 1	→ *myo*-inositol
7	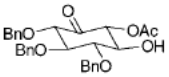	A	r.t., 24 h	37 %	78 : 22	
8		B	0 °C, 0.5 h	86 %	22 : 78	→ *scyllo*-inositol
9	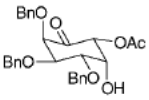	A	0 °C, 3 h	93 %	<1 : 99	→ *neo*-inositol
10		B	-78 °C, 0.5 h	88 %	98 : 2	
11	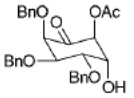	A	r.t., 48 h	N.R.	– : –	
12		B	0 °C, 0.5 h	96 %	<1 : 99	→ *allo*-inositol
13	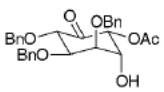	A	0 °C, 3 h	92 %	<1 : 99	→ L-*chiro*-inositol
14		B	-40 °C, 0.5 h	92 %	98 : 2	

Scheme 62. Reduction conditions towards the formation of different inositols, starting from the appropriate ketone

Marnera and d'Alarcao reported in 2006 the synthesis of D-*chiro*-inositol analogues starting from L-arabinose derivatives. [129] Treatment of carbohydrate **75** with an excess of vinyl magnesium bromide, followed by protection of the residual free hydroxyl groups as silyl ethers, afforded a mixture of anti:syn 2:1, with double bond undergoing a ozonolysis reaction and subsequent reduction w8ith $NaBH_4$ to give the bis-silyl ether **76**.

Protection as benzyl (or *p*-methoxybenzyl) ether of the secondary alcoholic portion and desilylation provided diol **77**, ready to undergo Swern oxidation and ring closure by SmI_2 to afford D-*chiro*-inositol derivative **78**. (Scheme 63)

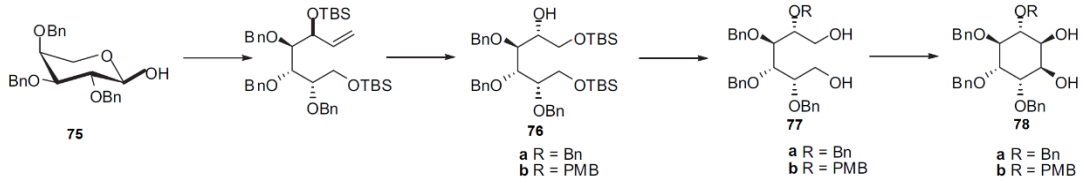

Scheme 63. Carbohydrate **75**, after treatment with vinylmagnesium bromide, was used as starting material for the selective obtainment of D-chiro inositol derivative **78**

Metha and Lakshminath designed the synthesis of *allo*-inositol derivatives from the norbornyl moiety of **79**. [130] Rearrangement to the deoxy-conduritol scaffold in presence of MeONa in MeOH was favored by the presence of the tosylate group in α position with respect to the bridge of the bicyclic system **80**. Dihydroxylation, reduction of the resulting ester **81** to the corresponding primary alcohol and its subsequent protection as tosylate gave **82**. Elimination provided the exocyclic double bond, then converted into ketone **83**, that was reduced and converted to alcohol and transformed into a good leaving group. Another elimination afforded the bis-acetonide conduritol-E **84**. Final cis-dihydroxylation of the double bond and acetal hydrolysis gave *allo*-inositol. (Scheme 64)

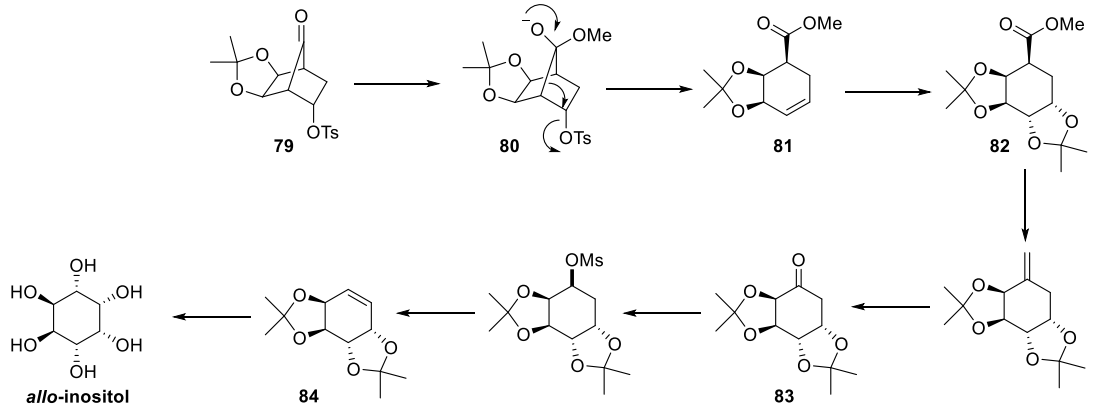

Scheme 64. Preparation of *allo*-inositol using norbornyl derivative **79**

3.5. *Myo*-inositol as starting material

Besides their role in intracellular pathways and as precursors of pharmacologically active agents, inositols were also widely studied as starting materials. The most important advantages in this direction are the cost and availability, together with the chemical similarity compared to other biologically active classes of compounds.

Polyhydroxy-benzenes are widely present in natural products and their activity ranges from antitumoral to antibacterial, antiviral, antifungal and anti-inflammatory. Presence of phosphate groups often allows them to act as inositol mimics in intracellular cascades. Having the possibility to obtain large quantity of inositol from natural sources, Gurale et al. proposed some synthetic pathway able to convert myo-inositol to 1,2,3,5-tetrahydroxy benzene derivatives with potential therapeutic activity. [131]

In particular, their approach provided for the 1,3-acetal protection on the *myo*-inositol analogue **85**, where a ketone is present at the C(5) and the residual hydroxyl groups are protected as benzyl ethers. Treatment of **85** with NaH at 0 °C for 5 minutes surprisingly afforded aromatic derivative **86**. This observation indicated the anomalous deprotection of a protecting group, such acetal is, generally very stable in alkaline reaction environment, whereas the aromatization took place because of intramolecular enolizations. Exposure of **85** to acidic conditions provided for the deprotected inositol **87**, but without racemization occurring. The same **87** was then treated to NaH, so that again **86** was obtained. Using Et_3N as the base, it was possible to isolate the unsaturated

ketone **88**, as key intermediate for the conversion to the aromatic scaffold, prior to NaH treatment. (Scheme 65)

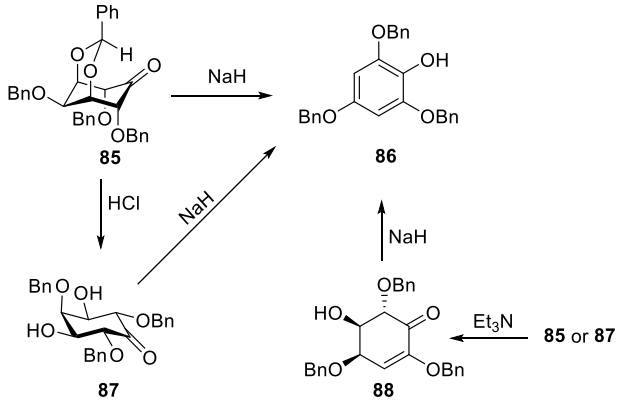

Scheme 65. Preparation of aromatic scaffold of **86** from NaH-based approach on inositols **85** and **87**

A new way to poly-hydroxy biaryl scaffold was developed, treating ketone **85** with PhMgBr and HCl, in order to deprotect the acetal moiety and afford triol **89**. Tosylation of one of the two equatorial hydroxyl groups (compound **90**) and subsequent treatment with NaH, allowed the aromatization and the isolation of the biaryl derivative **91**, as well as differently substituted benzene derivatives, when Grignard reagents other than PhMgBr were used. (Scheme 66)

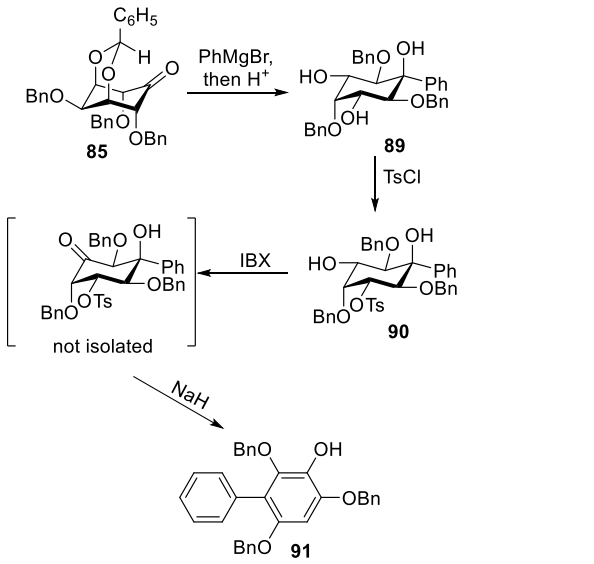

Scheme 66. Obtainment of biaryl scaffold **91** from treatment of ketone **85**

Chen et al. focused their research on *myo*-inositol as base scaffold for the synthesis of selective anticancer agents. [132] Starting from the observation that inositol phosphates represent important second messengers in intracellular signaling, they tried to prepare IP_3 analogs bypassing their polarity due to the negative charge induced by the phosphate presence. To improve their penetration through cellular membrane bio reversible phosphates were introduced, in order to better understand the mechanisms behind the intracellular signaling by PIPs. Taken inspiration from the functionalization on the antiviral phosphonoacetate, the authors proposed the protection in form of acyloxy benzyl ester, so that it was easier for the molecule to bypass the phospholipidic double layer. Once in the cytoplasmic environment, esterase would have hydrolyzed the acyloxy group, favoring the rearrangement and fragmentation to quinone methide, presumably due to the electron-donating contribution of hydroxyl group on the hydroxy-benzyl moiety. Esterase hydrolysis of the second benzyl acyloxy group and subsequent fragmentation would release the active drug within in the intracellular environment. (Scheme 67)

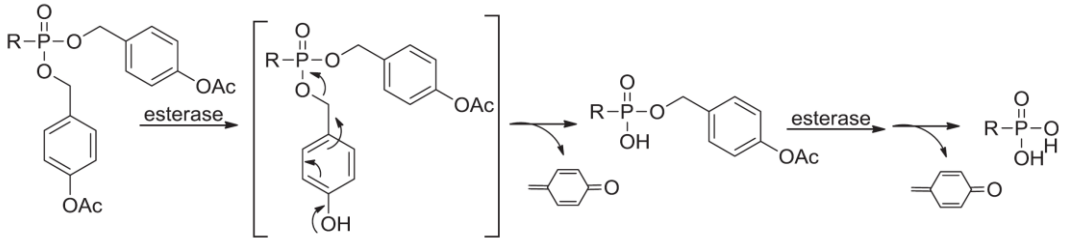

Scheme 67. Pro-drug like approach for the intracellular release of highly charged molecules, such as IP3 derivatives

Different PIP analogues were prepared, in order to test *myo*-inositol derivatives acting as false substrates within intracellular cascade signaling. Protection on the hydroxyl groups was performed, exploiting acetals, benzyl, *p*-methoxybenzyl and allyl ethers, so that one to three -OH could remain unprotected and free to be phosphorylated as benzyl phosphoesters. *In vitro* cytotoxic essays on different human cancer cell lines highlighted a good activity profile for most of the prepared products, with a better toxicological behavior than cis-platin, used as the reference; in general, more the phosphorylation degree, lower the cytotoxic activity. (Scheme 68)

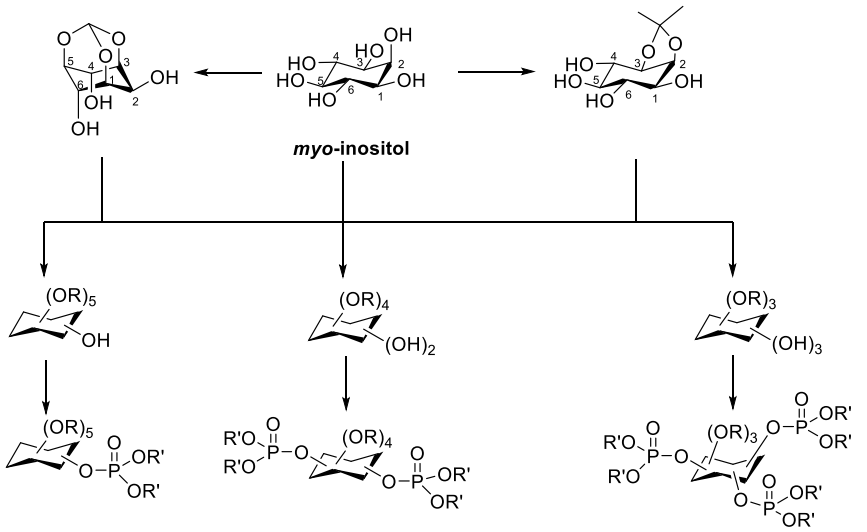

Scheme 68. Schematic representation of the possibilities offered by regioselective protections and phosphorylations

Due to their activity as glycosidase inhibitors, aminocyclitol derivatives have been considered interesting compounds containing the *myo*-inositol core. In particular, (-)-valiolamine, potent inhibitor towards maltase and sucrase, represents the direct precursor of the antidiabetic agent voglibose. [133] In nature it is isolated from the fermentation broth of validamycin and is present as component of validamycin G, [134] while several syntheses have been accomplished starting from D-glucose or through Diels-Alder reaction between furan and acrylic acid, among the others. [135,136] (Scheme 69)

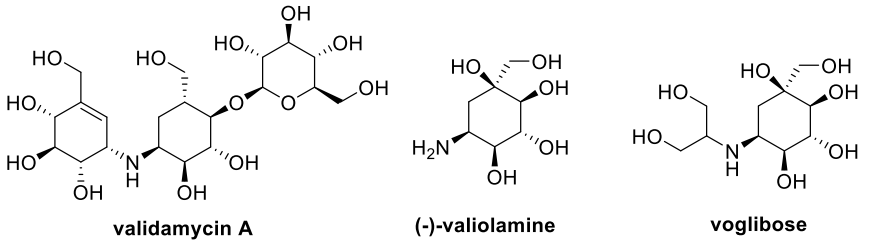

Scheme 69. Chemical structures of aminocyclitol derivatives validamycin A, (-)-valiolamine and voglibose

Ogawa and Kanto designed the synthesis of (-)-valiolamine, starting from *myo*-inositol in optically pure way, exploiting the bio-oxidation by *Salmonella typhimurium* to ketone **92**, that after dehydration led to unsaturated ketone **93**, in tautomeric equilibrium with the diketo derivative **94**. [137] Further bio-reduction afforded quercitols

96, **97** and **98**, obtained in different ratio even when hydrogenation on platinum catalyst was performed on the diketone **94**, affording (-)-*vibo*-quercitol **95** as the main product. (Scheme 70)

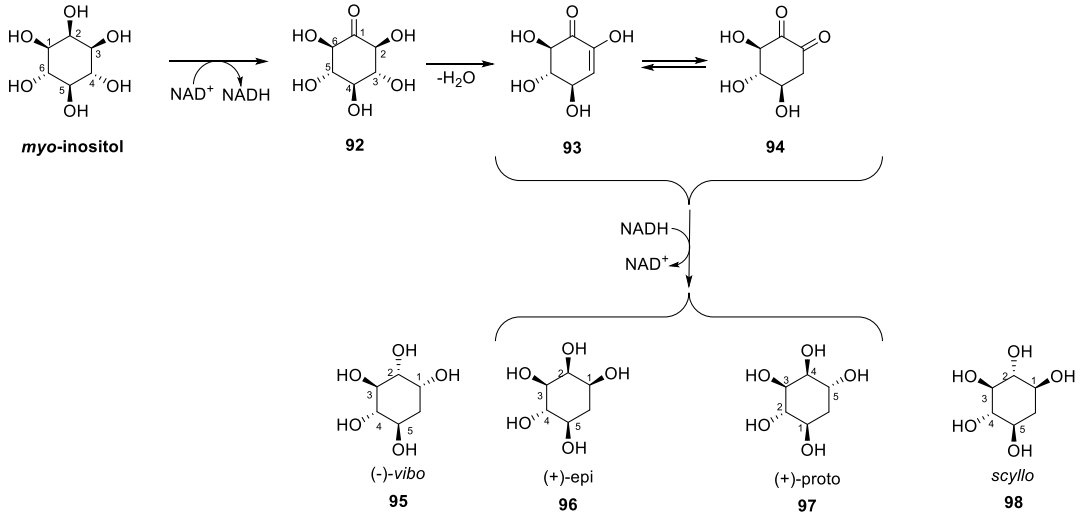

Scheme 70. Bio-oxidation of *myo*-inositol, followed by dehydration and further bio-oxidation, afforded enantiomerically pure **95-98**

Bio-oxidation of **95** by *Gluconobacter* sp. AB10277 afforded crude ketone **99**, that was converted to the spiro epoxide **100**, treated with KOH at 100 °C to obtain the primary alcohol **101**. Protection of **101** in form of benzylidene acetal afforded **102** as the main product, that was further protected in form of dimethyl acetonide, leading to a mixture of diastereoisomers **103** and **103diast**, easily separated by column chromatography. Exposure of **103** to an excess of tosyl chloride brought to the quantitatively formation of tosylate **104**, undergone nucleophilic substitution with NaN_3, providing **105** with inversion of the stereocenter at C(5). Hydrogenolysis in presence of acetic anhydride, followed by acidic hydrolysis of the resulting acetamide derivative, afforded pure **(-)-valiolamine**. (Scheme 71)

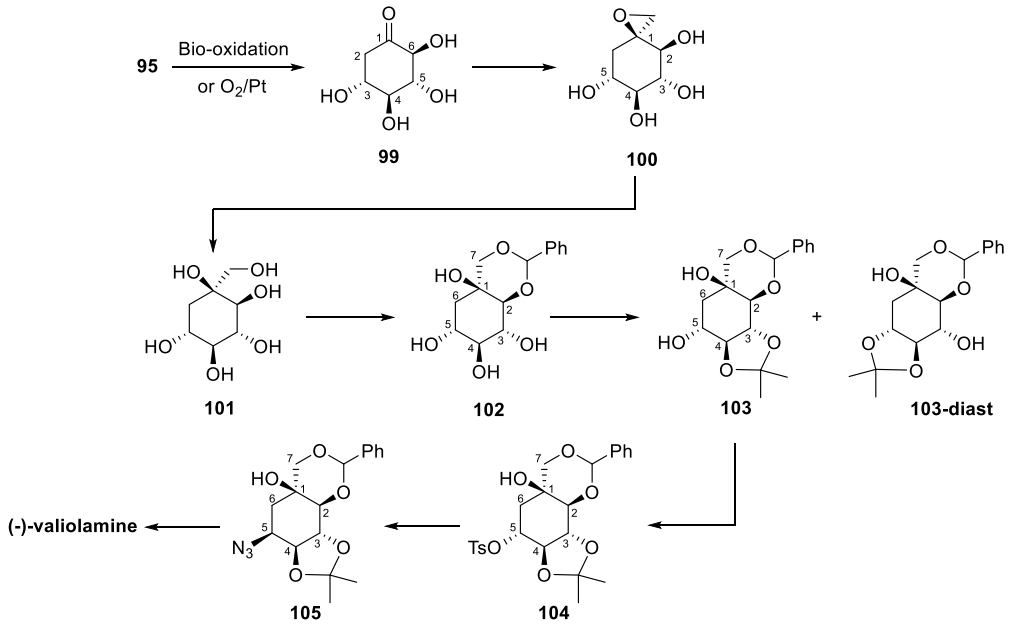

Scheme 71. Synthesis of (-)-valiolamine starting from (-)-*vibo*-quercitol **95**

Lipopolysaccharide (LPS) is a molecule produced by gram negative bacteria, found on the outer side of the membrane and essential for the activation of the immunological system of the host. [142] The monomeric structure taking part of LPS skeleton is represented by D-bradyrhizose, a bicyclic monosaccharide with a core characterized by a cis-decalin-like core and α1-7 (or α1-9) bonds to favorite the homopolymerization. Retrosynthetic analysis on D-bradyrhizose performed by Aboussafy et al. focused on, at first, the disconnection at the level of the carbohydrate moiety; [143] then, they identified in ethyl propiolate and adequately protected and functionalized *myo*-inositol derivative as the starting materials. (Scheme 72)

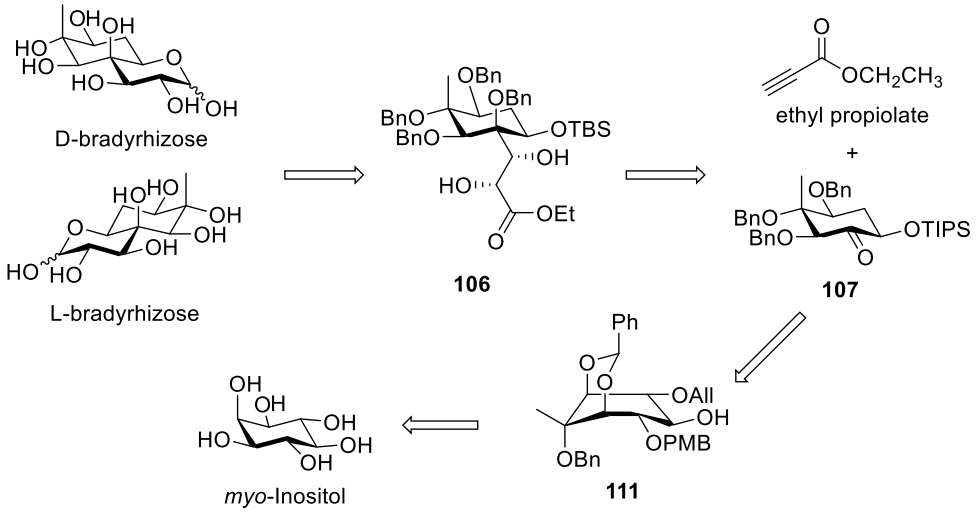

Scheme 72. Retrosynthetic approach for the synthesis of bradyrhizose

Protection of *myo*-inositol as orthobenzoate, followed by selective allylation and *p*-methoxybenzylation on the two axial hydroxyl groups afforded **109**, whose OH was oxidized to ketone and treated with MeMgBr to give tertiary alcohol **110**. Benzylation of **110** and orthobenzoate reduction by DIBAL afforded **111**, on which the alcoholic portion was protected as silyl ether and further treated with DIBAL on acetal moiety, affording a mixture of regioisomers (**112a** and **112b**), that anyway will be protected as tribenzylated **113**. Deallylation was performed in presence of $PdCl_2$, providing for alcohol **114**, that was then treated with LHMDS, CS_2 and CH_3I, to afford the xanthate ready to be deoxygenated. Addition of tributyl stannane in presence of AIBN allowed the Marton-McCombie deoxygenation (compound **115**), while PMB deprotection in acidic conditions and subsequent Swern oxidation provided for ketone **107**. (Scheme 73)

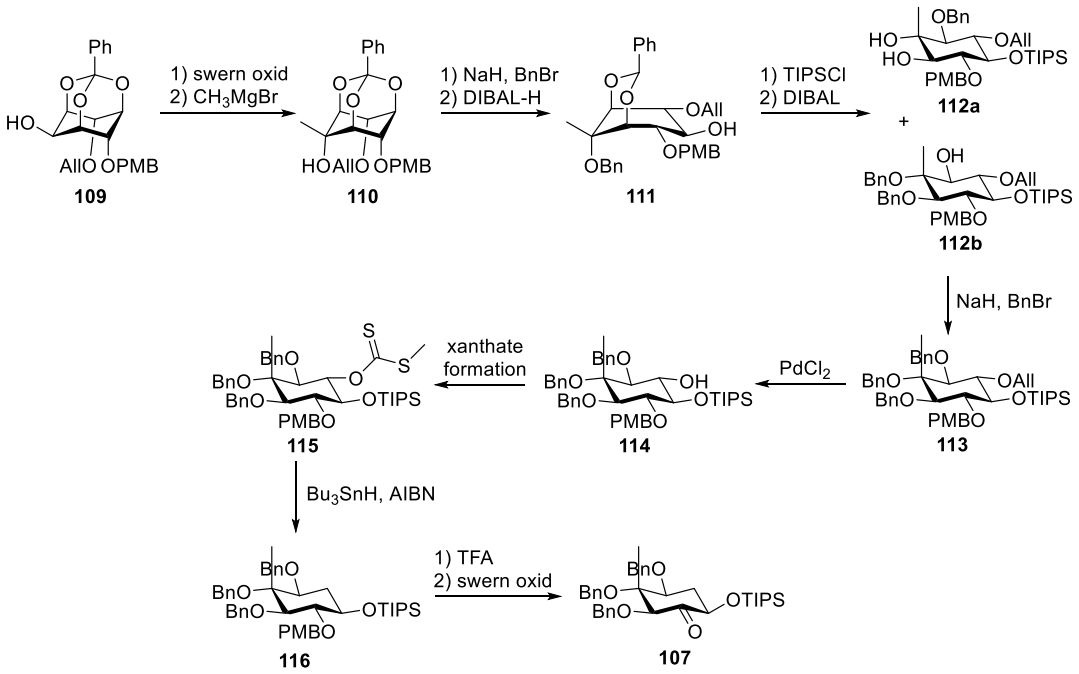

Scheme 73. Synthesis of the intermediate **107** starting from the orthobenzoate of *myo*-inositol

Lithium salt of ethyl propiolate was used as the nucleophile towards the ketone addition in a selective way from the less hindered side (equatorial, downside, compound **117**). Reduction by Red-Al® afforded trans-α,β-unsaturated ester **118**, that underwent silyl deprotection to give diol **119**, whose hydroxyl groups were protected as benzylidene acetal (compound **120**). Regioselective dioxolane ring opening by triethylsylane left the benzyl ether in axial position, whereas the free equatorial OH group was protected in form of TBDMS ether (compound **122**). Cis-dihydroxylation on the double bond and subsequent desilylation afforded a 3:1 mixture between the ester **123** and the bicyclic desired scaffold **124** in which the equatorial free OH group attacked the ethyl ester. Lactone reduction by DIBAL and debenzylation of **125** provided for the mixture of D- and L-bradyrhizose. (Scheme 74)

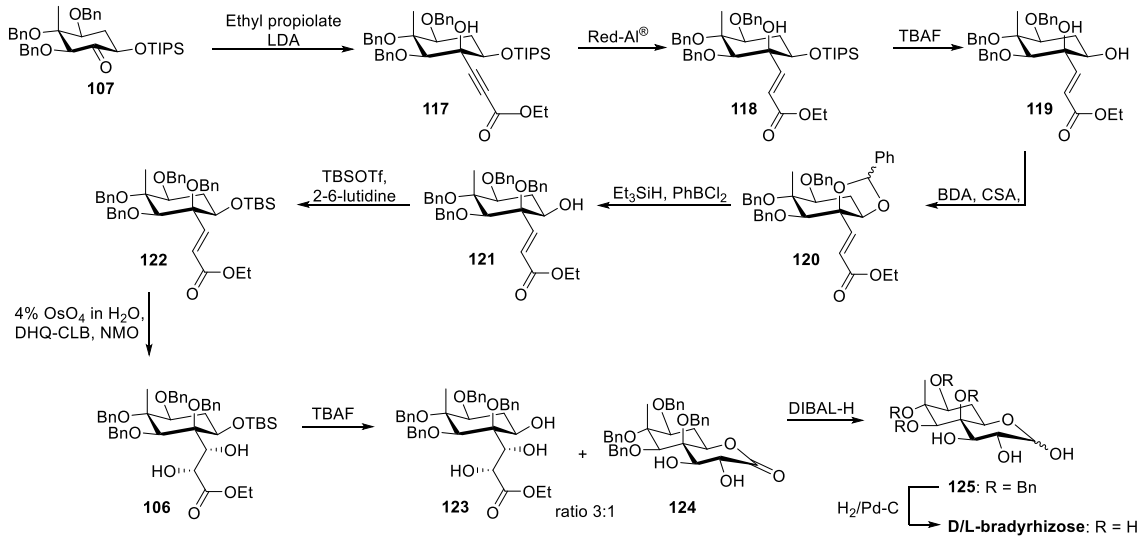

Scheme 74. Synthesis of mixture of D- and L-bradyrhizose

In order to obtain enantiomerically pure D-bradyrhizose, racemate diol was derivatize exploiting (S)-(−)-α-methoxy-α-(trifluoromethyl)phenylacetic acid to obtain the diastereoisomeric esters. Surprisingly, the chiral acid was able to react better with the undesired L-derivative, affording **L-126** while D-ester was esterified in minimum amount, so that most of the starting material remained unreacted (in form of the diol **D-106**) and diastereoisomerically pure. Desilylation of **D-106** afforded once again a 3:1 ratio of the opened and closed derivatives **D-123** and **D-124**, but treatment by DIBAL allowed to reduce the ester of **D-123** to aldehyde, furtherly favoring the formation of the lactone **D-124**, then reduced to the carbohydrate moiety of **D-125**. Debenzylation afforded in stereoselective manner D-bradyrhizose. (Scheme 75)

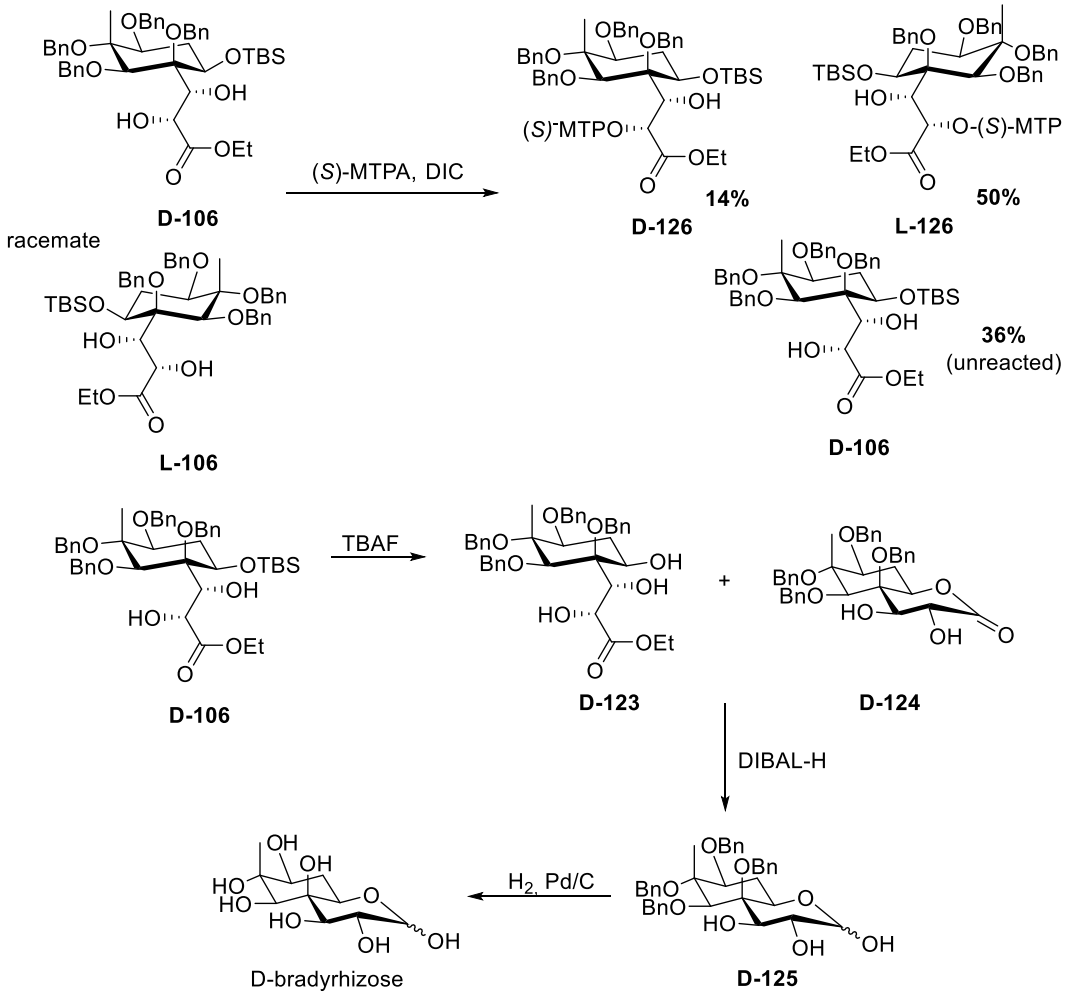

Scheme 75. Stereoconvergent approach to the obtainment of D-bradyrhizose

Oxyrapentins represent a class of highly oxidized chromene analogs, isolated from natural sources such as fungi of *Isaria felina*. [144] Sakai et al. focused their attention mostly on *oxyrapentin D*, presenting a 2,4,10-trioxaadamantane core, resulted active in preliminary biological studies as growth-inhibitor on *Staphylococcus aureus* and *Bacillus subtilis*. [145] Retrosynthetic approach provided for disconnection at the level of the tertiary alcohol, obtained from the addition of alkyne **I** to the ketone **II**, itself deriving from oxidation of the secondary alcohol of **III**. **IV** was considered as product of prenylation and hydrazone generation, starting from *myo*-inositol protected as orthoacetate x. (Scheme 76)

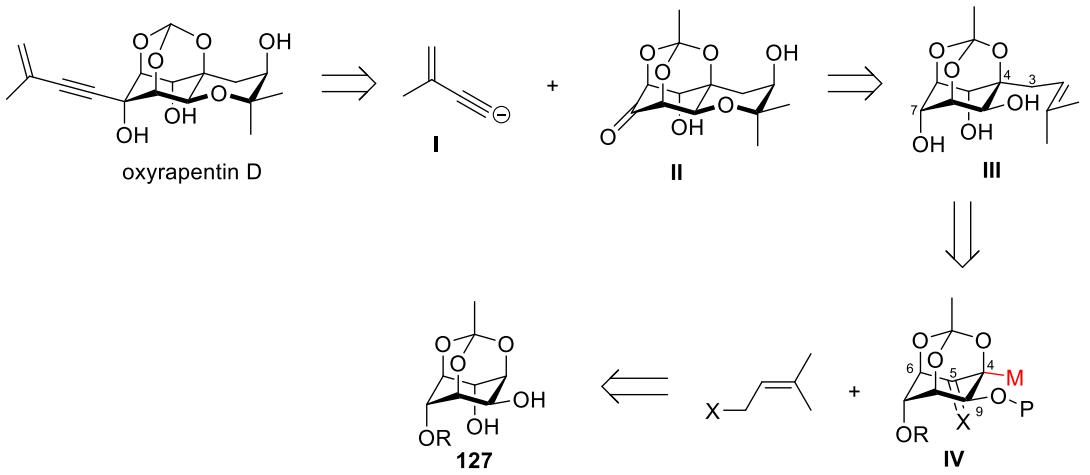

Scheme 76. Proposed retrosynthetic approach for the synthesis of oxyrapentin D

Myo-inositol was treated with trimethyl orthoacetate to give triol **127**, temporarily protected on the two axial hydroxyl groups in form of boronate, so that the residual free OH could be protected in presence of SEM-Cl. Alkaline oxidative cleavage of boronate protection afforded **128** as a cis-1,3-diol, ready to be selectively protected as silyl ether on one of the two axial OH (compound **129**). Oxidation to ketone **130** and treatment with methyl-methoxyethylenhydrazine afforded hydrazone derivative in a mixture of the two regioisomers **131-cis** and **131-trans**. Lithiation at the vicinal carbon with respect to SEM ether, in optimized conditions afforded the prenylation product **132**, as analogue intermediate of **IV**. (Scheme 80)

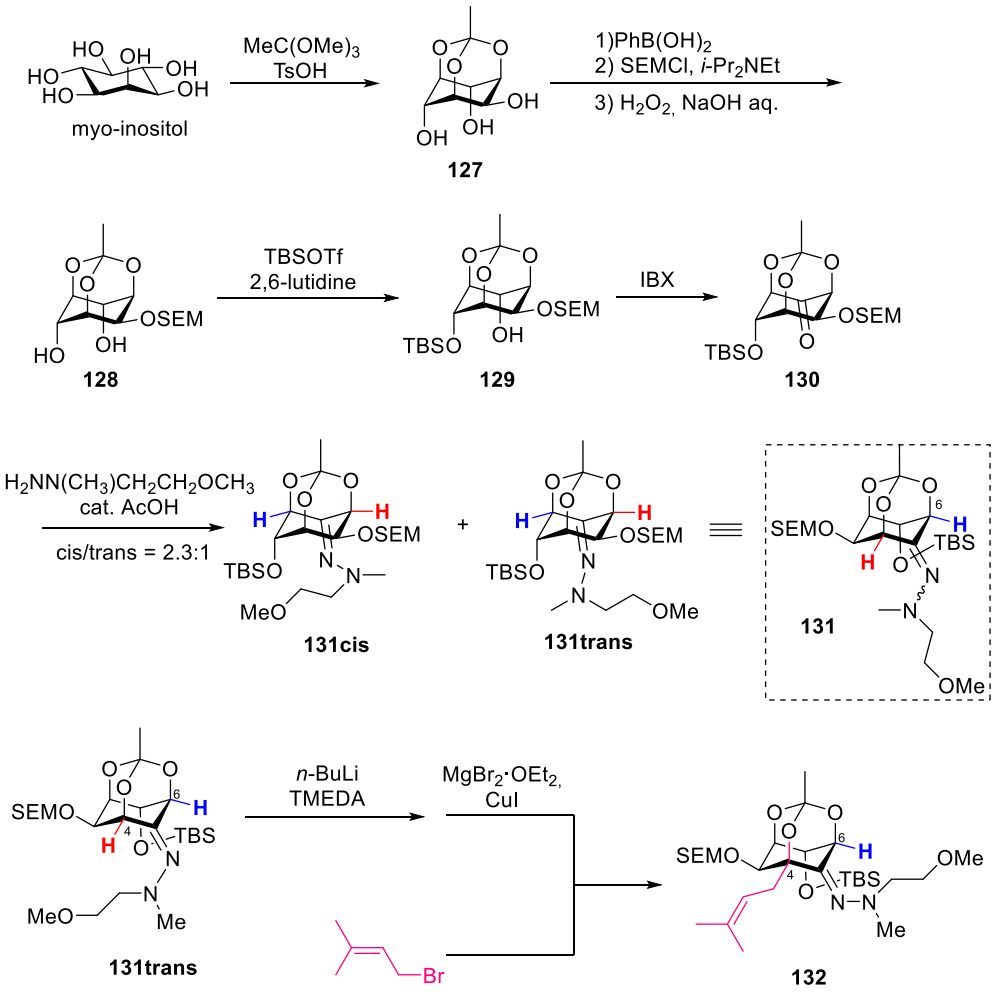

Scheme 77. Preparation of **132**, as analogue of **IV**, starting from *myo*-inositol

Conversion to ketone **133** was favored by treatment with methyl triflate, followed by $NaBH_4$ reduction, to provide selectively the alcohol in axial position (compound **134**), because of the more favorable hydrogen bond with the OTBS group. Deprotection of TBS and SEM ethers afforded triol **III**, ready to react with iodine to afford the not isolable iodonium intermediate, able to be attacked by equatorial hydroxyl group to afford iodotetrahydropyran **135**. (Scheme 78)

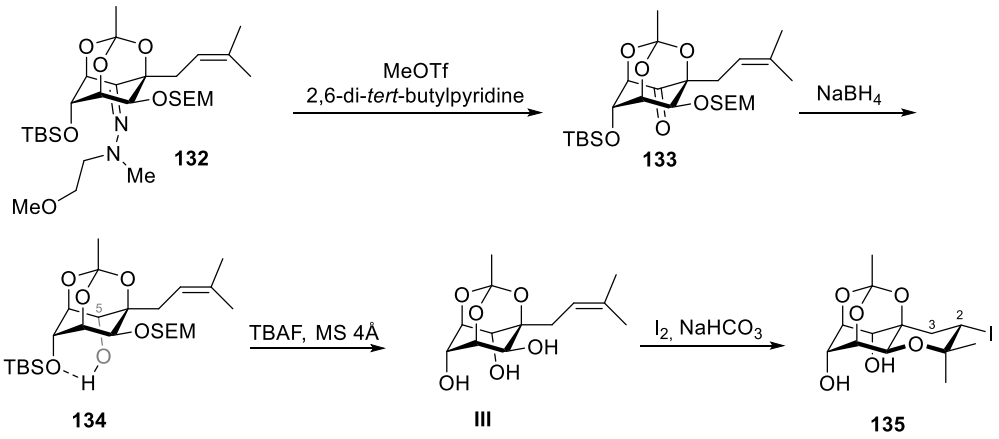

Scheme 78. Preparation of tetrahydropyran moiety of **135**

S_N2 on iodine did not allow the formation of the desired axial oxygen because of the steric hindrance given by the orthoacetate moiety. In order to overcome this difficulty double bond of the propenyl substituent on **III** was epoxidized in presence of $VO(acac)_2$ and peroxide, so that β-epoxide (obtained as the single diastereoisomer **136**) could be then attacked intramolecularly by the equatorial hydroxyl group, to give **137**. The solvent of choice for the ring closure was HFIP, because of its highly polarity (related to the polarity of the epoxide **136**), the less nucleophilicity compared to the defluorinated analogue and the relative acidity, able to activate the epoxide towards the nucleophilic attack. The tetrahydropyran triol **137** was ready to be oxidized selectively (due to the steric hindrance on the other positions) at the C(7) in presence of the BF_4^- ammonium salt of TEMPO, affording the desired ketone **II**, in equilibrium with its hydrate form **161**. Finally, treatment of the mixture of **II** and **138** with lithium acetylide **I** gave selectively *oxyrapentin D*. (Scheme 79)

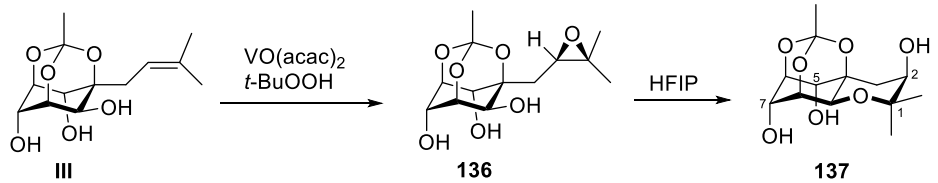

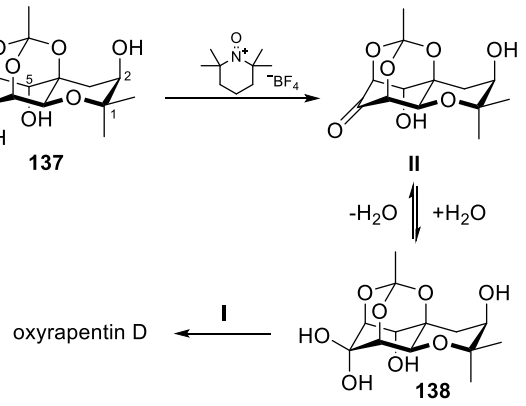

Scheme 79. Oxyrapentin D obtained from intermediate **III**

Phosphorylated, glycosylated and unmodified inositols are widely present in plants and animals and are easily affordable. On the other hand, methylated ones are only produced by plants, as they seem involved in important physiological roles, so that their isolation requires long and low-yielding extractions from natural sources. [146] To overcome these conditions and easily study the chemical and biological characteristics of these derivatives, Sureshan et al. proposed the total synthesis, in particular, of brahol (5-O-methyl-allo-inositol, isolated from *Stocksia brahuica*) and (+)-pinpollitol (dimethyl ether deriving from D-*chiro*-inositol, of which was not known the exact structure) starting from *myo*-inositol. [147]

From the retrosynthetic point of view, brahol can be obtained by methylating protected *allo*-inositol **139**, itself obtained by inversion of configuration of the stereocenter at C(2) of *myo*-inositol **141**. (Scheme 80)

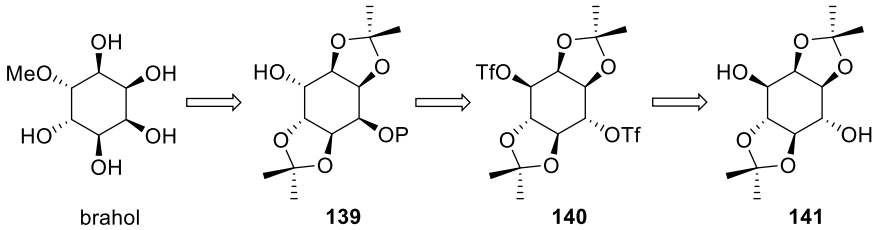

Scheme 80. Proposed retrosynthesis for *brahol*

Protection of *myo*-inositol as diketal derivative gave diol **141**, that was triflated on both OH groups that in this way can act as suitable leaving groups for the inversion of configuration. Treatment of ditriflate **140** with KOAc afforded the bis-acetate **142** that

was selectively hydrolyzed at the C(5) to afford alcohol **143**, ready to be methylated to **144** and completely deprotected, providing *brahol*. (Scheme 81)

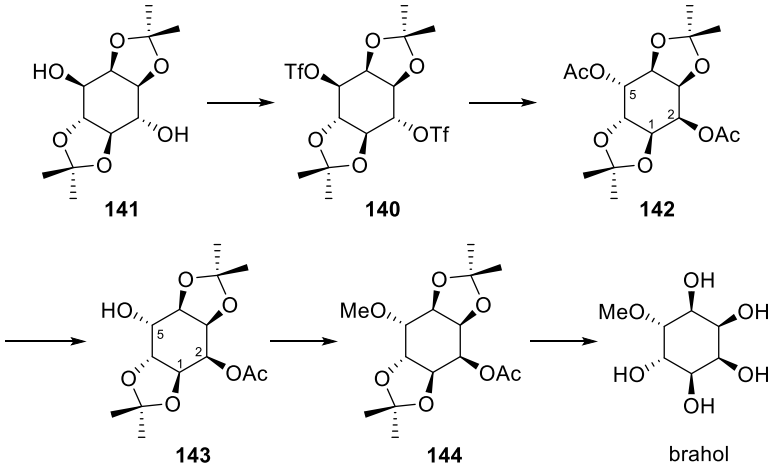

Scheme 81. Synthesis of brahol starting from *myo*-inositol diketal **141**

Because of the unconfirmed structure of (+)-pinpollitol, two different approaches were proposed: the first one (**145**) is related to the mono-inversion of the configuration at C(1); the second one (**146**) related to the inversion of configuration at C(1), exploiting different protecting groups. (Scheme 82)

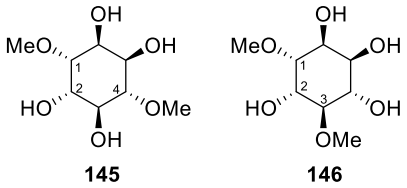

Scheme 82. Proposed structures for (+)-pinpollitol

Starting from the previously described diketal **141**, regioselective mono-O-triflation of hydroxyl group at the C(1) afforded **147**, undergone KOAc nucleophilic attack to give alcohol **148**. Acetylation of **148** provided for the diacetyl derivative **149**, that was then hydrolyzed and methylated to give **151**, ready to be deprotected, affording **145**. (Scheme 83)

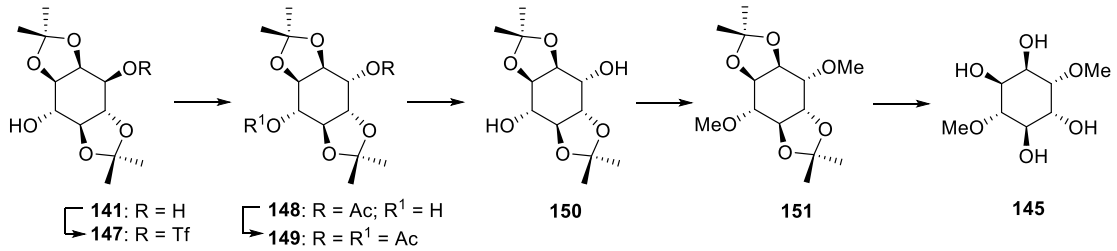

Scheme 83. Synthetic pathway for the obtainment of the first hypothesized structure for (+)-pinpollitol **145**.

Regioisomer (+)-pinpollitol II was obtained starting from tribenzyl orthoformate derivative of *myo*-inositol **152**. Hydrolysis of the orthoformate protection afforded triol **153**, that was regioselectively benzylated at the C(5), providing diol **154**, which in turn is mono-triflated at the C(1) (compound **155**). The residual free hydroxyl group was then acetylated to give **156**, undergone KOAc treatment with inversion of the stereocenter (compound **157**). Deacetalyzation and methylation afforded **159**, that was finally debenzylated to afford desired **146**. Comparison between the spectra of natural deriving with the synthetic compound revealed that the correct structure for (+)-pinpollitol is represented by **145**. (Scheme 84)

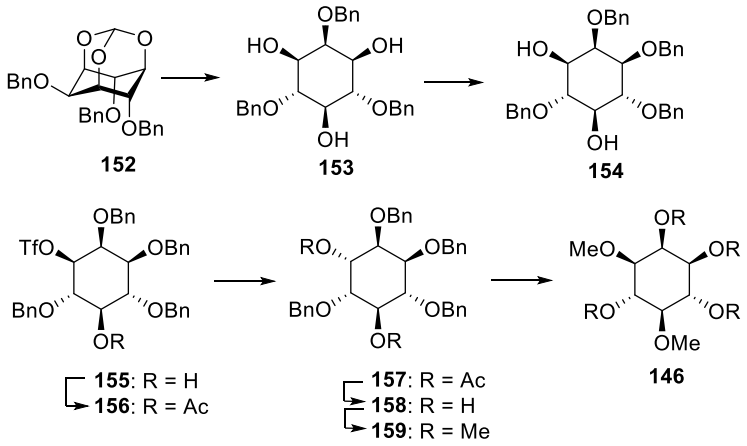

Scheme 84. Synthetic pathway towards the preparation of **146**

3.5 Desymmetrization approaches on inositol derivatives

Given that *myo*-inositol and most of its stereoisomers are *meso* forms, approaches for the desymmetrization of the molecule in this context were taken in consideration within several publications about inositols, [149] in order to avoid tedious and low-yielding pathways providing for the derivatization and the separation of

diastereoisomers, of which two significant examples will be reported. Amongst several ways to provide the enantiomerically pure inositol derivatives starting from the *meso* forms, the most representative four are listed below.

Garrett et al. dealt with the enantiomerically pure synthesis of Ins(1,4,5)P_3, starting from *myo*-inositol protected in form of orthoester. [150] The authors considered as very important the possibility to conduct such a synthetic pathway avoiding chromatographic purifications, together with the optimization of the reaction conditions in order to reduce the number of the steps needed for the obtainment of the enantiomerically pure compound. For these reasons, orthoformate was excluded as protecting group, because of its lability towards the acidic environment required for the obtainment of some intermediates. Orthoacetate **160** was then chosen as the protecting orthoester for *myo*-inositol, that was then di-O-acylated in presence of (S)-(-)-camphanoyl chloride and a catalytic mount of DMAP to afford the two diastereoisomeric dicamphanates **161** and **162**. Crystallization instead of chromatographic purification allowed the isolation of D-2,6-di-O-camphanate derivative in 37% yield **161**, while L-form **162** was recrystallized from methanol in 40-45% yield. Acidic hydrolysis by refluxing HCl of orthoacetate moiety of **161** afforded D-tetraol **163**. Selective conversion to monoacetate **164** was provided by treatment with 80% TFA and afforded also its regioisomers **165**. Phosphitylation in presence of phosphoramidite, followed by oxidation, gave derivative **166**, that underwent hydrogenolysis and aminolysis to afford **D-Ins(1,4,5)P_3**, tested for biological activities. (Scheme 85)

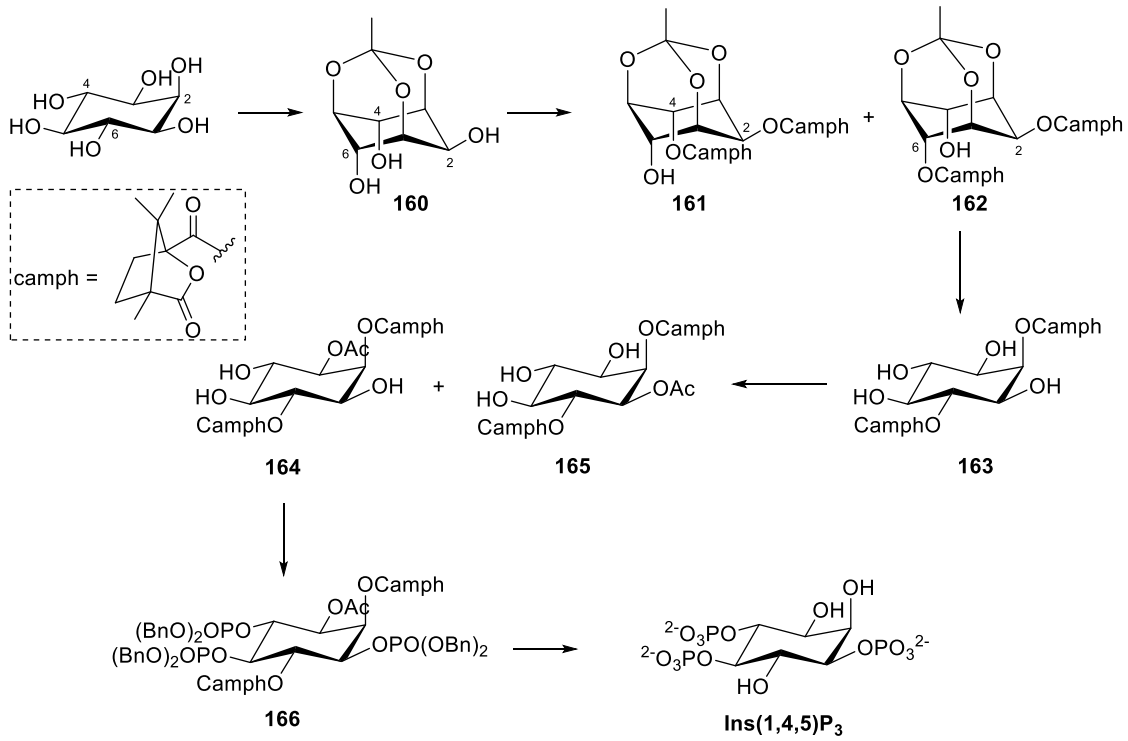

Scheme 85. Diastereoselective synthesis of **D-Ins(1,4,5)P$_3$** by using camphanate as chiral auxiliary.

Watanabe et al. reported in 2004 the resolution of derivatized triol **167** from 1,3,5-orthoformate protection of *myo*-inositol. [151] First of all, the triol was chosen as starting material because of the possibility to isolate it as pure with very high yield, if compared to the diketal derivatives (maximum yield 25%). Moreover, regioselective acylation on the free hydroxyl groups was widely studied, so that the di-functionalization in presence of 2 equivalents of acylating agent could have reasonably afforded the 2,4- and 2-6-di-O-diacylated orthoformate *myo*-inositol **168** and **169** The acylating agent that was described and used was the O-acetyl mandelic acid, as cheaper and more valid alternative to the previously reported camphanate derivatives. Functionalization of the two hydroxyl groups in position 2 and 4 in presence of (S)-(+)-O-acetyl mandeloyl chloride (or its enantiomeric R(-) form) provided for two great advantages: 1) the formation of chromatographically distinguishable diastereoisomers, that could be purified, characterized and further functionalized separately; 2) the possibility to recognize which diastereoisomer was the D- or the L-enantiomeric form, basing on the chiral anisotropy reagent O-acetyl mandelic acid, able at the NMR analysis to screen

certain protons when one enantiomer was used for the acylation instead of the other. [152] (Scheme 86)

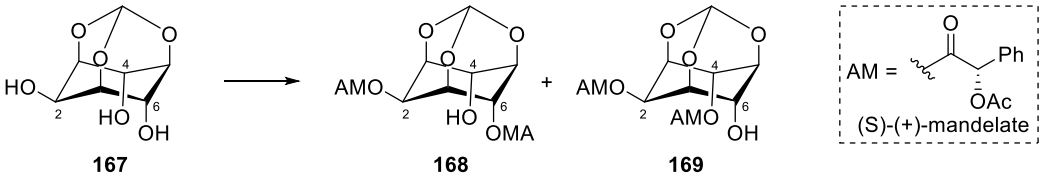

167 168 169

Scheme 86. Diastereoisomeric mixture of **168** and **169** from functionalization by optically pure (+)-mandelate

Using the acylating chloride (S)-(+)-acetyl mandeloyl chloride (**AMC**l), in presence of pyridine as the solvent in a cooled bath at 0 °C, a 3:7 mixture of 2,6- and 2,4-di-O-acylated-*myo*-inositol orthoformate **168** and **169** was afforded in good yield. It was worth noting that performing the reaction at higher temperatures, a 1:1 ratio was formed, probably because the dynamicity of the reaction brought to an easier acyl migration. Careful chromatographic purification, gave the alcohol **169**, that was protected in THP ether form **170**, hydrolyzed to the diol **171**, dibenzylated and deprotected from THP, to afford the known L-2,4-di-O-benzyl-*myo*-inositol **173**. Similar treatment was exploited for the characterization of D-2,4-di-O-benzyl derivative. (Scheme 87)

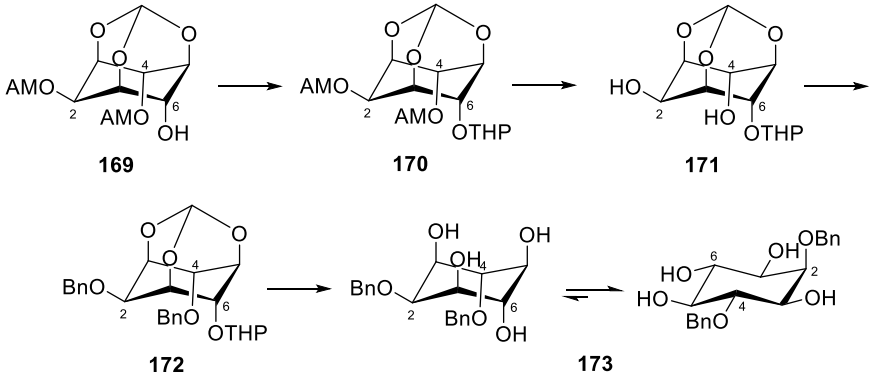

169 170 171

172 173

Scheme 87. Obtainment of optically pure dibenzylate **173**, exploiting acetyl mandeloyl chloride as chiral auxiliary

Enzymatic resolution of 1,3-di-O-benzyl-*myo*-inositol **174** was studied in presence of different commercially available immobilized lipases. Because of their ability to stereoselectively catalyzed a wide range of functionalization, three types of lipases were considered by Ribeiro et al. within its studies: Novozym 435, Lipozyme TL-IM

(from *Thermomyces lanuginosus*) and Lipozyme RM-IM (from *Rhizomucor riehei*). [153] In presence of vinyl acetate as the acyl donor and the solvent, Novozym 435 afforded with almost complete conversion meso 5-O-acetylated derivative **175**, whereas both of the Lipozymes provided for the enantioselective acetylation to give enantiomerically pure **L-(+)-176** with a >90% conversion. (Scheme 88)

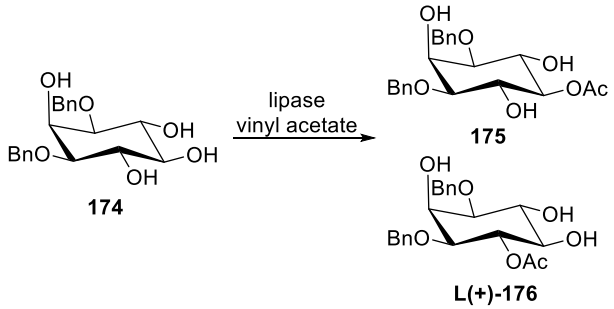

Scheme 88. Enzymatic resolution of meso **174** afforded acetylated optically pure **L(+)-176**

When vinyl acetate was replaced with ethyl acetate, in all of the cases worse results were obtained, though maintaining the same regio- and stereoselectivity of acylation. Explanation about these results was given taking in consideration that vinyl acetate, after acyl donation, gave acetaldehyde as byproduct, so that no competitive substrates were present within the reaction environment; on the other hand, ethyl acetate gave ethanol as byproduct, that can re-attack the acyl group preferentially in comparison with the hindered OH group of myo-inositol. Use of different co-solvents was studied, highlighting that a 1:1 mixture of vinyl acetate and ethyl acetate afforded the best performance when Lipozyme TL-IM was used for the acetylation of diether derivative of *myo*-inositol **174**, affording **L(+)-176** with higher conversion rate than RM-IM and complete regio- and stereoselectivity. The possibility for the biocatalyst to be reused was evaluated and it was evident that, in presence of ethyl acetate as the co-solvent TL-IM could be used for seven cycle (each lasting one hour) without any loss of conversion rate and/or selectivity. Configuration of **L(+)-176** was assigned on the base of known derivatives.

Padijar et al. proposed a completely new strategy in order to make viable the synthesis of natural polyphosphorylated inositols, and fully understand the mechanisms behind

the cytotoxic activity of this enantiomerically pure compound and its analogues on several cancer cell lines. [154] Because of the studies performed until now, *myo*-inositol orthoformate appeared to be appropriate as the feasible starting material, ready to be appropriately functionalized in regio- and stereoselective fashion, so to get through the limitations represented by several protection-deprotection steps, functional group migrations and isolation of unstable key intermediates. Based on previous publications made by the same group for the preparation of mannosyl derivatives for the *myo*-inositol desymmetrization, [155] a chiral anhydride-based approach was reported, in presence of a catalytic amount of metal triflate, $M(OTf)_3$. In fact, metal M^{3+} was able to simultaneously coordinate the oxygen of the dioxane used as the solvent, the two hydroxyl groups in axial position of *myo*-inositol orthoformate, as well as activated the anhydride and the acylating agent in the right conformation for the properly further attack by OH at C(4) or at C(6), giving the 2,6- or the 2,4-diol **177** and **178**, respectively. (Scheme 89)

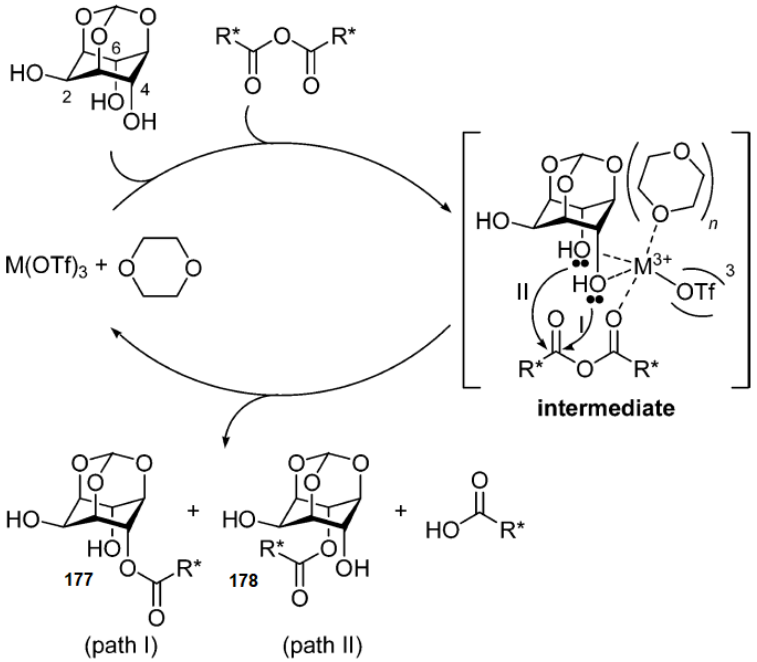

Scheme 89. Proposed mechanism for the regioselective acylation on *myo*-inositol orthoformate

Due to its small atomic radius and high catalytic activity, ytterbium drew attention as the best choice in terms of transition metal options, while different acid derivatives among the acylating agents were tested. At first, anhydride from O-acetyl mandelic

acid was used, affording in presence of 1 mol% of the catalyst the 4-mono ester **177a** in 49% yield, next to the 35% of the 6-mono ester **177b**. When some N-tosyl proline anhydride was employed the ratio between the two diastereoisomeric forms was inverted, so that the 6-mono **178b** ester was more represented (62% yield), with respect to the 4-mono ester **178a** (24% yield), affording the best regioselective result within these attempts. Increase of the catalyst charge (5 mol% instead of 1 mol%) resulted in lower yield, due to deprotection of orthoformate moiety, while other transition metal catalysts were screened (La, Pr, Nd, Sm, Eu, Gd) but with worse outcomes than Yb. To fully characterize the obtained ester and assign to it the correct configuration, benzylation followed by ester hydrolysis was performed. It was important to note that the classical Williamson etherification conditions were not compatible with the stability of the obtained ester, so that treatment of the isolated mono esters with N-phenyl-2,2,2-trifluoacetimidate in presence of triflic acid was needed for the dibenzylation. Finally, hydrolysis of the chiral ester portion gave dibenzylates **180a** and **180b**. (Scheme 90)

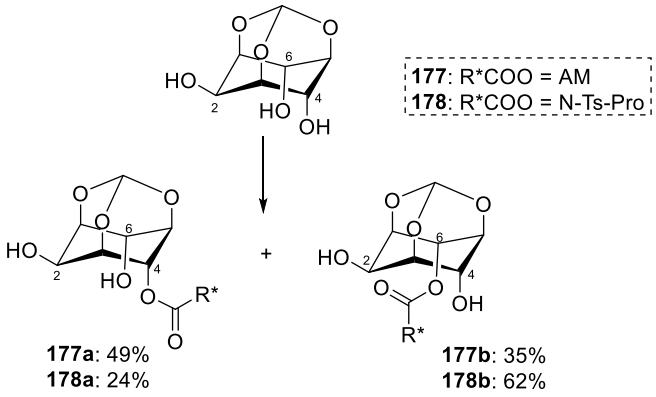

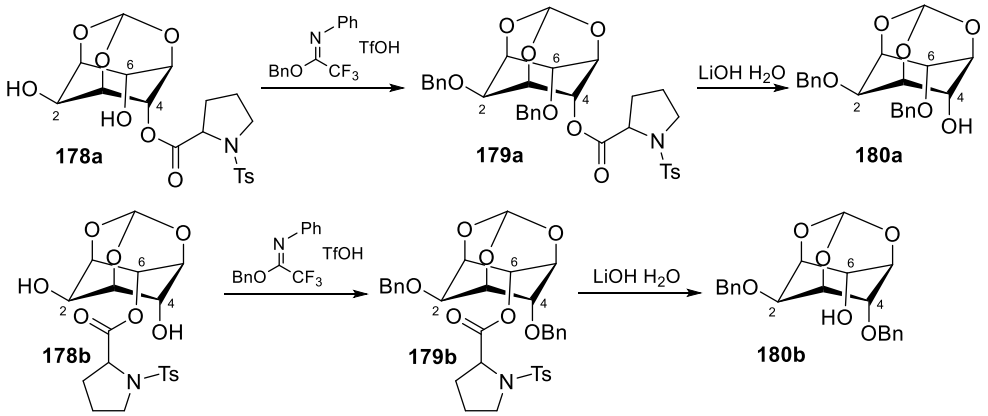

Scheme 90. Different derivatization on *myo*-inositol orthoformate gave different diastereoisomers **177** and **178**, hence diastereoisomeric dibenzylates **180**

In order to obtain enantiomerically pure phosphate derivative of *myo*-inositol treatment with dibenzyl-N,N-diisoproprylphosphoramidite in presence of tetrazole, followed by mCPBA oxidation, favored the formation of dibenzyl phosphate ester **181**. Hydrogenolysis, acidic hydrolysis and treatment by Na^+ ion-exchange resin afforded Ins(6)P **182**. In order to achieve the obtainment of Ins(2,4)P_2, 6-mono ester **178b** was treated to obtain the diphosphate moiety, then hydrogenated and hydrolyzed, before NaOH-mediated salification, to afford **184**. (Scheme 91)

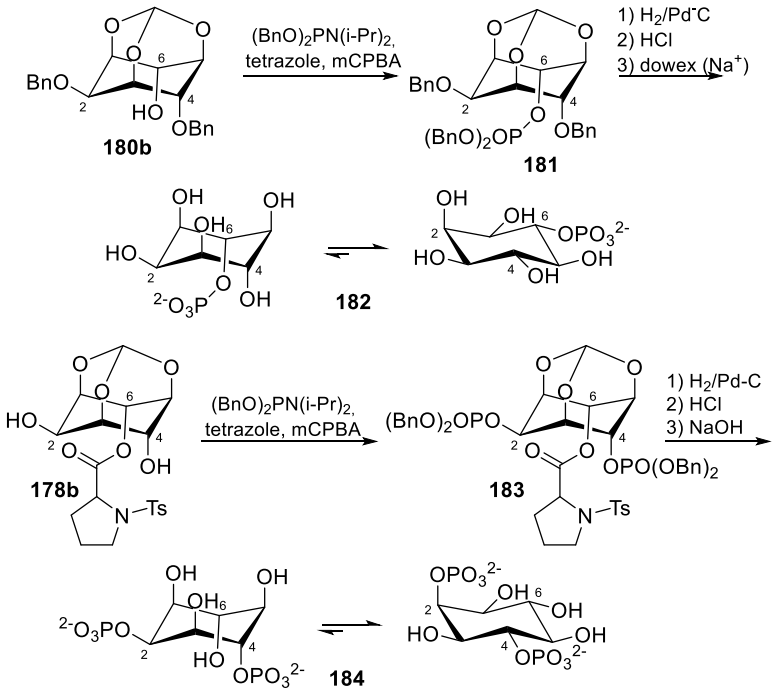

Scheme 91. Synthesis of Ins(6)P **182** and Ins(2,4)P_2 **184**

Triphosphates **Ins(1,4,5)P$_3$** and **Ins(3,4,5)P$_3$** were then prepared following a completely different protocol for the phosphate installation. After 6-mono ester **178b** was isolated, acidic hydrolysis provided for the orthoformate elimination, so that treatment with an excess of cyclohexylidene acetal in presence of different conditions (catalytic vs stoichiometric) pTSA afforded a mixture of differently acetal protected diastereoisomers. In particular, catalytic amount of acid followed by partial cleavage of the ketal moieties afforded 1,2-cyclohexylidene derivative **191** as the major product, whereas stochiometric amount of pTSA accounted for the selective formation of 2,3-cyclohexylidene derivative **190**. Phosphate formation on the three free hydroxyl groups, followed by hydrogenolysis, acidic hydrolysis and salification afforded **Ins(3,4,5)P$_3$** and **Ins(1,4,5)P$_3$**, respectively. (Scheme 92)

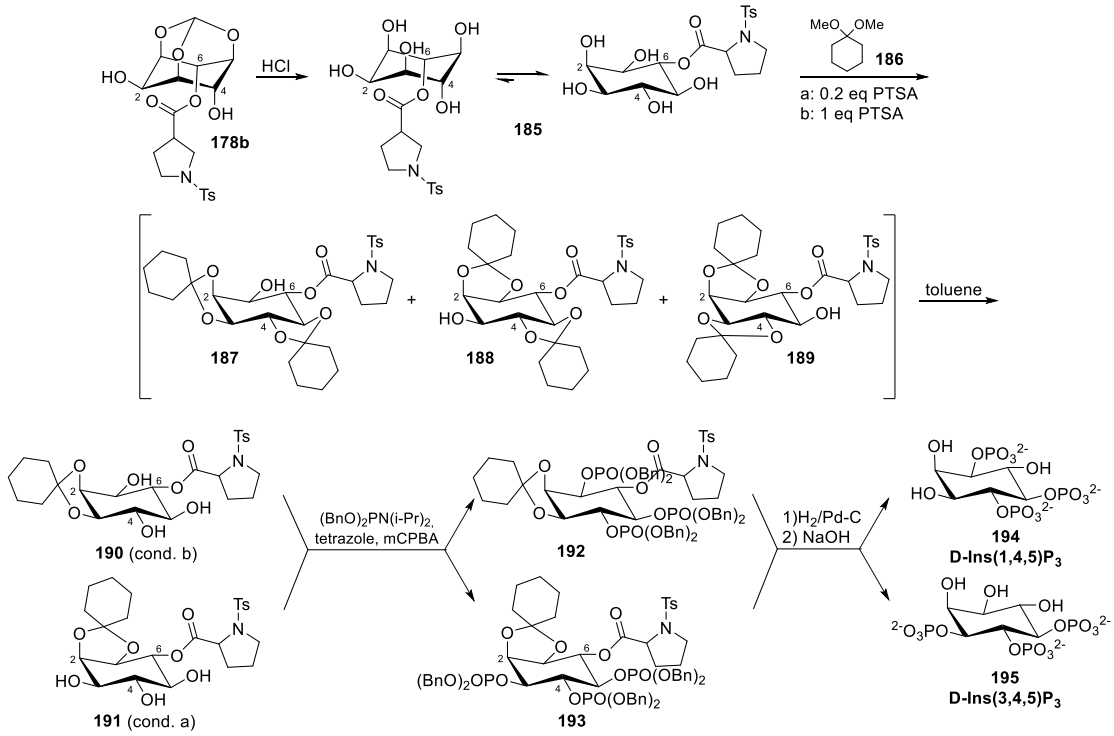

Scheme 92. Synthesis of **194** and **195**, optically pure products, starting from desymmetrized **178b**

4. Results and discussion

Taking in account the importance of myo-inositol for the synthesis of natural products, we decide to explore the selective functionalization of this ring in order to prepare different multifunctional intermediates for APIs synthesis.

In the context of this project, *myo*-inositol was always used in form of orthoformate derivative, because of the well-known regioselective functionalization framework.

Devaraj et al. studied in-depth aspects behind the selective hydroxyl group protections of the orthoformate triol, depending on the OH orientation (axial or equatorial), type of derivatization (acylation, etherification, nucleophilic substitution) and steric and electronic effects. [156] In particular, in presence of sterically hindered electrophiles and weak hindered bases (such as DBU, DIPEA, Et_3N, Py), substitution on the more available hydroxyl group (the equatorial one, at C(2)) takes place. On the other hand, when strong bases are exploited in presence of non-hindered electrophiles, protection occurs on one of the two axial hydroxyl groups. (Scheme 93)

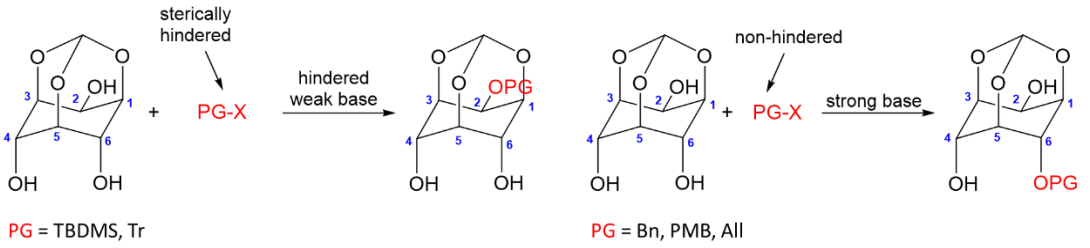

Scheme 93. Regioisomeric discrimination between equatorial and axial mono-O-protection

With this concepts in hands, orthoformate preparation was afforded, by the selective involvement of OH groups at C(1), C(3) and C(5), allowing the formation of an adamantane-like structure, able to switch the equilibrium towards the chair with 5 substituents in axial position. Catalytic amount of *p*-toluensulfonic acid (PTSA) was necessary in order to build the orthoester derivative in presence of triethyl orthoformate. Performing the reaction at 110-120 °C in dry DMF as the solvent, the triol **196** was isolated by recrystallization from methanol after 2 hours, in 65% yield. (Scheme 94)

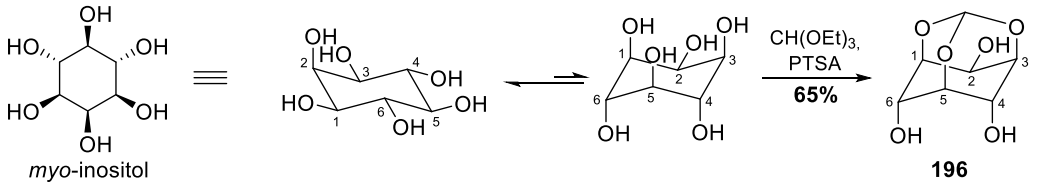

Scheme 94. Preparation of *myo*-inositol orthoformate **196**

In order to synthesize potential precursor of optically pure compound deriving from natural sources, it was thought, in first place, to perform some derivatization in presence of chiral auxiliary. In particular, regioselective acylation of hydroxyl groups in position 2 and 4 were attempted, following what was described by Watanabe and co-workers. Commercially available (R)-(-)-mandelic acid was acetylated in presence of acetyl chloride, so to obtain (R)-(-)-acetyl mandeloyl chloride **(-)-AMCl**, ready to react with the triol **196** to give the diastereoisomeric mixture of 2,4- and 2,6-diacylated derivatives **AM_2,4** and **AM_2,6**, respectively, in presence of of dichloromethane and pyridine as the solvent, at 0 °C for 1 hour, then for other 3 hours until room temperature was reached. (Scheme 95)

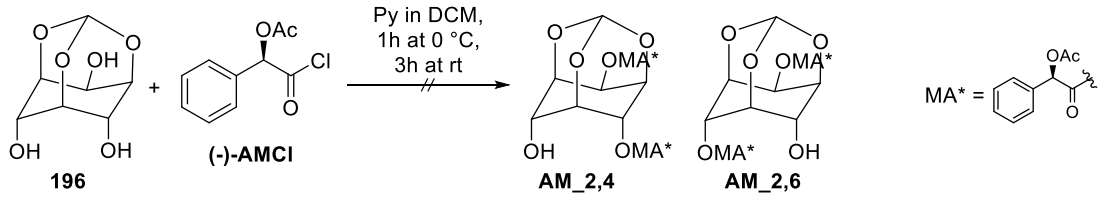

Scheme 95. Derivatization of **196** as 2,4- or 2,6-di-mandelate **AM_2,4** and **AM_2,6**

Unfortunately, even repeating the reaction several times, even for longer reaction times and at different temperature, it was not possible to isolate other than the starting triol **196**. Even if the resolution did not afford the desired enantiomerically pure derivative, it was necessary to desymmetrize in some way the orthoformate *myo*-inositol structure, still in *meso* form. With this in mind, it was a priority to variously functionalize, in a regioselective manner, the orthoformate derivative **196**.

4.1 Strategies towards orthogonal protections on *myo*-inositol orthoformate

Synthesis of orthogonally protected *myo*-inositol orthoformate was then afforded. To do that, interesting data deriving from Devaraj et al. were exploited. [156] In particular, the directing cation effect was introduced, in order to explain the regioselectivity of the OH protection depending on the basis counterion that was used. Protection of the hydroxyl group is considered like a nucleophilic attack by the oxygen to the electrophilic center, typically bringing a halide. Increase of the oxygen nucleophilicity could be reach converting it in an alcoholate, so that the secondary alcohol needs for some strong base to be deprotonated to the corresponding alkoxide. Once the deprotonation occurred, the electrophile could be more easily attacked, with subsequent protection of the hydroxyl group and formation of the salt deriving from the base counterion and the halide from the electrophile.

It was observed that in presence of a non-coordinating counterion (for example Na^+), the exploited base acted deprotonating in first place one of the two axial OH. (Scheme 96) The reason for this kind of selectivity is explained by the less steric hindrance, though the unfavorable 1,3-diaxial interaction between hydroxyl groups in position 4 and 6. Then, if a second deprotonation is required, it is more favorite the formation of the equatorial alcoholate and subsequent 2,4-diprotected system, here highlighted in green.

When the exploited strong base shows a small and coordinating counterion (for example Li^+), the degree of the regioselectivity for the hydroxyl groups protection is higher and more reproducible. This observation was rationalized considering that, after the first axial protection, lithium cation would allow the formation of a very stable intermediate, in which it behaves as Lewis acid simultaneously towards the two axial oxygens. In these conditions, the residual proton is more acidic and easier to be deprotonated by the base, affording the lithium alcoholate ready to be protected on also in position 6, affording with complete regioselectivity the equatorial alcohol highlighted in blue.

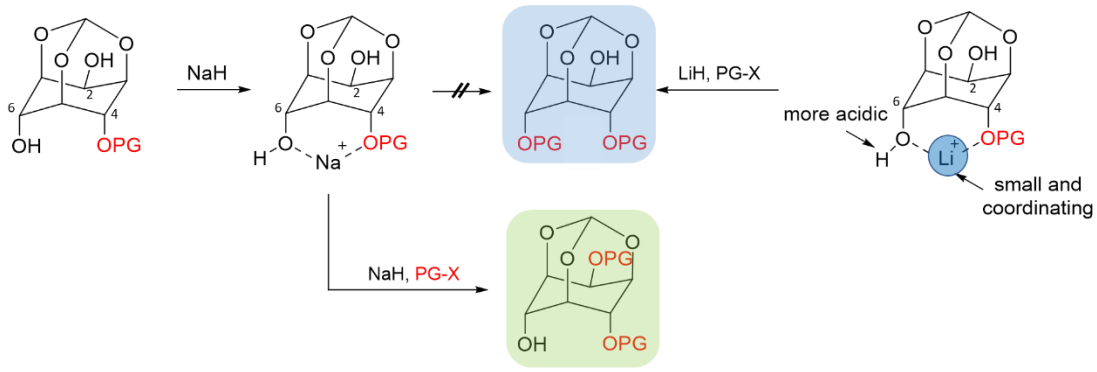

Scheme 96. Schematic representation of the rationale behind 2,4- and 4,6-di-O-protection

4,6-Deprotonation was then performed by exploiting a strong base presenting lithium as the counterion; subsequent reaction with the appropriate protecting group afforded the 4,6-di-O-protected *myo*-inositol orthoformate **197**. In particular, lithium hydride was used as the base, added to a solution of orthoformate **196** in dry DMF. After 30 minutes, the desired electrophile **RX** was added dropwise and the reaction was left stirring for 16 hours, until complete disappearing of starting triol **196**. Residual free hydroxyl group of 4,6-di-O-protected orthoformate **197** was then deprotonated in presence of sodium hydride, prior to protecting group **R_2X** addition, to afford the protected *myo*-inositol **198**. Table 1 reported the different orthogonal protections afforded following this procedure.

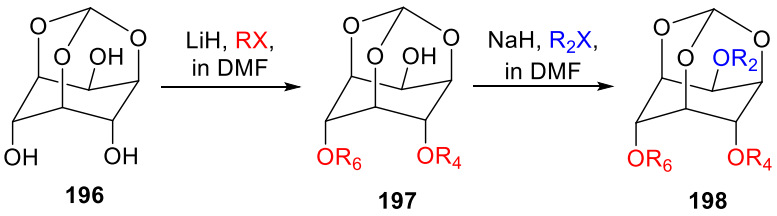

Entry	$R_4 = R_6$	Yield 197	R_2	Yield 198
a	PMB	**99%**	Bn	**99%**
b	All	**70%**	Bn	**94%**
c	Bn	**82%**	All	**82%**

d	Bn	**82%**	MEM	**48%**
e	All	**71%**	Me	**99%**
f	Bn	**81%**	Me	**99%**
g	PMB	**71%**	Me	**99%**

Table 1. Orthogonal protection of OH in position 4 and 6 to give **197a-g**, followed by protection of residual OH at C(2), afford **198a-g** [PMB = p-methoxybenzyl; Bn = benzyl; All = allyl; MEM = methoxyethoxymethyl]

It is evident that such compounds **198a-g**, although obtained in good to excellent yields, were still in *meso* form, so that some kind of desymmetrization of the molecule was necessary before derivatization. At the best of our knowledge, the presence of the same protection on the two symmetric OH (position 4 and 6) and because of the equatorial substituent placed along the plane of symmetry, the desymmetrization target is represented by the orthoformate moiety. In fact, any other modification would have not result in any improvement from the stereochemical point of view. (Scheme 99)

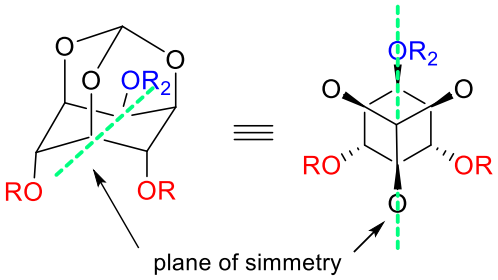

Scheme 97. Plane of symmetry pass through C(2) and C(5), because OR_4 = OR_6. Only orthoformate cleavage could desymmetrize the molecule.

Among the methods described in literature for the orthoformate opening, one was considered the most suitable for the desymmetrization of **198**. [159] Methyl magnesium iodide was indeed reported to be an excellent nucleophile towards the orthoformate scaffold, having also very high stereoselectivity of attack, thanks to the coordination of the magnesium cation with the equatorial oxygen. With the aim to obtain a mixture of diastereoisomers to be resolved, all of the protected *myo*-inositols **198a-g** underwent reaction in presence of MeMgI 3.0 M in diethyl ether, at a temperature between 25 °C and 70 °C for 3 to 16 hours. (Table 2)

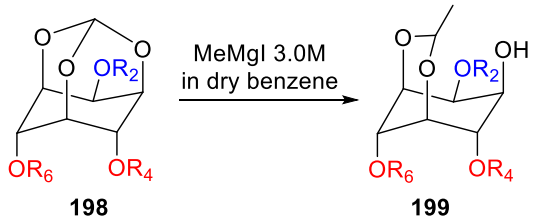

198 199

Entry	$R_4 = R_6$	R_2	Yield 199
a	PMB	Bn	-
b	All	Bn	-
c	Bn	All	-
d	Bn	MEM	-
e	All	Me	**54%***
f	Bn	Me	**57%**
g	PMB	Me	**55%***

Table 2. Reported yields from the reaction of **198a-g** with Grignard reagent
***** = calculated yield based on the NMR analysis of the crude

It is worth noting that opening of the orthoformate afforded the alcohol **199** only when methyl ether was present as the equatorial substituent (R_2 = Me, entry **e**, **f**, **g**). This aspect suggested that steric hindrance on the coordinating oxygen should have been minimized as much as possible, in order not only to direct the attack following its particular stereoselectivity, but also to allow the nucleophilic attack itself to occur. (Scheme 98)

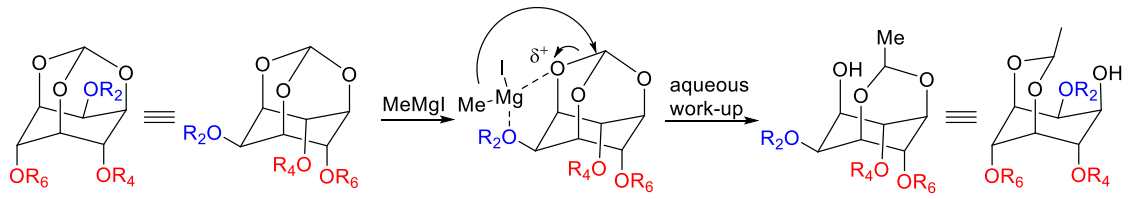

Scheme 98. Orthoformate opening mechanism, by Grignard reagent employment

Nonetheless, 20-25% of the starting material **198** remained unreacted, while the reproducibility of the reaction turned out to be strictly dependent on the quality of Grignard reagent and on the air moisture inside the laboratory. Besides, it was possible

to notice from the purification of the crude that 1) **199** was not obtained as pure in none of the entries, but always eluted together with a fraction of the residual starting **198** (typically 75:25 ratio); 2) at least one of the two axial positions (in form of benzyl and allyl ethers, entry **e** and **f**) suffered nucleophilic attack by the Grignard reagent. Probably electron-positive carbons of both the substituents could be involved in the organometallic methylation, with consequent mono-deprotection and formation of deprotected starting material **200e** and **200f**. (Scheme 99)

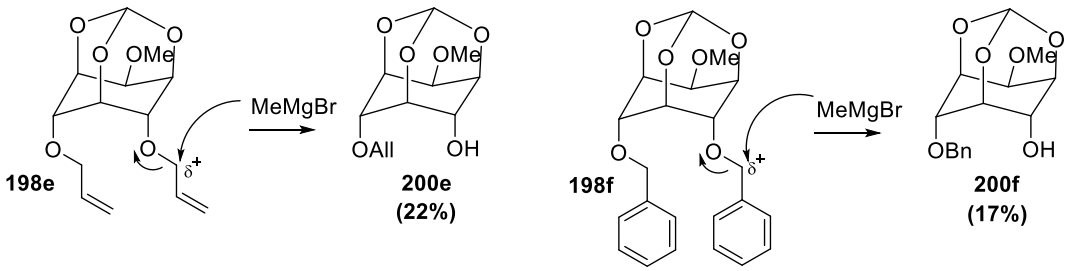

Scheme 99. Hypothesis about the formation of mono-deprotected **200e** and **200f** after MeMgI treatment

Unfortunately, most of the entries did not show positive results, considering that analysis by TLC and chromatographic purification of the crude confirmed the predominant presence of unreacted starting material **198**, together with traces of deprotection products: deallylation from entry **b** and **c**, debenzylation from entry **d**, acetal cleavage from entry **h**.

Particularly surprising was the outcome from entry **d**, considering that equatorial hydroxyl group was protected as methoxy-ethyl-methyl ether (O-MEM), as an ideal coordination site for magnesium. (Scheme 100)

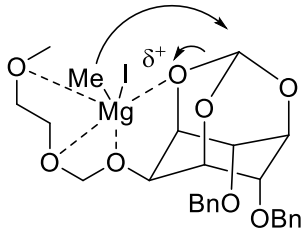

Scheme 100. Rationalization for O-MEM protection: better coordination of magnesium with the substituent at C(2) could have favored orthoformate opening

Due to this result, it is possible that steric factors have more influence in this kind reaction with respect to the coordination capability of the substituent towards the nucleophile. However, considering the low reproducibility of this protocol and its weak appeal towards potential total synthesis approaches (due to the harsh deprotection conditions that are required), an alternative way to desymmetrize the molecule was taken in consideration. Orthogonal protection on *myo*-inositol orthoformate **196** was then performed following a different strategy, with subsequent obtainment of regioisomeric derivatives, with respect to the already synthesized compounds: mono-functionalization on the hydroxyl group in position 4 and, then, double protection of OH at C(2) and C(6), provided for compound **201** with general formula reported in scheme 101.

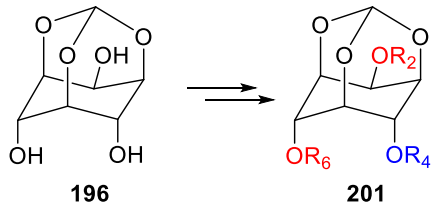

Scheme 101. Functionalization of **196**, so to have R_2 = R_6 on compound **201**

Differently from the previously described pathway, in this case it was not necessary to employ different bases with different counterions, keeping always in mind that a hindered protecting group could favor one particular regioselectivity instead of some others. To maintain our purpose, sodium hydride was used as the base to allow the deprotonation of **196**, while relatively small electrophiles were employed for the OH functionalization. In a first attempt to obtain **201**, double deprotonation of **196** in presence of 2 equivalents of sodium hydride was performed, followed by the addition of 2 equivalents of the electrophile, in order to obtain the intermediate **202**. Unfortunately, in this case no satisfying regioselectivity of the attack was observed; indeed, a mixture of 2,4- and 4,6-di-O-protected derivatives (**202a** and **202b,** respectively) were obtained and identified by NMR analysis after purification of the crude, indicating that exploiting a base with a non-coordinating counterion only regioisomeric mixture of two products **202a** and **202b** could be afforded. (Scheme 102)

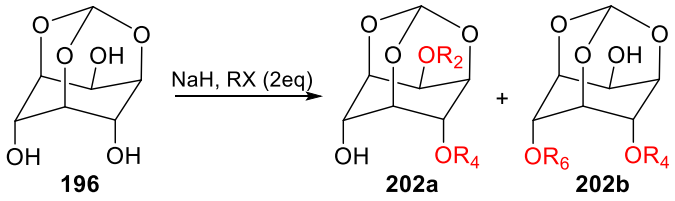

Scheme 102. Treatment of **196** with 2 equivalents of non-coordinating base and 2 equivalents of electrophile gave a mixture of 2,6-di-O-protected **202a** and 4,6-di-O-protected **202b**

On the contrary, deprotonation by sodium hydride (1 eq) and subsequent addition of the appropriate halide easily afforded the 4-O-protected *myo*-inositol orthoformate derivative **203**. Further deprotonation in presence of excess of the base and reaction with the same excess of the electrophile, typically afforded the tri-O-protected *myo*-inositol orthoformate **201** in very high yields. (Table 3)

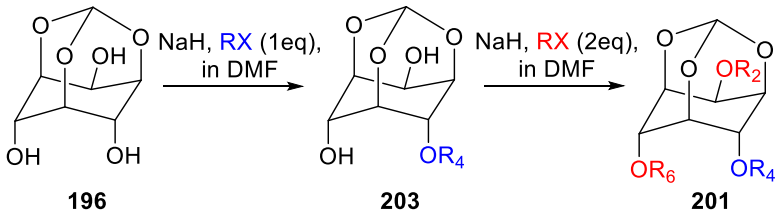

Entry	R_4	Yield 203	$R_2 = R_6$	Yield 201	Yield 201 one-pot
a	All	**87%**	Bn	**82%**	**42%**
b	All	**87%**	PMB	**58%**	**19%**
c	Bn	**88%**	All	**82%**	**38%**
d	Bn	**88%**	PMB	**73%**	**20%**
e	PMB	**79%**	All	**88%**	*
f	PMB	**79%**	Bn	**89%**	*
g	Ts	*	Bn	*	**73%**
h	Ts	*	PMB	*	**19%**

Table 3. Mono-protection of **196** in presence of NaH gave **203**, further protected to give **201**
***** = not performed

Given that, in this last case, both the steps exploited the same solvent reaction and base (dry DMF and NaH, respectively) it was thought to perform these two steps within the same flask, in the same reaction environment. In particular, once the first mono-protection finished (TLC analysis and mass spectrometry), the excess of the base and of the orthogonal halide were added directly to the crude, so that one purification could be avoided and that less solvent could be employed. (Scheme 103)

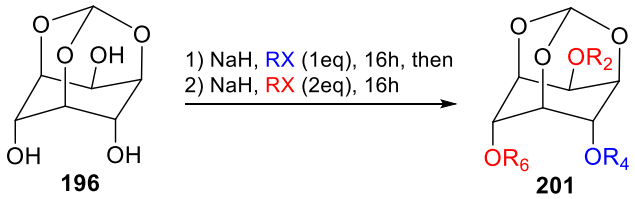

Scheme 103. One-pot approach for the synthesis of **201**

Actually, this approach worked quite well when the first protection was R_4 = Ts, and the second protecting group was $R_2 = R_6$ = Bn (73% yield, Table 4, entry **g**). In all of the other cases (Table 4), at the end of this one-pot approach several byproducts hard to be separated were present and the yield of the desired product was generally discrete but not good. Of course, this kind of approach was performed using, in first place, exactly 1 equivalent of the base and 1 equivalent of the halide: more base would have deprotonated also some other hydroxyl group, with the possibility to obtain di-O-protected derivatives, even when the triol was still available for the deprotonation and functionalization; obviously, the presence of more than 1 equivalent of the electrophile would have brought to the more like formation of **238a** and **238b**, so that the next exhaustive protection step was limited by the number of free OH within the crude. However, this one-pot approach appeared to be low reproducible and, for this reason, not further considered for the preparation of **237**.

Considering the different substitutions on the *myo*-inositol orthoformate scaffold **237**, the molecule was already desymmetrized, but with no functionalization anchors, other than orthoformate moiety. Among the feasible alternatives, Grignard reagent was ruled out, because of its non-reproducibility and its sufferings from steric hindrance:

protection of the hydroxyl group at C(2) with groups more hindered than methyl ether made this alternative not viable for the considered purposes.

In literature, orthoformate opening by diisobutylaluminum hydride (DIBAL-H) was widely described. [160] Differently from what happened with MeMgI, DIBAL-H acted with different stereoselectivity, providing acetal **240** containing a methylene moiety. (Table 5) Clearly, it was not possible to exploit on **237** protecting groups sensitive to the presence of hydride sources. However, the stereoselective attack from DIBAL-H would afford the opening of the orthoformate bond between OH at C(5) and the orthoester carbon, so that **240** could be afforded, stereoselectively and with reproducible high yields. (Table 4)

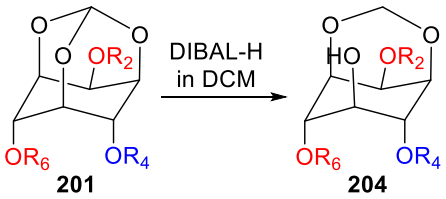

201 **204**

Entry	R_2	R_4	R_6	Yield 204
a	Bn	PMB	PMB	**65%**
b	Bn	Bn	Bn	**96%**
c	All	All	All	**92%**
d	Bn	All	Bn	**88%**

Table 4. DIBAL-H-based orthoformate **201** opening, to afford selectively **204**

While with MeMgI the most important factor were the coordination with the equatorial oxygen and the reduced steric hindrance in that position, DIBAL-H needed for at least 2.5 equivalents to work properly: the first equivalent was used as Lewis acid, so that aluminum could properly activate the less hindered oxygen, that one at C(5); the remaining reactant acted at this point as hydride source, so that the weakest bond could be broken by the nucleophilic substitution from the hydride, affording the alcohol **204**. (Scheme 104)

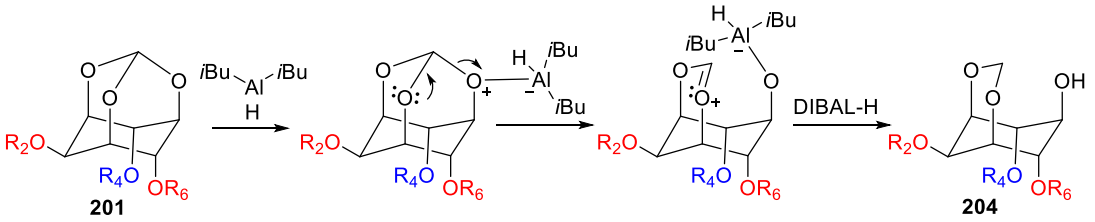

Scheme 104. Reaction mechanism providing for DIBAL-H-mediated orthoformate opening to give alcohol **204**

Once the *myo*-inositol moiety was desymmetrized, it was possible to further functionalize it, prior to perform the derivatization and resolution. Alcohol oxidation in form of ketone would represent a suitable modification for the preparation of some total synthesis product intermediates. (Scheme 105)

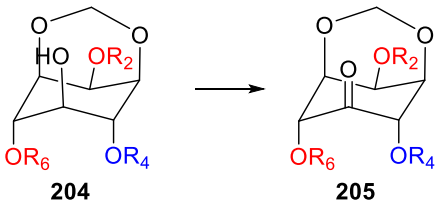

Scheme 105. Oxidation of secondary alcohol **204**, to afford ketone **205**

In this sense, one of the most exploited approach consist of the Swern oxidation, where oxalyl chloride and dimethylsulfoxide allowed the formation of the dimethylchlorosulphonium intermediate, ready to react with primary and secondary alcohols, to afford the alkoxysulphonium derivative **206**. Treatment with a base favored the carbonyl formation and, at the same time, the dimethylsulfide generation, as the byproduct. (Scheme 106)

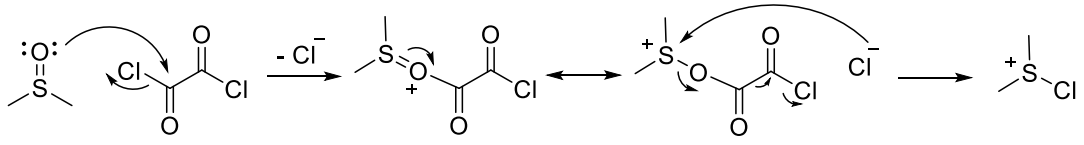

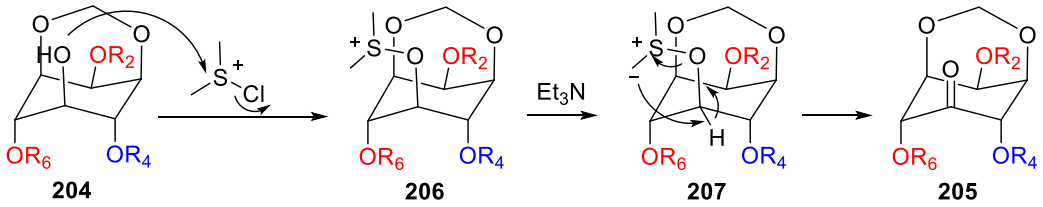

Scheme 106. Swern oxidation mechanism and conversion of **204** to ketone **205**

In conclusion, different regioselective protocols for the protection of *myo*-inositol orthoformate **196** were used. Orthoformate opening by Grignard reagent and DIBAL-H were performed, demonstrating a decidedly better reproducibility in the latter case and favoring the desymmetrization of the inositol moiety when trisubstituted compounds similar to **201a-f** were involved. Due to intellectual property reasons, it is not possible to further discuss about the next developments of this synthetic pathways. Though, it is clear that *myo*-inositol could represent a suitable substrate to be modified and functionalized, in order to be obtained in optically pure form, within the context of total synthesis of different, pharmacologically active natural products.

5. Experimental procedures

5.1 General

All reagents were used as purchased from standard commercial suppliers without further purification, if not differently specified. Solvents were dried and purified by conventional methods prior to use or, if available, purchased in anhydrous form.

For the reactions carried out under anhydrous conditions, all glassware and syringes were dried overnight in an oven at 140 °C and allowed to cool in a desiccator. For the transfer of some reagents sterile packaged one-way plastic syringes were employed. Hypodermic needles for medicinal use were used together with metal needles (specially to transfer anhydrous solvents) and the latter dried in an oven as described previously. The inert gas used for all reactions were nitrogen or argon.

Vacuum distillations were accomplished with standard equipment using oil pumps. Flash column chromatography was performed with Merck silica gel 60, 0.040-0.063 mm (230-400 mesh). Merck aluminum backed plates pre-coated with silica gel 60 (UV254) were used for analytical thin layer chromatography (TLC) and were visualized by staining either with a $KMnO_4$ solution or a ninhydrin solution.

5.2 Analytical instruments

NMR spectra were recorded at 25 °C with a Bruker AC 400 MHz both for ^{1}H and ^{13}C. Deuterated solvents were used as purchased. The solvent is specified for each spectrum. Splitting patterns are designated as s, singlet; d, doublet; t, triplet; q, quartet; m, multiplet; br, broad. Chemical shifts (δ) are given in part-per-million (ppm) relative to the resonance of tetramethylsilane (TMS) as internal standard.

GC/MS analysis were performed with a GC Varian 3900 couple to a MS Varian Saturn 2000. The capillary column containing the stationary phase VF-5 ms has the following dimensions: 30 m x 0.25 mm x 0.25 nm (L x ID x OD).

MS. Mass spectra were recorded with the LC/ SD chromatographic system equipped with an inline UV detector, Agilent 1100 series. Test conditions: 95% MeOH + 5%

H_2O, flow 0.4 mL/min, direct injection, ESI ionization, desiccant gas (N_2) flow equal to 9 l/min, temperature 350 °C, atomizing pressure 40 psi, fragmentation 70 eV.

HPLC/MS analysis were performed with the chromatographic LC/MSD system Agilent 1100 series, connected with UV detector (254 nm) using an Intersil ODS-3V C18 column (5µm, 4.6 x 250mm), flow 1 mL/min, MeCN/H_2O gradient from 55:45 to 80:20 in 30 minutes.

5.3 Synthetic procedures

5.3.1 Experimental procedures about maytansinoids

*Synthesis of 3-(methyldithio)propanoic acid **10***

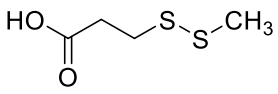

10

To a cooled solution (ice bath) of 3-mercaptopropanoic acid **8** (580 mg, 5.46 mmol) in water (15 mL), was added S-methyl-methanethiosulfonate (780 mg, 1.1 eq) in absolute ethanol (7.5 mL) and the reaction was left stirring for 16 hours. The crude was then diluted with saturated sodium chloride solution and extracted with diethyl ether. The collected organic phase was washed with brine, dried over sodium sulfate, evaporated and purified by chromatographic column (chloroform + 0.1% formic acid), to afford 780 mg of **10** (94% yield).

*Synthesis of N-Methyl-N-[(3-methyldithio)-1-oxopropyl]-L-alanine **12***

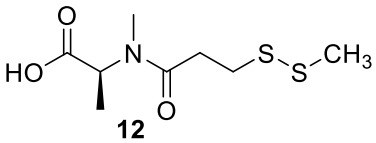

12

To a solution of **10** (775 mg, 5.09 mmol) in THF (10 mL), isobutyl chloroformate (0.65 mL, 1 eq) was added and the solution was stirred at -10 °C for 10 minutes. Triethylamine (0.71 mL, 1 eq) was dropwise added and, after 15 minutes at the same

temperature, N-methyl-L-alanine (1105 mg, 1 eq) in water (10 mL) and triethylamine (1.5 mL) was dropwise added. After 16 hours, the crude was quenched by carefully adding HCl 1N and extracted with ethyl acetate. The collected organic phase was washed with brine, dried over sodium sulfate, evaporated and purified by chromatographic column (chloroform/methanol 97:3), to afford 580 mg of **12** (48% yield).

*Synthesis of maytansinol **5***

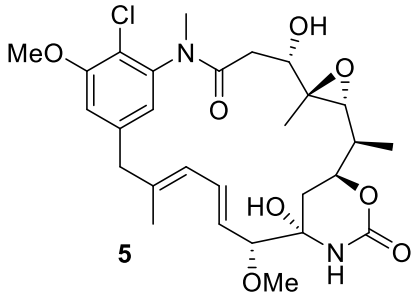

5

In a round bottom flask, dried at 140 °C for two hours and containing 4Å molecular sieves, $LiAlH_4$ 1M in THF (13.5 mL, 13.5 mmol) was treated at -45 °C with MeOH (2 mL, 40.5 mmol) in THF (4.5 mL). After for 15 minutes, this solution was cannulated to ansamitocin P3 (960 mg, 1.5 mmol) in THF (12 mL) at the same temperature under argon atmosphere. After stirring for 4.5 h at a temperature between -35 °C and -45 °C, water (1.6 mL) was added dropwise and the mixture left stirring for 30 minutes at -30 °C. Then, formic acid (0.45 mL) was added dropwise and the reaction mixture let warming to room temperature and diluted with ethyl acetate. Filtration of aluminum salts gave a crude that was evaporated to give a mixture to be purified by chromatographic column, 0-10% gradient of methanol in dichloromethane to obtain the desired alcohol maytansinol (770 mg, 1.4 mmol, 92%).

^{1}H NMR (400 MHz, CDCl3) δ 7.03 (s, 1H), 6.98 (s, 1H), 6.78 (s, 1H), 6.40 (dd, J = 14.8, 11.1 Hz, 1H), 6.12 (d, J = 10.8 Hz, 1H), 5.48 (dd, J = 15.1, 9.3 Hz, 1H), 4.34 (t, J = 11.2 Hz, 1H), 3.95 (s, 3H), 3.47 (m, 3H), 3.33 (s, 3H), 3.18 (s, 3H), 3.09 (d, J = 12.8 Hz, 1H), 2.54 (d, J = 9.6 Hz, 1H), 2.27 (t, J = 12.0 Hz, 1H), 2.17 (d, J = 13.9 Hz, 1H), 2.05 (s, 3H), 1.65 (s, 3H), 1.26 (d, J = 6.1 Hz, 3H), 0.81 (s, 3H).

*Synthesis of **DM1-SMe***

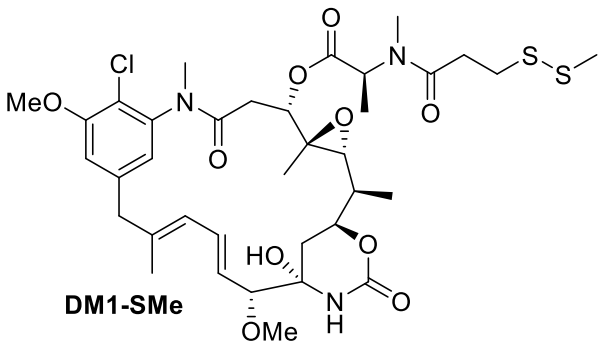

DM1-SMe

To a solution of the acid **12** (130 mg, 0.5 mmol) in dry DCM (1.5 mL), DCC (160 mg, 0.6 mmol) in dry DCM (1.5 mL) and zinc chloride 1.9 M in 2-Me-THF (0.052 mL, 0.1 mmol), then maytansinol **5** (60 mg, 0.1 mmol) in dry DCM (1.5 mL) were added dropwise under argon. After 4.5h at room temperature, the reaction mixture was filtrated from the urea with DCM and the filtrate was evaporated at reduced pressure. Purification performed by preparative TLC (0.2 mm, two runs 6% of methanol in chloroform) afforded to bands with R_f between 0.7 and 0.6, that were separated and extracted with ethyl acetate. The lower band was identified as the L-aminoacyl derivative **DM1-SMe** (10 mg, 4% yield, after preparative TLC).

^{1}H-NMR ($CDCl_3$) δ 6.85 (d, J = 1.5 Hz, 1H), 6.77 (d, J = 11 Hz, 1H), 6.67 (d, J = 1.5 Hz, 1H), 6.47 (dd, J = 15, 11 Hz, 1H), 6.25 (s, 1H), 5.69 (dd, J = 15, 9 Hz, 1H), 5.45 (q, J = 7 Hz, 1H), 4.82 (dd, J = 12, 3 Hz, 1H), 4.31 (t, J = 11 Hz, 1H), 4.02 (s, 3H), 3.72 (d, J = 13 Hz, 1H), 3.54 (d, J = 9 Hz, 1H), 3.39 (s, 3H), 3.28 (s, 3H), 3.14 (d, J = 12 Hz, 1H), 3.08 (d, J = 9 Hz, 1H), 3.03 – 2.92 (m, 2H), 2.90 (s, 3H), 2.86 – 2.73 (m, 2H), 2.65 (dd, J = 15, 12 Hz, 1H), 2.30 (s, 3H), 2.24 (dd, J = 15, 12 Hz, 1H), 1.97 (d, J = 9 Hz, 1H), 1.68 (s, 3H), 1.52 – 1.46 (m, 1H), 1.35 (d, J = 6 Hz, 3H), 1.31 (d, J = 6 Hz, 3H), 1.23 – 1.11 (m, 1H), 0.84 (s, 3H).

*Synthetic procedure for the obtainment of N-carboxyanhydride **18***

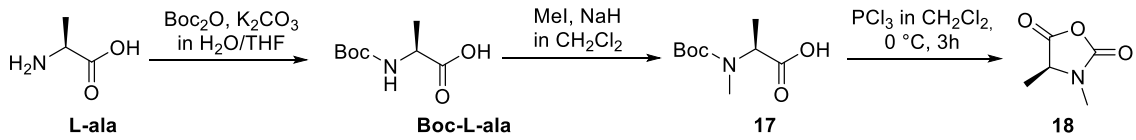

To a suspension of L-alanine (81 mg, 1 mmol) and K_2CO_3 (251 mg, 2 eq) in water (0.7 mL) in an ice bath, Boc_2O (200 mg, 1 eq) in THF (0.4 mL) was dropwise added. After 30 minutes the ice bath was removed and the reaction left stirring for 16 hours. Evaporation of the organic solvent was followed by treatment with 5% citric acid solution until pH = 4 and extraction with ethyl acetate. The collected organic phase was washed with brine, dried over sodium sulfate and evaporated, then used without any further purification for the next step.

A solution of Boc-L-ala (280 mg, 1.48 mmol) in dry THF (5 mL) was cooled at 0 °C and treated with NaH 60% in mineral oil (180 mg, 10 eq) and, after 30 minutes at the same temperature, with MeI (0.93 mL, 10 eq), dropwise added. After 16 hours the solution was acidified with HCl 1N, until pH = 2 and extracted with ethyl acetate. The collected organic phase was washed with brine, dried over sodium sulfate and evaporated, then used without any further purification for the next step.

A solution of Boc-N-methyl-L-alanine **17** (184 mg, 0.9 mmol) in dry DCM (5 mL) was cooled at 0 °C and treated with PCl_3 (0.1 mL, 1.2 eq) and the reaction was left stirring at the same temperature for 2 hours. Evaporation of the solvent at reduced pressure under nitrogen afforded crude **18**, used without any further purification for the next step.

*Synthesis of N-deacetyl-maytansine **16***

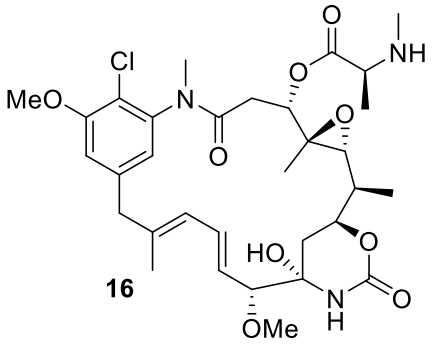

16

To a solution of maytansinol **5** (100 mg, 0.18 mmol) in a 3:1 mixture of dry THF (1.5 mL) and dry DMF (0.4 mL), DIPEA (0.2 mL, 6 eq), $Zn(OTf)_2$ (200 mg, 3 eq) and NCA **18** (160 mg, 5 eq) were added. After 72 hours, dilution with ethyl acetate followed by filtration afforded a crude that was purified by chromatography (chloroform/methanol 97:3), to afford 95 mg of deacetyl-maytansine **16** (15% yield).

*Synthesis of N-nitrophenylsulfenyl-N-methyl-L-alanine **22***

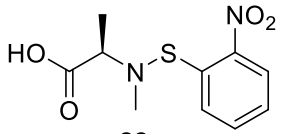

22

To a cooled solution of N-methyl-L-ala (200 mg, 1.94 mmol) and Nps-Cl (1 eq) in acetone (20 mL), water (5 mL) and triethylamine (0.27 mL, 1 eq) were added and the reaction was left stirring for 16 hours at room temperature. Careful HCl 1N addition and extraction with ethyl acetate, were followed by saturated sodium chloride solution washing and drying on sodium sulfate. Evaporation of the solvent and chromatographic purification by Sepa-Core system (ethyl acetate in petroleum ether 0-50% in 4', 50-80% in 8') afforded 485 mg of **22** (98% yield).

^{1}H NMR (400 MHz, $CDCl_3$) δ 10.61 (brs, 1H), 8.27 (d, J = 8.2 Hz, 1H), 8.00 (d, J = 8.2 Hz, 1H), 7.65 (t, J = 7.7 Hz, 1H), 7.25 (t, J = 7.7 Hz, 1H), 3.92 (m, 1H), 2.96 (s, 3H), 1.49 (brs, 3H).

*Synthesis of N-nitrophenylsulfenyl-N-methyl-L-alanine-L-mentholate **23***

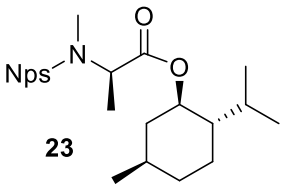

23

To a solution of Nps-N-methyl-L-alanine **22** (500 mg, 1.95 mmol) and L-menthol (80 mg, 0.49 mmol) in dry DCM (20 mL), DCC (450 mg, 4.5 eq) and $ZnCl_2$ 1.9M in 2-Me-THF (0.28 mL, 1.1 eq) were added and the reaction was left stirring for 4 hours. Filtration and evaporation of the crude was followed by chromatographic purification

by Sepa-Core system (ethyl acetate in petroleum ether, 0-15% in 13', 15-40 in 11'), affording 180 mg of **23**, pure enough to be used for the next step.

*Synthesis of imidazolyl sulfonyl azide hydrochloride **28 HCl***

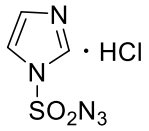

28 HCl

Sulfuryl chloride (2.5 mL, 30.76 mmol) was added dropwise to a suspension of sodium azide (2.0 g, 30.76 mmol) in acetonitrile (25 mL) at 0 °C. The mixture was left stirring for 16 h at room temperature and then treated with imidazole (4.0 g, 58.44 mmol) at 0 °C. After 3 h stirring, the crude was diluted with ethyl acetate, washed with water, saturated $NaHCO_3$, brine, dried over sodium sulfate and filtered. The filtrate was treated at 0 °C by adding dropwise HCl in EtOH to obtain a precipitate. The solid was filtered and washed with ethyl acetate, to give imidazolyl sulfonyl azide hydrochloride **28 HCl** (4.65 g, 22.15 mmol, 72%), as white needles.

^{1}H NMR (400 MHz, D_2O) δ 9.41 (s, 1H), 7.98 (s, 1H), 7.57 (s, 1H).

*Synthesis of L-azido-alanine **27***

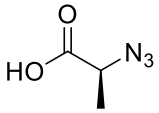

27

L-alanine (150 mg, 1.68 mmol), potassium carbonate (5.42 mmol) and $CuSO_4$ $5H_2O$ (10 mg, 0.04 mmol) in MeOH (10 mL) were treated with sulfonyl azide hydrochloride **28 HCl** (500 mg, 2.87 mmol) and the resulting mixture was left stirring at room temperature. After 16 h MeOH was evaporated and the residue was solubilized in water, added of HCl conc, extracted with ethyl acetate and dried over sodium sulfate. Evaporation of the solvent and treatment with petroleum ether, gave in the ethereal phase the azido acid (190 mg, 1.66 mmol, 99%), as colorless oil.

^{1}H NMR (400 MHz, $CDCl_3$) δ 10.11 (s, 1H), 4.11 – 3.94 (m, 1H), 1.50 (dd, J = 7.1, 1.7 Hz, 3H).

*Synthesis of L-azido-alanyl-maytansinol **29***

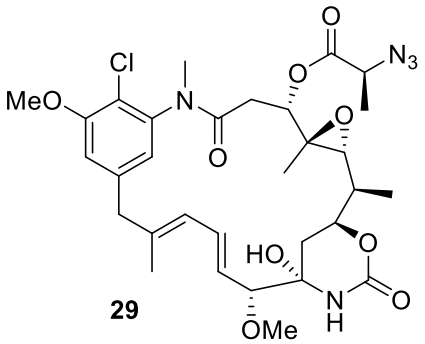

29

To a mixture of maytansinol **5** (320 mg, 0.57 mmol) and L-azido-alanine **27** (120 mg, 1.05 mmol) in dry DCM (10 mL), in presence of 4Å molecular sieves and under argon atmosphere, DCC (300 mg, 1.14 mmol) in dry DCM (1.5 mL) was added dropwise, followed after 20 minutes by $ZnCl_2$ 1.9M in 2Me-THF (0.33 mL, 0.63 mmol). After 6 hours the reaction mixture was quenched by adding cold ethyl acetate and washed with ice, in order to precipitate DCU (as DCC byproduct). Washing with $NaHCO_3$ and brine, gave an organic residue to be dried over sodium sulfate and purified by chromatographic column. Elution with 0-10% methanol in dichloromethane gave azido ester derivative (56 mg, 0.08 mmol, 15%), as pale-yellow solid.

^{1}H NMR (400 MHz, $CDCl_3$) δ 7.10 (s, 1H), 6.82 (s, 1H), 6.42 (dd, J = 15.3, 11.1 Hz, 1H), 6.33 (s, 1H), 6.19 (d, J = 10.8 Hz, 1H), 5.44 (dd, J = 15.3, 8.8 Hz, 1H), 5.30 (s, 1H), 4.95 (dd, J = 11.9, 2.6 Hz, 1H), 4.19 (t, J = 10.6 Hz, 1H), 3.96 (s, 3H), 3.92 – 3.88 (m, 1H), 3.50 (d, J = 6.5 Hz, 1H), 3.47 (s, 3H), 3.33 (s, 3H), 3.16 (s, 3H), 2.82 (d, J = 9.7 Hz, 1H), 2.57 (dd, J = 14.0, 12.1 Hz, 1H), 2.20 (dd, J = 14.1, 2.5 Hz, 1H), 1.90 (d, J = 9.7 Hz, 1H), 1.77 (m, 3H), 1.66 (s, 3H), 1.54 (d, J = 6.8 Hz, 3H), 1.25 (d, J = 6.4 Hz, 3H), 0.83 (s, 3H).

*Synthesis of N-deacetyl-maytansine **33** and its corresponding primary amine **34***

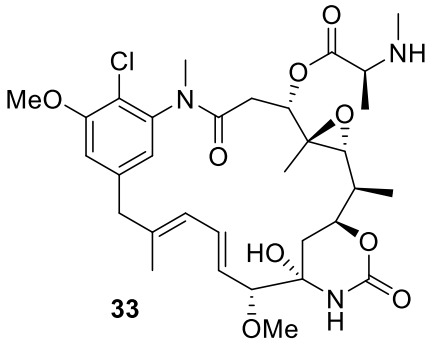

33

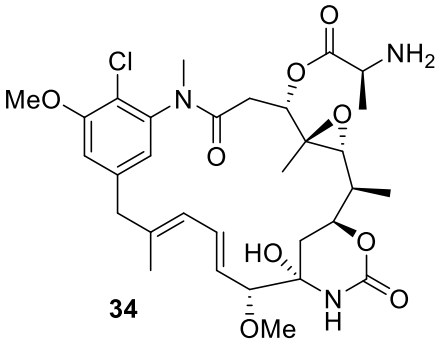

34

To a solution of azido ester **29** (30 mg, 0.08 mmol) in dry DCM (2 mL), PPh_3 was added in one portion and the mixture was left stirring at room temperature under argon atmosphere. After 16 h paraformaldehyde (12 mg, 0.40 mmol) was added and left reacting for 5 h. Then, $NaBH_4$ (15 mg, 0.04 mmol) in MeOH (1 mL) was added dropwise at 0 °C and the resulting mixture left stirring at the same temperature for 40 minutes. Quenching by $NaHCO_3$ and extraction with DCM gave an organic phase to be dried over sodium sulfate and evaporated. Chromatographic column purification eluting with 0-10% methanol in dichloromethane + 0.1 % Et_3N gave methylamino derivative **33** (14 mg, 27% yield), together with primary amine **34** (75 mg, 67%)

33: ^{1}H NMR (400 MHz, CDCl3) δ 6.87 (s, 1H), 6.83 (s, 1H), 6.43 (dd, J = 15.1, 11.1 Hz, 1H), 6.25 (d, J = 11.9 Hz, 1H), 6.16 (d, J = 10.9 Hz, 1H), 5.49 (dd, J = 15.6, 9.0 Hz, 1H), 5.00 – 4.91 (m, 1H), 4.24 (t, J = 10.9 Hz, 1H), 3.98 (s, 3H), 3.34 (s, 3H), 3.13 (s, 3H), 2.84 (d, J = 9.7 Hz, 1H), 2.63 – 2.51 (m, 1H), 2.40 (s, 3H), 2.23 (d, J = 11.7 Hz, 1H), 1.86 (s, 3H), 1.67 (s, 3H), 1.37 (d, J = 6.7 Hz, 3H), 1.28 (d, J = 6.3 Hz, 3H), 0.84 (s, 3H).

34: ^{1}H-NMR (400 MHz, $CDCl_3$) δ 6.83 (s, 1H), 6.79 (s, 1H), 6.40 (dd, J = 18.4, 7.9 Hz, 2H), 6.16 (d, J = 10.9 Hz, 1H), 5.52 (dd, J = 15.4, 8.9 Hz, 1H), 4.92 (dd, J = 11.9, 3.0 Hz, 1H), 4.28 (t, J = 11.1 Hz, 1H), 3.97 (s, 3H), 3.66 (m, 1H), 3.54 – 3.41 (m, 4H), 3.32 (s, 3H), 3.14 (s, 3H), 2.86 (d, J = 9.6 Hz, 1H), 2.57 (dd, J = 14.0, 12.1 Hz, 1H), 2.21 (dd, J = 14.1, 2.9 Hz, 1H), 1.65 (s, 3H), 1.46 (d, J = 6.8 Hz, 3H), 1.26 (d, J = 6.3 Hz, 3H), 0.83 (s, 3H).

*Synthetic procedure for the mono-amino methylation of **34***

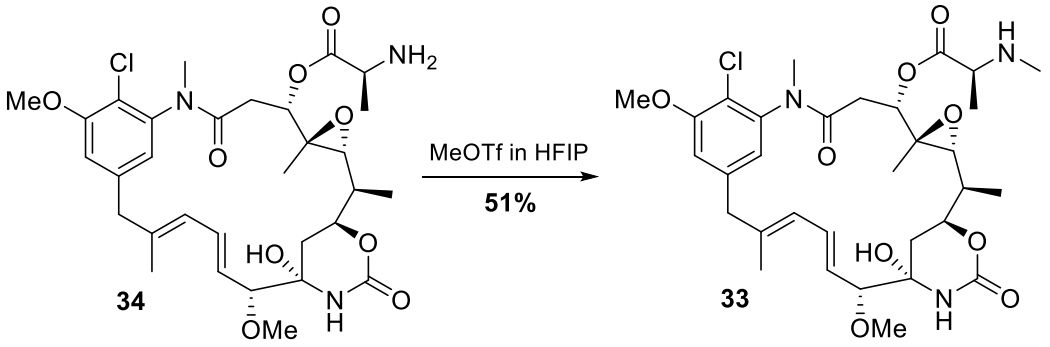

To a solution of primary amine **34** (40 mg, 0.063 mmol) in 1,1,1-3,3,3-Hexafluoro-2-propanol (HFIP, 1 mL) cooled at 0 °C, methyl triflate (10 μL, 0.09 mmol) was added dropwise and the solution was left stirring for 50 minutes. Then, ammonia 2.0 M in ethanol (60 μL, 0.13 mmol) was added to quench the alkylating agent and the crude was evaporated at reduced pressure. Very careful flash chromatography, eluting with a mixture between 0 and 10% of methanol in dichloromethane, allowed us to obtain dimethyl amino derivative **35** (13 mg, 31%), followed by residual starting material **34** (5 mg, 13%), along with the desired methyl amino derivative **33** (21 mg, 51%).

*Synthetic procedure for the acylation of **33***

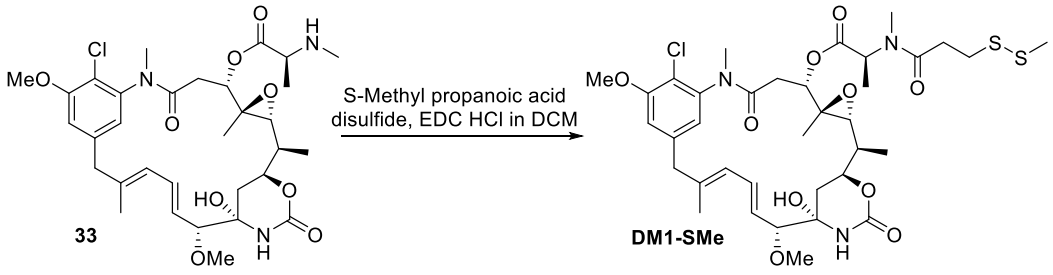

To a solution of the methyl amino derivative **33** (15 mg, 0.023 mmol) in 2 mL of dry DCM, in presence of molecular sieves (4 Å), S-Methyl propanoic acid disulfide **10** (11 mg, 0.046 mmol) was added, followed by EDC HCl (5 mg, 0.025 mmol) and the reaction was left stirring at room temperature. After 16 h, the crude was diluted with DCM and washed with saturated aqueous $NaHCO_3$, then with brine. The organic phase was dried over sodium sulfate, filtered and evaporated at reduced pressure.

HPLC analysis of the crude mixture was performed with a C18 column. The column was eluted following a gradient of acetonitrile in water, from 55% to 80% in 30 minutes. R_t = 13.27 min.

5.3.2 Experimental procedures about *myo*-inositol

*Synthesis of myo-inositol orthoformate **196***

A solution of *myo*-inositol (9g, 50 mmol) in dry DMF (50 mL) was treated with triethyl orthoformate (15 mL, 1.7 eq) and heated at 110 °C under Argon. After 10 minutes, pTsOH monohydrate (2.5 g, 25 mol%) in dry DMF (5 mL) was quickly added. After 3 hours at 110-120 °C, the crude was left cooling and evaporated at the high vacuum pump. The residue was treated with pyridine (30 mL) and cooled at 0 °C prior to the addition of acetic anhydride (30 mL). After 16 hours, the solid was filtered and dried at the high vacuum pump. Recrystallization from methanol, gave pure **196** (65% yield) as a white crystal.

^{1}H NMR (400 MHz, D_2O) δ 5.52 (s, 1H), 4.49 (s, 2H), 4.23 (s, 1H), 4.17 s, 2H), 4.15 – 4.13 (m, 1H).

*General procedure for the synthesis of 4,6-di O-substituted myo-inositol orthoformate **197a-h***

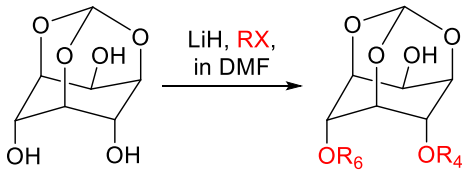

196 **197**

To an ice bath cooled solution of *myo*-inositol orthoformate **196** (1 eq) in dry DMF (0.25 M), LiH (2.2 eq) was added. After 30 minutes at the same temperature, the corresponding electrophile RX (2.1 eq) was added in one portion and left stirring for 16 hours at room temperature. Residual LiH was quenched by carefully adding water to the chilled stirring solution, then the suspension was dried through the high vacuum pump. The residue was dissolved in DCM, and washed with water. The collected

organic phase was treated with saturated solution of sodium chloride, dried over sodium sulfate and evaporated at reduced pressure. The crude was purified by chromatography, through Sepa-Core system (ethyl acetate in petroleum ether, typically 0-60% in 12'), to afford the desired product **197**

197a: ^{1}H NMR (400 MHz, $CDCl_3$) δ 7.17 (d, *J* = 8.5 Hz, 4H), 6.81 (d, *J* = 8.5 Hz, 4H), 5.45 (s, 1H), 4.54 (m, 4H), 4.39 (s, 1H), 4.32 (m, 2H), 4.18 (s, *J* = 1.4 Hz, 1H), 3.78 (s, 6H).

197b: ^{1}H NMR (400 MHz, $CDCl_3$) δ 5.81 (ddd, *J* = 22.3, 10.6, 5.4 Hz, 2H), 5.43 (s, 1H), 5.23 (dd, *J* = 17.2, 0.9 Hz, 2H), 5.13 (d, *J* = 10.4 Hz, 2H), 4.34 (s, 1H), 4.21 (s, 1H), 4.15 (s, 1H), 4.08 – 3.92 (m, 4H), 3.56 (s, 1H), 3.53 (s, 1H).

197c: ^{1}H NMR (400 MHz, $CDCl_3$) δ 7.29 – 7.25 (m, 10H), 5.45 (s, 1H), 4.61 (dd, *J* = 32.2, 11.5 Hz, 4H), 4.48 – 4.43 (m, 1H), 4.36 (m, 2H), 4.26 – 4.20 (m, 2H), 3.09 (s, 1H), 3.06 (s, 1H).

*General procedure for the protection at C(2) of **197a-g** to afford **198a-g***

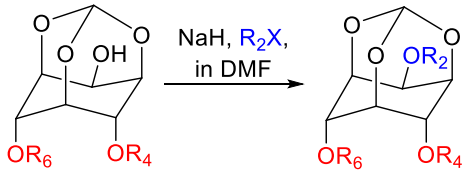

197 **198**

To an ice bath cooled solution of **197** (1 eq) in dry DMF (0.25 M), NaH 60% dispersion in mineral oil (1.5 eq) was added in one portion and left stirring for 30 minutes. Corresponding electrophile R_2X (1.5 eq) was then added and the reaction left stirring for other 16 hours. Residual NaH was quenched by carefully adding water, then the crude was diluted with DCM and washed with water. The collected organic phase was treated with saturated solution of sodium chloride, dried over sodium sulfate and evaporated at reduced pressure. The crude was purified by chromatography, through Sepa-Core system (ethyl acetate in petroleum ether, typically 0-30% in 11'), to afford the desired product **198**.

198a: ^{1}H NMR (400 MHz, $CDCl_3$) δ 7.41 – 7.23 (m, 5H), 7.12 (d, *J* = 8.5 Hz, 4H), 6.81 (d, *J* = 8.5 Hz, 4H), 5.51 (s, 1H), 4.63 (s, 2H), 4.53 (d, *J* = 11.2 Hz, 2H), 4.39 (d, *J* = 11.2 Hz, 3H), 4.30 (t, *J* = 3.5 Hz, 2H), 4.26 (s, 2H), 4.01 (s, 1H), 3.79 (s, 6H).
198b: ^{1}H NMR (400 MHz, $CDCl_3$) δ 7.45 – 7.22 (m, 5H), 5.80 (ddd, *J* = 22.6, 10.6, 5.4 Hz, 1H), 5.51 (s, 1H), 5.22 (dd, *J* = 17.2, 1.6 Hz, 1H), 5.14 (dd, *J* = 10.4, 1.3 Hz, 1H), 4.69 (s, 2H), 4.36 (dd, *J* = 3.2, 1.6 Hz, 1H), 4.27 – 4.25 (m, 1H), 4.22 (t, *J* = 3.6 Hz, 1H), 4.06 – 3.91 (m, 2H).
198c: ^{1}H NMR (400 MHz, $CDCl_3$) δ 7.29 (s, 10H), 5.97 (ddd, *J* = 16.2, 10.9, 5.8 Hz, 1H), 5.52 (s, 1H), 5.30 (dd, *J* = 17.2, 1.4 Hz, 1H), 5.20 (dd, *J* = 10.3, 1.0 Hz, 1H), 4.62 (dd, *J* = 48.0, 11.6 Hz, 4H), 4.45 (s, 1H), 4.36 (t, *J* = 3.6 Hz, 2H), 4.32 (s, 2H), 4.10 (d, *J* = 5.8 Hz, 2H), 3.99 (s, 1H).
198d: ^{1}H NMR (400 MHz, $CDCl_3$) δ 7.27 (s, 10H), 5.51 (s, 1H), 4.89 (s, 2H), 4.61 (dd, *J* = 29.7, 11.6 Hz, 4H), 4.44 (s, 1H), 4.35 (s, 3H), 4.24 (s, 1H), 3.79 (dd, *J* = 5.4, 3.7 Hz, 2H), 3.54 (dd, *J* = 5.4, 3.8 Hz, 2H), 3.33 (s, 2H).
198e: ^{1}H NMR (400 MHz, $CDCl_3$) δ 5.85 (ddd, *J* = 22.7, 10.7, 5.5 Hz, 2H), 5.46 (s, 1H), 5.26 (dd, *J* = 17.2, 1.5 Hz, 2H), 5.16 (dd, *J* = 10.4, 1.2 Hz, 2H), 4.42 – 4.34 (m, 1H), 4.32 – 4.26 (m, 2H), 4.24 (t, *J* = 3.7 Hz, 2H), 4.04 (tdd, *J* = 12.8, 9.2, 3.3 Hz, 4H), 3.69 (s, 1H), 3.47 (s, 3H).
198f: ^{1}H NMR (400 MHz, $CDCl_3$) δ 7.31 (s, 10H), 5.51 (s, 1H), 4.64 (dd, *J* = 51.3, 11.6 Hz, 4H), 4.48 (s, 1H), 4.38 (dd, *J* = 8.3, 4.9 Hz, 2H), 4.35 (s, 2H), 3.82 (s, 1H), 3.44 (s, 3H).
198g: ^{1}H NMR (400 MHz, $CDCl_3$) δ 7.24 – 7.15 (m, 4H), 6.83 (m, 4H), 5.47 (s, 1H), 4.53 (dd, *J* = 49.7, 11.2 Hz, 4H), 4.39 (s, 1H), 4.30 (dd, *J* = 15.0, 2.2 Hz, 2H), 3.77 (s, 6H), 3.42 (s, 3H).

*General procedure for the orthoformate opening of **198** by Grignard reagent*

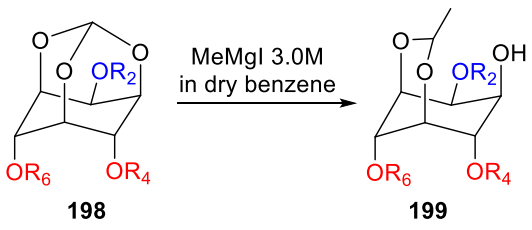

198 **199**

To an ice-bath cooled solution of **198** (1 eq) in dry benzene (or toluene) (0.07 M), MeMgI 3.0 M in Et_2O (Aldrich) (2 eq) was added dropwise and the reaction was left stirring for 5 hours. Quenching by NH_4Cl was followed by extraction with Et_2O and washing of the collected organic phase with saturated sodium chloride solution and drying over sodium sulfate. Evaporation at reduced pressure afforded a crude residue that was attempted to be purified by chromatography (Sepa-Core system, typically ethyl acetate in petroleum ether 0-40% in 14'), affording a mixture of **199** and unreacted **198** (entry **f**)

General procedure for the synthesis of 4-mono-O-protected myo-inositol orthoformate ***203a-f***

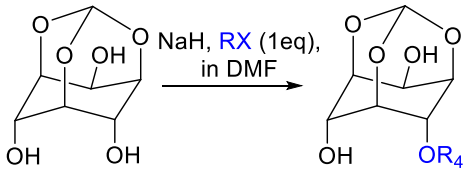

196 **203**

To an ice bath cooled solution of **196** (1 eq) in dry DMF (0.25 M), NaH 60% dispersion in mineral oil (1.05 eq) was added in one portion and left stirring for 30 minutes. Corresponding electrophile R_4X (1 eq) was then added and the reaction left stirring for other 16 hours. Residual NaH was quenched by carefully adding water, then the suspension was dried through the high vacuum pump. The residue was dissolved in DCM, and washed with water. The collected organic phase was treated with saturated solution of sodium chloride, dried over sodium sulfate and evaporated at reduced pressure. The crude was purified by chromatography, through Sepa-Core system (ethyl acetate in petroleum ether, typically 0-40% in 3', 40-80% in 8'), to afford the desired product **203**

203a: ^{1}H NMR (400 MHz, $CDCl_3$) δ 5.80 (ddd, *J* = 23.0, 11.0, 5.9 Hz, 1H), 5.40 (s, 1H), 5.28 – 5.18 (m, 2H), 4.37 (ddd, *J* = 13.4, 8.8, 4.8 Hz, 1H), 4.31 – 4.27 (m, 1H), 4.22 (ddd, *J* = 8.6, 3.8, 1.9 Hz, 2H), 4.13 (dd, *J* = 3.9, 1.8 Hz, 1H), 4.08 (t, *J* = 5.5 Hz, 2H), 3.98 (d, *J* = 11.2 Hz, 1H), 3.69 (dd, *J* = 19.0, 10.8 Hz, 2H).

*General procedure for the protection at C(2) and C(6) of **203a-f** to afford **201a-f***

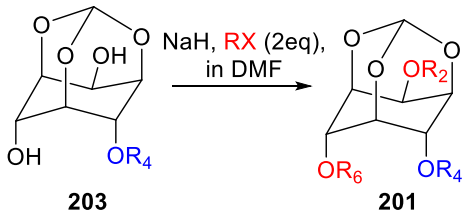

203 **201**

To an ice bath cooled solution of **203** (1 eq) in dry DMF (0.25 M), NaH 60% dispersion in mineral oil (2.5 eq) was added in one portion and left stirring for 30 minutes. Corresponding electrophile RX (2.5 eq) was then added and the reaction left stirring for other 16 hours. Residual NaH was quenched by carefully adding water, then the crude was diluted with DCM and washed with water. The collected organic phase was treated with saturated solution of sodium chloride, dried over sodium sulfate and evaporated at reduced pressure. The crude was purified by chromatography, through Sepa-Core system (ethyl acetate in petroleum ether, typically 0-20% in 12'), to afford the desired product **201**.

201a: ^{1}H NMR (400 MHz, $CDCl_3$) δ 7.51 – 7.08 (m, 10H), 5.80 (ddd, *J* = 22.1, 10.7, 5.6 Hz, 1H), 5.52 (s, 1H), 5.17 (dd, *J* = 24.1, 13.8 Hz, 2H), 4.67 (s, 2H), 4.53 (dd, *J* = 56.1, 11.8 Hz, 2H), 4.40 (s, 1H), 4.32 – 4.27 (m, 2H), 4.26 (s, 2H), 4.12 – 3.89 (m, 3H).

201b: ^{1}H NMR (400 MHz, $CDCl_3$) δ 7.29 (d, *J* = 8.5 Hz, 2H), 7.17 (d, *J* = 8.6 Hz, 2H), 6.90 – 6.80 (m, 4H), 5.80 (ddd, *J* = 22.7, 10.7, 5.5 Hz, 1H), 5.49 (d, *J* = 1.0 Hz, 1H), 5.17 (ddd, *J* = 13.8, 11.7, 1.4 Hz, 2H), 4.59 (s, 2H), 4.45 (dd, *J* = 54.3, 11.4 Hz, 2H), 4.34 (dd, *J* = 3.2, 1.5 Hz, 1H), 4.27 – 4.21 (m, 3H), 4.18 (dd, *J* = 3.7, 1.7 Hz, 1H), 4.13 – 3.90 (m, 3H), 3.79 (s, 3H), 3.76 (s, 3H).

*General procedure for the synthesis of **201a-h** by one-pot approach*

To an ice bath cooled solution of **196** (1 eq) in dry DMF (0.15 M), NaH 60% dispersion in mineral oil (1 eq) was added in one portion and left stirring for 30 minutes. Corresponding electrophile R_4X (1 eq) was then added and the reaction left stirring for

other 16 hours. Then, NaH 60% dispersion in mineral oil (2.2 eq) was added in one portion, followed by the addition of the electrophile RX (2.2 eq) in one portion. After 6 hours residual NaH was quenched by carefully adding water, then the crude was diluted with DCM and washed with water. The collected organic phase was treated with saturated solution of sodium chloride, dried over sodium sulfate and evaporated at reduced pressure. The crude was purified by chromatography, through Sepa-Core system (ethyl acetate in petroleum ether, typically 0-20% in 12'), to afford the desired product **201**.

201g: ^{1}H NMR (400 MHz, $CDCl_3$) δ 7.70 (d, *J* = 8.2 Hz, 2H), 7.39 – 7.17 (m, 12H), 5.49 (s, 1H), 5.17 (t, *J* = 3.7 Hz, 1H), 4.59 (m, 4H), 4.42 (m, 2H), 4.26 (ddd, *J* = 6.7, 5.8, 3.5 Hz, 3H), 3.96 (s, 1H), 2.43 (s, 3H).
201h: ^{1}H NMR (400 MHz, $CDCl_3$) δ 7.73 (dd, *J* = 25.1, 7.2 Hz, 2H), 7.30 (dd, *J* = 34.3, 6.8 Hz, 4H), 7.13 (dd, *J* = 22.9, 7.1 Hz, 2H), 6.82 (d, *J* = 21.9 Hz, 4H), 5.44 (s, 1H), 5.06 (s, 1H), 4.56 – 4.46 (m, 3H), 4.45 – 4.26 (m, 3H), 4.26 – 4.06 (m, 3H), 3.80 (s, 6H), 2.43 (s, 3H).

*General procedure for the orthoformate opening of **201** by DIBAL-H*

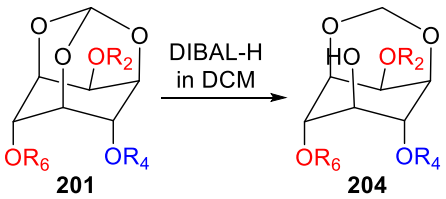

201 **204**

To an ice bath cooled solution of **201** (1 eq) in dry DCM (0.1 M), DIBAL-H 1M in hexanes (Aldrich) (2.5 eq) was dropwise added and left stirring for 16 hours. Residual DIBAL-H was quenched by carefully adding water withing the chilled solution, then the aluminum salts were filtered out and the resulting filtrate was diluted with DCM and washed with water. The collected organic phase was treated with saturated solution of sodium chloride, dried over sodium sulfate and evaporated at reduced pressure. The crude was purified by chromatography, through Sepa-Core system (ethyl acetate in petroleum ether, typically 0-30% in 12'), to afford the desired product **204**

204a: ^{1}H NMR (400 MHz, $CDCl_3$) δ 7.36 – 7.26 (m, 5H), 7.20 (d, *J* = 8.5 Hz, 2H), 6.84 (d, *J* = 8.5 Hz, 2H), 5.54 (d, *J* = 4.9 Hz, 1H), 4.66 (d, *J* = 4.9 Hz, 2H), 4.59 (t, *J* = 5.6 Hz, 4H), 4.50 (d, *J* = 11.5 Hz, 2H), 4.40 (s, 2H), 4.26 (s, 1H), 3.99 (s, 2H), 3.92 (d, *J* = 10.2 Hz, 1H), 3.80 (s, 6H), 2.96 (d, *J* = 10.2 Hz, 1H).

204d: ^{1}H NMR (400 MHz, $CDCl_3$) δ 7.42 – 7.24 (m, 10H), 5.87 (ddd, *J* = 16.6, 10.6, 5.4 Hz, 1H), 5.55 (d, *J* = 4.9 Hz, 1H), 5.23 (dd, *J* = 33.8, 13.8 Hz, 2H), 4.71 – 4.60 (m, 5H), 4.57 (d, *J* = 12.0 Hz, 1H), 4.40 (s, 2H), 4.25 (s, 1H), 4.18 – 4.03 (m, 2H), 3.96 (m, 3H), 3.07 (d, *J* = 10.0 Hz, 1H)

Bibliography

(1) Kupchan, S. M.; Komoda, Y.; Branfman, A. R.; Dailey, R. G.; Zimmerly, V. A. *J. Am. Chem. Soc.* **1974**, *96* (11), 3706–3708..

(2) Asai, M.; Mizuta, E.; Izawa, M.; Haibara, K.; Kishi, T. *Tetrahedron* **1979**, *35* (9), 1079–1085.

(3) Kupchan, S. M.; Sneden, A. T.; Branfman, A. R.; Howie1, G. A.; Rebhun, L. I.; Mclvor, W. E.; Wang, R. W.; Schnaitman, T. C. *J. Med. Chem.* **1978**, *21* (1), 31–37.

(4) Issell, B. F. *Cancer Treat. Rev.* **1978**, *5*(4), 199–207.

(5) Kupchan, S. M.; Komoda, Y.; Branfman, A. R.; Sneden, A. T.; Court, W. A.; Thomas, G. J.; Hintz, H. P. J.; Smith, R. M.; Karim, A.; Howie, G. A.; et al. *J. Org. Chem.* **1977**, *42* (14), 2349–2357.

(6) Tanida, S.; Hasegawa, T.; Higashide, E.; Yoneda, M. **1980**, 192–198.

(7) Luduena, R. F.; Anderson, W. H.; Prasad, V.; Jordan, M. A.; Ferrigni, K. C.; Roach, M. C.; Horowitz, P. M.; Murphy, D. B.; Fellous, A. *Ann. N. Y. Acad. Sci.* **1986**, *466* (1), 718–732.

(8) Huang, A. B.; Lin, C. M.; Hamel, E. *Biochem. Biophys. Res. Commun.* **1985**, *128* (3), 1239–1246.

(9) Mandelbaum-Shavit, F.; Wolpert-DeFilippes, M. K.; Johns, D. G. *Biochem. Biophys. Res. Commun.* **1976**, *72* (1), 47–54.

(10) Remillard, S.; Rebhun, L. I.; Howie, G. A.; Kupchan, S. M. *Science* **1975**, *189* (4207), 1002–1005.

(11) Jordan, M. A.; Wilson, L. *Nat. Rev. Cancer* **2004**, *4* (4), 253–265.

(12) Raxworthy, M. J. *Biochem. Educ.* **1988**, *16* (1), 2–9.

(13) Wallin, M. Microtubules: Structural, Functional, and Clinical Aspects. In *Neuronal and glial proteins: structure, function and clinical application*; Academic Press, San Diego, 1988; pp 321–338.

(14) Kamath, M. A. J. and K. *Current Cancer Drug Targets*. 2007, pp 730–742.

(15) Lopus, M.; Oroudjev, E.; Wilson, L.; Wilhelm, S.; Widdison, W.; Chari, R.; Jordan, M. A. *Mol. Cancer Ther.* **2010**, *9* (10), 2689–2699.

(16) Kirschning, A.; Harmrolfs, K.; Knobloch, T. *Comptes Rendus Chim.* **2008**, *11* (11–12), 1523–1543.

(17) Cassady, J. M.; Chan, K. K.; Floss, H. G.; Leistner, E. *Chem. Pharm. Bull.* **2004**, *52* (1), 1–26.

(18) Chari, R. V. J.; Martell, B. A.; Gross, J. L.; Cook, S. B.; Shah, S. A.; Blättler, W. A.; McKenzie, S. J.; Goldmacher, V. S. *Cancer Res.* **1992**, *52* (1), 127–131.

(19) Lambert, J. M.*Curr. Opin. Pharmacol.* **2005**, *5* (5 SPEC.ISS.), 543–549.

(20) Carter, P.; Presta, L. E. N.; Gorman, C. M.; Ridgway, J. B.; Henner, D.; Wong, W. L.; Rowland, A. M.; Kotts, C.; Carver, M. E.; Shepard, H. M. *Proc. Natl. Acad. Sci.* **1992**, *89* (10), 4285–4289.

(21) Diane E. Handy, Rita Castro, J. L. *Bone* **2011**, *23* (1), 1–7.

(22) Lewis Phillips, G. D.; Li, G.; Dugger, D. L.; Crocker, L. M.; Parsons, K. L.; Mai, E.; Blättler, W. A.; Lambert, J. M.; Chari, R. V. J.; Lutz, R. J.; et al. *Cancer Res.* **2008**, *68* (22), 9280–9290.

(23) Tsuchikama, K.; An, Z. Antibody-Drug Conjugates: *Protein Cell* **2016**, *9*.

(24) Segraves, N. L.; Yazzie, D.; Deese, A. J. *Magn. Reson. Chem.* **2012**, *50* (3), 256–259.

(25) Cantuzumab Mertansine. *https://adisinsight.springer.com/drugs/800007546* **2005**.

(26) Erickson, H. K.; Park, P. U.; Widdison, W. C.; Kovtun, Y. V.; Garrett, L. M.; Hoffman, K.; Lutz, R. J.; Goldmacher, V. S.; Blättler, W. A. *Cancer Res.* **2006**, *66* (8), 4426–4433.

(27) Junttila, T. T.; Li, G.; Parsons, K.; Phillips, G. L.; Sliwkowski, M. X. *Breast Cancer Res. Treat.* **2011**, *128* (2), 347–356.

(28) Jiang, Z.; Yang, Z.; Li, F.; Li, Z.; Fishkin, N.; Burgess, K. *Bioconjug. Chem.* **2018**, *29* (9), 2920–2926.

(29) Oroudjev, E.; Lopus, M.; Wilson, L.; Audette, C.; Provenzano, C.; Erickson, H.; Kovtun, Y.; Chari, R.; Jordan, M. A. *Mol. Cancer Ther.* **2010**, *9* (10), 2700–2713.

(30) Sun, X.; Widdison, W.; Mayo, M.; Wilhelm, S.; Leece, B.; Chari, R.; Singh, R.; Erickson, H. *Bioconjug. Chem.* **2011**, *22* (4), 728–735.

(31) Dosio, F. D.; Brusa, P.; Cattel, L. *Toxins (Basel).* **2011**, *3* (7), 848–883.

(32) Kovtun, Y. V.; Audette, C. A.; Mayo, M. F.; Jones, G. E.; Doherty, H.; Maloney, E. K.; Erickson, H. K.; Sun, X.; Wilhelm, S.; Ab, O.; et al. *Cancer Res.* **2010**, *70* (6), 2528–2537.

(33) Aller, S. G.; Yu, J.; Ward, A.; Weng, Y.; Chittaboina, S.; Zhuo, R.; Harrell, P. M.; Trinh, Y. T.; Zhang, Q.; Urbatsch, I. L. *Science* **2009**, *323* (5922), 1718–1722.

(34) Homolya, L.; Holló, Z.; Germann, U. A.; Pastan, I.; Gottesman, M. M.; Sarkadi, B. *J. Biol. Chem.* **1993**, *268* (29), 21493–21496.

(35) Diamantis, N.; Banerji, U. *Br. J. Cancer* **2016**, *114* (4), 362.

(36) Ogitani, Y.; Hagihara, K.; Oitate, M.; Naito, H.; Agatsuma, T. *Cancer Sci.* **2016**, *107* (7), 1039–1046.

(37) Kovtun, Y. V; Goldmacher, V. S. *Cancer Lett.* **2007**, *255* (2), 232–240.

(38) Kovtun, Y. V.; Audette, C. A.; Ye, Y.; Xie, H.; Ruberti, M. F.; Phinney, S. J.; Leece, B. A.; Chittenden, T.; Blättler, W. A.; Goldmacher, V. S. *Cancer Res.* **2006**, *66* (6), 3214–

(39) Kupchan, S. M.; Sneden, A. T.; Branfman, A. R.; Howie, G. A.; Rebhun, L. I.; McIvor, W. E.; Wang, R. W.; Schnaitman, T. C. *J. Med. Chem.* **1978**, *21* (1), 31–37.

(40) Widdison, W. C.; Wilhelm, S. D.; Cavanagh, E. E.; Whiteman, K. R.; Leece, B. A.; Kovtun, Y.; Goldmacher, V. S.; Xie, H.; Steeves, R. M.; Lutz, R. J.; et al. *J. Med. Chem.* **2006**, 4392–4408.

(41) Scebach, D.; Thaler, A.; Blaser, D.; Ko, S. Y. *Helv. Chim. Acta* **1991**, *74* (5), 1102–1118.

(42) Burger, J. S.; Zietek, K. A.; Cadwallader, A. B.; Bedison, J. E.; Smielewska, M. M. *Synlett* **2003**, *7*, 991–992.

(43) Shinada, T.; Hamada, M.; Miyoshi, K.; Higashino, M.; Umezawa, T.; Ohfune, Y. *Synlett* **2010**, *4* (14), 2141–2145.

(44) Nicolaou, K. C.; Estrada, A. A.; Zak, M.; Lee, S. H.; Safina, B. S. *Angew. Chem. Int. Ed.* **2005**, *44* (9),1378–1382.

(45) Salomon, C. J.; Mata, E. G.; Mascaretti, O. A. *J. Org. Chem.* **1994**, *59* (24), 7259–7266.

(46) Krasik, P. *Tetrahedron Lett.* **1998**, *39* (24), 4223–4226.

(47) Grasa, G. A.; Kissling, R. M.; Nolan, S. P. *Org. Lett.* **2002**, *4* (21), 3583–3586.

(48) Lai, C. L.; Lee, H. M.; Hu, C. H. *Tetrahedron Lett.* **2005**, *46* (37), 6265–6270.

(49) Akssira, M.; Boumzebra, M.; Kasmi, H.; Dahdouh, A.; Roumestant, M.-L.; Viallefont, P. *Tetrahedron* **1994**, *50* (30), 9051–9060.

(50) Patent Carrozzella US7598375B2NCA-Maytansine

(51) Dev, D.; Palakurthy, N. B.; Thalluri, K.; Chandra, J.; Mandal, B. *J. Org. Chem.* **2014**, *79* (12), 5420–5431.

(52) Zervas, L.; Borovas, D.; Gazis, E. *J. Am. Chem. Soc.* **1963**, *85* (22), 3660–3666.

(53) Goddard-borger, E. D.; Stick, R. V. *Org. Lett.* **2007**, 4, 7515–7517.

(54) Lebleu, T.; Ma, X.; Maddaluno, J.; Legros, J. *Chem. Commun.* **2014**, *50* (15), 1836–1838.

(55) Holub, B. J. *Annu. Rev. Nutr.* **1986**, *6* (1), 563–597.

(56) Croze, M. L.; Soulage, C. O. *Biochimie* **2013**, *95* (10), 1811–1827.

(57) Yu, J.; Choi, S.; Park, E.-S.; Shin, B.; Yu, J.; Lee, S. H.; Takami, M.; Kang, J. S.; Meong, H.; Rho, J. *J. Clin. Immunol.* **2012**, *32* (6), 1360–1371.

(58) Xia, T.; Wang, Q. *J. Pharm. Pharmacol.* **2006**, *58* (11), 1527–1532.

(59) Bates, S. H.; Jones, R. B.; Bailey, C. J. *Br. J. Pharmacol.* **2000**, *130* (8), 1944–1948.

(60) Sethi, G.; Ahn, K. S.; Sung, B.; Aggarwal, B. B. *Mol. Cancer Ther.* **2008**, *7* (6), 1604 LP – 1614.

(61) Lin, T.-H.; Tan, T.-W.; Tsai, T.-H.; Chen, C.-C.; Hsieh, T.-F.; Lee, S.-S.; Liu, H.-H.; Chen, W.-C.; Tang, C.-H. *Int. J. Mol. Sci.* **2013**, *14* (5), 9790–9802.

(62) Yap, A.; Nishiumi, S.; Yoshida, K.; Ashida, H. *Cytotechnology* **2007**, *55* (2), 103–108.

(63) Kim, A. R.; Zou, Y. N.; Park, T. H.; Shim, K. H.; Kim, M. S.; Kim, N. D.; Kim, J. D.; Bae, S. J.; Choi, J. S.; Chung, H. Y. *Phyther. Res.* **2004**, *18* (1), 1–7.

(64) de Olinda, T. M.; Lemos, T. L. G.; Machado, L. L.; Rao, V. S.; Santos, F. A. *Phytomedicine* **2008**, *15* (5), 327–333.

(65) Clements, R.; Darnell, B. *Am. J. Clin. Nutr.* **1980**, *33*, 1954–1967.

(66) Hauser, G.; Finelli, V. N. *J Biol Chem* **1963**, *238* (3224–28), 64.

(67) Deranieh, R. M.; Greenberg, M. L. Cellular Consequences of Inositol Depletion. Portland Press Limited 2009.

(68) Schlemmer, U.; Frølich, W.; Prieto, R. M.; Grases, F. *Mol. Nutr. Food Res.* **2009**, *53* (S2), S330–S375.

(69) Coady, M. J.; Wallendorff, B.; Gagnon, D. G.; Lapointe, J. *J. Biol. Chem.* **2002**, *277* (38), 35219–35224.

(70) Fu, H.; Li, B.; Hertz, L.; Peng, L. *Neurochem. Int.* **2012**, *61* (2), 187–194.

(71) Xie, Y.; Wang, Q.; Liu, J.; Xie, J.; Xue, K.; Tang, Q. *J. Chinese Mater. medica* **2010**, *35* (15), 1996–2000.

(72) Michell, R. H. Inositol Derivatives : Evolution and Functions. **2008**, *9* (February), 151–161.

(73) Takai, Y.; Kishimoto, A.; Kikkawa, U.; Mori, T.; Nishizuka, Y. *Biochem. Biophys. Res. Commun.* **1979**, *91* (4), 1218–1224.

(74) Unger, R. H. *Science* **1991**, *251* (4998), 1200–1205.

(75) Henry, R. R. *Am. J. Med.* **1998**, *105* (1), 20S-26S.

(76) Chang, H.-H. Mechanisms Underlying the Abnormal Inositol Metabolisms in Diabetes Mellitus. *Doctoral Thesis*, 2011.

(77) Winegrad, A. I. Banting *Diabetes* **1987**, *36* (3), 396 – 406.

(78) a) Jones, D. R.; Varela-Nieto, I. *Mol. Med.* **1999**, *5* (8), 505–514; b) Laganà, A.; Garzon, S.; Casarin, J.; Franchi, M.; Ghezzi, F. *Trends in Endocrinology and Metabolism*, **2018**, *29*, 768-780.

(79) Pak, Y.; Huang, L. C.; Lilley, K. J.; Larner, J. *J. Biol. Chem.* **1992**, *267* (24), 16904–16910.

(80) Asplin, I.; Galasko, G.; Larner, J. *Proc. Natl. Acad. Sci.* **1993**, *90* (13), 5924 LP – 5928.

(81) Özturan, A.; Arslan, S.; Kocaadam, B.; Elibol, E.; İmamoğlu, İ.; Karadağ, M. G. *Critical Reviews in Food Science and Nutrition* **2019**, *8398*.

(82) Llewelyn, J. G. *J. Neurol. Neurosurg. Psychiatry* **2003**, *74* (suppl 2), ii15–ii19.

(83) ESHRE, T. R.; Group, A.-S. P. C. W. *Fertil. Steril.* **2004**, *81* (1), 19–25.

(84) Bremer, A. A. P *Metab. Syndr. Relat. Disord.* **2010**, *8* (5), 375–394.

(85) Carlomagno, G.; Nordio, M.; Chiu, T. T.; Unfer, V. *Eur. J. Obstet. Gynecol. Reprod. Biol.* **2011**, *159* (2), 267–272.

(86) Artini, P. G.; Di Berardino, O. M.; Papini, F.; Genazzani, A. D.; Simi, G.; Ruggiero, M.; Cela, V. *Gynecol. Endocrinol.* **2013**, *29* (4), 375–379.

(87) Papaleo, E.; Unfer, V.; Baillargeon, J.-P.; De Santis, L.; Fusi, F.; Brigante, C.; Marelli, G.; Cino, I.; Redaelli, A.; Ferrari, *Gynecol. Endocrinol.* **2007**, *23* (12), 700–703.

(88) Genazzani, A. D.; Lanzoni, C.; Ricchieri, F.; Jasonni, V. M. *Gynecol. Endocrinol.* **2008**, *24* (3), 139–144.

(89) Unfer, V.; Carlomagno, G.; Papaleo, E.; Vailati, S.; Candiani, M.; Baillargeon, J.-P. *Reprod. Sci.* **2014**, *21* (7), 854–858.

(90) Benelli, E.; Del Ghianda, S.; Di Cosmo, C.; Tonacchera, M. *Int. J. Endocrinol.* **2016**, *2016*.

(91) Pizzo, A.; Laganà, A. S.; Barbaro, L. *Gynecol. Endocrinol.* **2014**, *30* (3), 205–208.

(92) Benvenga, S.; Antonelli, A. *Rev. Endocr. Metab. Disord.* **2016**, *17* (4), 471–484.

(93) Song, Y.; Driessens, N.; Costa, M.; De Deken, X.; Detours, V.; Corvilain, B.; Maenhaut, C.; Miot, F.; Van Sande, J.; Many, M.-C. *J. Clin. Endocrinol. Metab.* **2007**, *92* (10), 3764–3773.

(94) Fruman, D. A.; Bismuth, G. *Immunol. Rev.* **2009**, *228* (1), 253–272.

(95) Kopp, P. Thyroid Hormone Synthesis. *Werner Ingbar's Thyroid A Fundam. Clin. Text. Tenth Ed. Lippincott Williams Wilkins, Philadelphia* **2012**, 48–74.

(96) Field, J. B.; Ealey, P. A.; Marshall, N. J.; Cockcroft, S. *Biochem. J.* **1987**, *247* (3), 519–524.

(97) Ohye, H.; Sugawara, M. *Exp. Biol. Med.* **2010**, *235* (4), 424–433.

(98) Dunn, J. T. Thyroglobulin Chemistry, Biosynthesis, and Proteolysis. *Werner Ingbar's Thyroid* **2000**.

(99) Gumbleton, M.; Kerr, W. G. *Front. Immunol.* **2013**, *4*, 47.

(100) Ferrari, S. M.; Elia, G.; Ragusa, F.; Ruffilli, I.; Paparo, S. R.; Caruso, C.; Gugliemi, G.; Fallahi, P.; Antonelli, A. *Int J Med Device Adjuv Treat* **2018**, *1*, e166.

(101) Fong, P. *J. Physiol.* **2011**, *589* (24), 5929–5939.

(102) Shamsuddin, A. M.; Elsayed, A. M.; Ullah, A. *Carcinogenesis* **1988**, *9* (4), 577–580.

(103) Vucenik, I.; Shamsuddin, A. M. *J. Nutr.* **1994**, *124* (6), 861–868.

(104) Vucenik, I.; Tomazic, V. J.; Fabian, D.; Shamsuddin, A. M. *Cancer Lett.* **1992**, *65* (1), 9–13.

(105) Deliliers, G. L.; Servida, F.; Fracchiolla, N. S.; Ricci, C.; Borsotti, C.; Colombo, G.; Soligo, D. *Br. J. Haematol.* **2002**, *117* (3), 577–587.

(106) Wattenberg, L. Chalcones, *J. Cell. Biochem.* **1995**, *59* (S22), 162–168.

(107) Menniti, F. S.; Oliver, K. G.; Putney Jr, J. W.; Shears, S. B. *Trends Biochem. Sci.* **1993**, *18* (2), 53–56.

(108) Huang, C.; Ma, W.-Y.; Hecht, S. S.; Dong, Z. *Cancer Res.* **1997**, *57* (14), 2873–2878.

(109) Morrison, R. S.; Shi, E.; Kan, M.; Yamaguchi, F.; McKeehan, W.; Rudnicka-Nawrot, M.; Palczewski, K. *Vitr. Cell. Dev. Biol.* **1994**, *30* (11), 783–789.

(110) Thompson, L. U.; Zhang, L. *Carcinogenesis* **1991**, *12* (11), 2041–2045.

(111) Baten, A.; Ullah, A.; Tomazic, V. J.; Shamsuddin, A. M. *Carcinogenesis* **1989**, *10* (9), 1595–1598.

(112) Vucenik, I.; Tantivejkul, K.; Ramakrishna, G.; Anderson, L. M.; Ramljak, D. *Proc. Am. Assoc. Cancer Res*; 2000; Vol. 41, p 339.

(113) TANTIVEJKUL, K.; VUCENIK, I.; SHAMSUDDIN, A. M. Inositol Hexaphosphate (IP 6) Inhibits Key Events of Cancer Metastasis: I. In Vitro Studies of Adhesion, Migration and Invasion of MDA-MB 231 Human Breast Cancer Cells. *In Vivo (Brooklyn)*. **2003**, *10*, 12.

(114) Vucenik, I.; Passaniti, A.; Tantivejkul, K.; Eggleton, P.; Vitolo, M.; Shamsuddin, A. M. *Rev. Oncol.* **2002**, *4* (Suppl 1), 79.

(115) Singh, A.; Singh, S. P.; Bamezai, R. *Cancer Lett.* **1997**, *117* (1), 1–6.

(116) Druzijanic, N.; Juricic, J.; Perko, Z.; Kraljevic, D. *Rev Oncol* **2002**, *4* (171), 480.

(117) Grases, F.; March, J. G.; Prieto, R. M.; Simonet, B. M.; Costa-Bauzá, A.; García-Raja, A.; Conte, A. *Scand. J. Urol. Nephrol.* **2000**, *34* (3), 162–164.

(118) Grases, F.; Isern, B.; Sanchis, P.; Perello, J.; Torres, J. J.; Costa-Bauza, A. *Front Biosci* **2007**, *12* (1), 2580–2587.

(119) Grases, F.; Sanchis, P.; Perello, J.; Isern, B.; Prieto, R. M.; Fernandez-Palomeque, C.; Saus, C. *Front Biosci* **2008**, *13* (7115), 22.

(120) Curhan, G. C.; Willett, W. C.; Knight, E. L.; Stampfer, M. J. *Arch. Intern. Med.* **2004**, *164* (8), 885–891.

(121) Rodan, G. A.; Fleisch, H. A. *J. Clin. Invest.* **1996**, *97* (12), 2692–2696.

(122) Podeschwa, M.; Plettenburg, O.; Block, O.; Adelt, S.; Altenbach, H. *Eur. J. Org. Chem.* **2003**, *10*, 1958-1972.

(123) Gultekin, M. S.; Celik, M.; Balci, M. *Curr. Org. Chem.* **2004**, *8* (13), 1159–1186.

(124) Worawalai, W.; Rattanangkool, E.; Vanitcha, A.; Phuwapraisirisan, P.; Wacharasindhu, S. *Bioorg. Med. Chem. Lett.* **2012**, *22* (4), 1538–1540.

(125) Hudlicky, T.; Restrepo-Sánchez, N.; Kary, P. D.; Jaramillo-Gomez, L. M. A Short, *Carbohydr. Res.* **2000**, *324* (3), 200–203.

(126) Conrad, R. M.; Grogan, M. J.; Bertozzi, C. R. *Synthesis* **2002**, 10387–10388.

(127) Kang, B.; Sutou, T.; Wang, Y.; Kuwano, S.; Yamaoka, Y.; Takasu, K.; Yamada, K. N- *Advanc. Synth. Cat.* **2015**, *357* (1), 131-147

(128) Takahashi, H.; Kittaka, H.; Ikegami, S. *J. Org. Chem.* **2001**, *66* (8), 2705–2716.

(129) Marnera, G.; Alarcao, M. *Carbohydr. Res.* **2006**, *341*, 1105–1116.

(130) Mehta, G.; Lakshminath, S. *Tetrahedr. Lett.* **2000**, *41*(18), 3509–3512.

(131) Gurale, B. P.; Shashidhar, M. S.; Sardessai, R. S.; Gonnade, R. G. *Carbohydr. Res.* **2018**, *461*, 38–44.

(132) Chen, W.; Deng, Z.; Chen, K.; Dou, D.; Song, F.; Li, L.; Xi, Z. *Eur. J. Med. Chem.* **2015**, *93*, 172–181.

(133) Horii, S.; Fukase, H.; Matsuo, T.; Kameda, Y.; Asano, N.; Matsui, K. *J. Med. Chem.* **1986**, *29* (6), 1038–1046.

(134) Kameda, Y.; Asano, N.; Yoshikawa, M.; Takeuchi, M.; Yamaguchi, T.; Matsui, K.; Horii, S.; Fukase, H. *J. Antibiot. (Tokyo).* **1984**, *37* (11), 1301–1307.

(135) Ogawa, S.; Shibata, Y. *Carbohydr. Res.* **1986**, *148* (2), 257–263.

(136) Fukase, H.; Horii, S. *J. Org. Chem.* **1992**, *57* (13), 3651–3658.

(137) Ogawa, S.; Kanto, M. *J. Nat. Prod.* **2007**, 493–497.

(138) Narahashi, T.; Moore, J. W.; Scott, W. R. *J. Gen. Physiol.* **1964**, *47* (5), 965–974.

(139) Noguchi, T.; Jeon, J.-K.; Arakawa, O.; Sugita, H.; Deguchi, Y.; Shida, Y.; Hashimoto, K. *J. Biochem.* **1986**, *99* (1), 311–314.

(140) Sato, K.; Kajihara, Y.; Nakamura, Y.; Yoshimura, J. *Chem. Lett.* **1991**, *20* (9), 1559–1562.

(141) Sato, K.; Akai, S.; Sugita, N.; Ohsawa, T.; Kogure, T. *Chem. Asian J.* **2006**, 1, 125

(142) Gnauck, A.; Lentle, R. G.; Kruger, M. C. *Int. Rev. Immunol.* **2016**, *35* (3), 189–218.

(143) Bettina, L.; Gersby, A.; Molinaro, A.; Newman, M.; Lowary, T. L. *J. Org. Chem.* **2018**, *84* (1), 14-41.

(144) Takahashi, S.; Itoh, Y.; Takeuchi, M.; Furuya, K.; Kodama, K.; Naito, A.; Haneishi, T.; Sato, S.; Tamura, C. *J. Antibiot. (Tokyo).* **1983**, *36* (10), 1418–1420.

(145) Sakai, T.; Suzuki, K.; Ohmori, K. *Synlett* **2018**, *14*(10), 1351–1357.

(146) Yu, R.; Li, B.-G.; Ye, Q.; Zhang, G.-L. *Nat. Prod. Res.* **2005**, *19* (4), 359–362.

(147) Sureshan, K. M.; Murakami, T.; Watanabe, Y. *Tetrahedron* **2009**, *65*, 3998–4006.

(148) Kwon, Y.; Lee, C.; Chung, S.; Five, F. *J. Org. Chem.* **2002**, *67*(10), 3327–3338.

(149) Potter, B. V. L.; Lampe, D. *Angew. Chemie Int. Ed. English* **1995**, *34* (18), 1933–1972.

(150) Garrett, S. W.; Liu, C.; Riley, A. M.; Potter, B. V. L. *J. Che. Soc. Perk. Trans. 1* **1998**, *57*, 1367–1368.

(151) Sureshan, K. M.; Watanabe, Y. *Tetrahedr. Asymm.* **2004**, *15*, 1193–1198.

(152) Sureshan, K. M.; Kiyosawa, Y.; Han, F.; Hyodo, S. *Tetrahedr. Asymm.* **2005**, *16*, 231–

241.

(153) Ribeiro, M. F. P.; Pais, K. C.; Jesus, B. S. M. De; Fernandez-, R.; Freire, D. M. G.; Manoel, E. A.; Simas, A. B. C. *Eur. J. Org. Chem.* **2018**, *3*, 386–391.

(154) Padiyar, L. T.; Zulueta, M. M. L.; Sabbavarapu, N. M.; Hung, S. *J. Org. Chem.* **2017**, *82* (21), 11418–11430.

(155) Patil, P. S.; Hung, S. *Chem. Eur. J.* **2009**, *15* (5), 1091–1094.

(156) Devaraj, S.; Shashidhar, M. S.; Dixit, S. S. *Tetrahedron* **2005**, *61*, 529–536.

(157) Lee, H. W.; Kishi, Y. *J. Org. Chem.* **1985**, *50*, 4402-4404.

(158) Chen, J.; Lin, J-H.; Xiao, C. *Org. Lett.* **2018**, *20*(10), 3061-3064.

(159) Yeh, S.-M.; Lee, G.H.; Tien, Y.W.; Luh, Y. *J. Org. Chem.* **1997**, *62* (24), 8315-8318.

(160) Gilbert, I.H.; Holmes, A.B.; Pestchanker, M.J.; Young, R.C. *Carbohydr. Res.* **1992**, *234*, 117.